THE ROLE OF UHRF1

IN

THE FANCONI ANEMIA PATHWAY

Bao Zhan

DPhil. in Chromosome and Developmental Biology

Green Templeton College, University of Oxford

Supervisor: Dr. Martin Cohn

Co-supervisor: Dr. Nicholas Lakin

December, 2013

Abstract

Fanconi Anemia (FA) is a genetic disease caused by mutations in any one of the identified 16 genes. The corresponding proteins are known as FA proteins and compose the FA pathway, which is critical for the cellular response to DNA inter-strand cross-links (ICLs). Many efforts have been drawn to understand the individual role of the FA proteins, yet the mechanism of the initiation of the pathway remains elusive, and in particular, no sensor protein for ICLs has been identified. The aims of this study are to identify such a putative factor and to investigate the role of this factor in DNA ICL repair.

We have analyzed the DNA binding activity of two up-stream players in the FA pathway, i.e. FANCD2 and FANCI, which do not seem to be able to detect the damage directly. We then designed a novel biochemical purification strategy using biotin-labeled ICL DNA to isolate ICL interacting proteins from HeLa nuclear extract. By using mass-spectrometry following the purification, we identified an E3 ligase named UHRF1. We cloned, expressed and purified UHRF1 from Sf9 cells. *In vitro* data demonstrate that UHRF1 specifically and directly interacts with cross-linked DNA. *In vivo* experiments indicate that UHRF1 participates in the FA pathway, potentially by recruiting FANCD2 to the sites of DNA damage, and the reduction of cellular levels of UHRF1 by RNA interference (RNAi) sensitizes cells to MMC. We also identified the SRA domain as the region of UHRF1 that is responsible for DNA ICL binding, and the interference of this region results in defects in the cells in ICL repair.

With the unique feature of ICL DNA binding, UHRF1 is identified as a new player in the FA pathway. Future clinical studies will help to determine if UHRF1 is indeed an FA gene of which mutations can generate phenotypes of the disease. Also, a better understanding of the molecular mechanisms underlying UHRF1 in the FA pathway will enable us to develop better and more targeted modes of cancer therapies.

Acknowledgement

Realizing my DPhil study is coming to an end as I am typing away this thesis, I feel extremely thankful to all the people around me who made my study at Oxford possible and enjoyable. First and foremost, I would like to express my sincerest gratitude to my supervisor, Dr. Martin Cohn, who has been a great teacher, a coach and a mentor to guide me through my DPhil study with his knowledge, patience and support. It is with his encouragement and help that I discovered such an amazing topic to study and conducted the subsequent exciting research. I firmly believe that one simply could not have wished for a better scientific training experience. I am also deeply grateful to the Wellcome Trust and Green Templeton College. All my research and my life in Oxford would have never happened without the generous financial support from them.

Secondly, I would like to thank my co-supervisor, Dr. Nicholas Lakin, who has kindly devoted so much of his time and effort to help and advise me at many different stages of my study. Moreover, a genuine thank you goes to Prof. David Sherratt and Prof. Matthew Whitby, who have been on my thesis committee in the past three years, and have given me very critical and constructive advices throughout my study. I also would like to take this opportunity to thank Dr. Fumiko Esashi, who examined me for my transfer, together with Prof. Sherratt. The discussion we had during the transfer viva was proven to be very important to direct my following study into a better shape. In addition, I want to thank my rotation supervisors, Prof. Tariq Enver, Prof. Kim Nasmyth and the members of their labs, who provided me with caring trainings and brilliant opportunities to

explore different areas of research. A big thank you also goes to my college advisor, Prof. John Furlong, who has always given me his best encouragement for my study, and all the advisors on the board of the Wellcome Trust Programme in Chromosome and Developmental Biology lead by Prof. Matthew Whitby. I still vividly remember the inspiring tutorials we were given in the first year, and the immense amount of support I received in many aspects of my DPhil study.

I want to take this opportunity thank all our collaborators, especially Prof. Steven Gygi and his team from Harvard Medical School, whose amazing work helped us to identify UHRF1 and lead to the core discovery of this study. I am very grateful for having the chance to collaborate with Prof. Johannes Walter and his laboratory from Harvard Medical School as well, whose excellent research will enable us to better understand the function of UHRF1 in the process of DNA inter-strand cross-link repair. It is also thanks to the generosity on reagents and advices from several other groups that this study was made possible, including Dr. Rob Klose, Prof. Neil Brockdorff, Dr. Fumiko Esashi, Dr. Catherine Pears, Dr. Lynne Cox, Prof. Ilan Davies, Prof. Francis Barr, Dr. Lidia Vasilieva, Dr. Haruhiko Koseki from RIKEN Institute of Allergy and Immunology, Dr. Masaki Okano from RIKEN Centre of Developmental Biology, Dr. Johan de Winter from VU University Medical Center and Micron Oxford Advanced Bioimaging Unit.

I have to send my earnest gratitude to all my colleagues and friends during my study in Oxford, especially to Chih-Chao Liang, who has been a wonderful partner and a true friend to me at work. The current and past colleagues also contributed significantly to this study and supported my work greatly, including

Jean Tian, Maarten van der Velden, Ragna de Jonge, Dr. Yasunaga Yoshikawa, Caroline Schneider, and Alicja Bulsiewicz. It is with dear friends like Stella Lempidaki, Dr. Duen-Wei Hsu, Dr. Hong-Yu Wang, Dr. Edgar Pogna, Dr. Denis Krndija, Dr. Jayati Jain, Gianluca Vegiani, Dr. Claudia Anne-Marie Couto, Dr. Amanda Unsworth, Alina Rakhimova, Dr. Penelope Mason, Dr. Nick Crump, Caroline Schneider, Kira Fischer, Dr. Keiko Watanabe, Hannah Long, Catarina Vicente, Anne Grijzenhout, Claudia Gruber, Dr. Jean-Yves Bleuyard, and Dr. Keiko Yata, etc., that I have had such an enjoyable study at Oxford. Also, thanks to my lovely teammates and friends at Green Templeton College, GTC Boat Club, Oxford University Symphonic Band, and Oxford International Relations Society, my DPhil life formed an extraordinarily colorful memory that I will always cherish.

Finally, I would like to convey a special thank you to my parents and all my family, for giving me their unconditional love and enormous amount of support to help me come this far and complete my study; and to my dearest companion, Jeremy Bourg, who has always been there for me in the past four years, and given me the best care one could ever ask for. At the end, I want to dedicate this study to my beloved grandma, who was the one encouraged me to study biomedical science when I was eight, but unfortunately left us during my study before I had a chance to show her that I had proudly followed her advice. I will always remember the very words she spoke to me and I will always love her.

Bao Zhan

University of Oxford

September 2013

List of Abbreviations

BER	Base Excision Repair
DDR	DNA Damage Response
DSBs	Double-strand Breaks
EMSA	Electrophoretic-mobility Shift Assay
FA	Fanconi Anemia
FACS	Fluoresence-activated Cell Sorting
hESCs	Human Embryonic Stem Cells
HJ	Holliday junction
HR	Homologous Recombination
HU	Hydroxyurea
ICLs	Inter-strand Cross-links
IF	Immuno-fluoresence
IR	Ionizing-radiation
KD	Knock-down
LIF	Leukemia Inhibitory Factor
mESCs	Mouse Embryonic Stem Cells
NER	Nucleotide Excision Repair
MMC	Mitomycin C
MMR	Mismatch Repair
MNNG	Methylnitronitrosoguanidine
NHEJ	Non-homologous End Joining
PCR	Polymerase Chain Reaction
PHD	Plant-homeo Domain
PIP	PCNA-interacting Protein
RING	Really-interesting-new-gene
RNAi	RNA Interference
ROS	Reactive Oxidative Substances
shRNA	Small-hairpin RNA

SRA	SET-and RING-finger-associated
TLS	Translesion Synthesis
WB	Western-blot
WT	Wild Type

Table of Contents

Figure Index

Chapter 1 Introduction

1.1 Fanconi Anemia and ICLs repair

1.1.1 DNA damage response overview

Cellular DNA is facing both endogenous and exogenous damages everyday. Endogenous factors include the DNA replication process for cell division and certain metabolic processes, and exogenous damages are from environmental sources such as exposure to mutagens and UV radiation. Thousands of lesions have to be repaired efficiently to preserve genomic integrity. The machinery, which facilitates the repair, is known as DNA Damage Response (DDR). It is a sophisticated network of multiple repair pathways. Thanks to this machinery, cells can develop, replicate and function properly within an organism. Depending on the type of the damage, cells first go through a decision-making process, and then select one or a combination of a few repair pathways, including base-excision repair (BER), mismatch repair (MMR), nucleotide-excision repair (NER), homologous recombination (HR), non-homologous end joining (NHEJ) and translesion synthesis (TLS) (*1*).

It is generally believed that the DDR is primarily regulated by DNA damage response kinases, e.g. the holoenzyme DNA-dependent protein kinase (DNA-PK), ataxia telangiectasia-mutated protein (ATM), and ATM and Rad3-related protein (ATR) (*2*). The catalytic subunit of DNA-PK, DNA-PKcs, and ATM are mostly

involved in DNA double-strand breaks (DSBs) repair, whereas ATR is required in a wide range of DNA damage repair (*3*).

1.1.2 Diseases caused by DNA repair defects and the relevant pathways

Defects in coordinating these DNA damage response and repair pathways result in genome instability and underlie a series of human genetic diseases. Patients are usually diagnosed at a very early stage, but all tend to develop cancer later in the life. Some commonly known examples are listed below (Table 1.1).

Genetic Defect	Disease Examples	Common Symptoms
Damage detection and response	Ataxia telangiectasia, Li–Fraumeni syndrome, Seckel syndrome	Defects in DNA damage signalling, and predisposition to cancer
NER	Xeroderma pigmentosum, Cockayne syndrome, Trichothiodystrophy	Photosensitivity, and predisposition to cancer
BER	Alzheimer's disease	Dementia, neurologic disorders
DSBs repair	Nijmegen breakage syndrome (NBS), Werner syndrome, Bloom syndrome, Riddle syndrome	Growth retardation, immunodeficiency, photosensitivity, and predisposition to cancer
ICLs repair	Fanconi anemia	Developmental defects and predisposition to leukemia
MMR	Herediatary nonpolyposis colon cancer	Predisposition to colon cancer

Table 1.1 Genetic diseases caused by defects in DNA damage repair (*4, 5*).

1.1.2.1 Nucleotide excision repair

Nucleotide excision repair (NER) is an important repair mechanism that can remove bulky DNA adducts, that are commonly caused by ultraviolet light (UV). Defects in this pathway can cause diseases, such as Xeroderma pigmentosum. Patients are characterized by hypersensitivity to UV light, which causes cyclobutane pyrimidine dimers (CPDs, including thymine dimers) and 6,4-photoproducts in the DNA (*6*). These DNA distortions results in a bulge on one of the strands on the DNA double helix structure, which can be recognized by NER proteins.

NER pathway is evolutionarily conserved, and recognizes distortions either throughout the genome, or selectively from the transcribed strand of active genes (*7*). The Xeroderma pigmentosum complementation group C (XPC) forms a complex with several other proteins, scanning the genomic DNA (*8*). Once a damage is detected, the DNA around the lesion is unwound and stabilized for incision by a multi-subunit complex including transcription factor II H (TFIIH), XPB, XPD, XPG, RPA etc. (*9, 10*). Then excision repair cross-complementation group 1 protein (ERCC1)-XPF, and XPG, structure-specific endonucleases, cleave off the nucleotide fragment containing the damaged DNA. PCNA is loaded near the excision site, and activates replicative DNA polymerases δ and ε or the translesion DNA polymerase κ to fill the single-strand gap (*11*). The final step involves DNA ligase IIIα and X-ray cross complementing protein-1 (XRCC1) and DNA ligase I to seal the nascent DNA fragment (*12*).

1.1.2.2 Base excision repair

Endogenous hydrolysis, and reactive oxidative substances (ROS) are the most common source of DNA damage in a cell, which is usually repaired by the base excision repair (BER) pathway. Inefficient BER has been suggested to be involved in Alzheimer's disease (*13*). In BER, the damaged DNA base is removed by DNA glycosylases, and the phophodiester backbone is incised by AP endonuclease-1 (APE1). The complementary nucleotide is added by polymerase β, and the DNA backbone is sealed by a complex of XRCC1 and DNA ligase IIIα (*14*).

1.1.2.3 DNA DSB repair

Defects in DNA DSB repair can result in severe diseases, such as Nijmegen breakage syndrome (NBS) and Werner syndrome. Both are autosomal recessive diseases. NBS is caused by mutations in gene NBS1, which is critical for the repair pathway activation and checkpoint signaling. The genetic deficiency of Werner syndrome has been identified as WRN, which encodes a member of RecQ DNA helicase family (*15*). The protein has been proposed to participate in DNA replication, double-strand break (DSB) repair, and telomere maintenance (*16*). It has been shown that cells from patients with DSB repair defects are hypersensitive to DNA damage inducing agents, e.g. ionizing radiation (IR) and camptothecin (CPT) (*17, 18*). CPT inhibits the rejoining activity of toperisomerase I, which removes DNA supercoils during DNA transcription and

replication, and leads to DNA single-strand break. As DNA replication progresses during S phase of the cell cycle, the single-strand break can convert into a double-strand break.

1.1.2.3.1 DSB DDR activation

DNA DSBs are considered as the most detrimental lesion in cells, because they can cause replication fork collapse and genomic re-arrangement. Typically, IR is a source to introduce DSBs directly, and collapsed replication forks can also transform into DNA DSBs. This type of damage is mainly repaired using two pathways, HR and NHEJ, depending on the availability of a homologous repair template. In case of a double-stranded DNA break being created, for example by IR, the complex of meiotic recombination protein-11 (MRE11), RAD50 and Nijmegen breakage syndrome protein-1 (NBS1) (MRN complex) is recruited to the break (Fig. 1.1, step A), and the dimeric, inactive form of ATM is separated to generate a monomeric and phosphorylated form, which is also recruited (*3, 19*) (step B). ATM binds to MRN and is further activated by phosphorylation. In G1 or S phase of the cell cycle, the activated ATM phosphorylates the C-terminal tail of the histone variant H2AX, producing γH2AX, and other downstream targets, including CHK2, which leads to cell-cycle arrest, inhibition of the origin firing in S phase, and DSB repair (*3*) (step C). Mediator of DNA damage checkpoint protein 1 (MDC1) then forms a complex with MRN and γH2AX (step D) to recruit more of ATM to the flanking region of chromatin, and to propagate the phosphorylation of H2AX (*2, 20*).

Similar to phosphorylation, ubiquitination is also an important type of protein post-translational modification, controlling protein intra-cellular signalling transduction. It is involved in regulating many aspects of biological processes, such as DNA replication and repair. This modification requires an enzymatic cascade that is composed by an E1 activating enzyme, E2 conjugating enzyme and an E3 ubiquitin ligase. A protein can be mono-, multi- or poly-ubiquitinated, and the type of modification usually decides the fate of the protein. For example, a protein poly-ubiqutinated at the Lys 48 position of ubiquitin is typically subject to degradation mediated by 26S proteasomes, but not when it is at Lys 63 (*21, 22*). Lys 63 poly-ubiquitination can change the substrate's activity or location (*22*). Phosphorylated MDC1 can recruit RNF8, to poly-ubiquitinate H2A/H2AX, forming Lys 63 ubiquitin chain, following its mono-ubiquitination by RNF168 (*23, 24*). Rap80 is also recruited, probably through the interaction with H2AX poly-ubiquitination, and brings in BRCA1 or 53BP1 (*23, 25, 26*). Moreover, ATM and NBS1 promote the nuclease-mediated resection of DNA ends to generate RPA-coated single-stranded DNA (ssDNA), probably mediated by CtIP (*27, 28*) (steps G&J). DNA-PKcs can stabilize ATM, and also trigger H2AX phosphorylation (*29*) (steps H&I).

Fig. 1.1

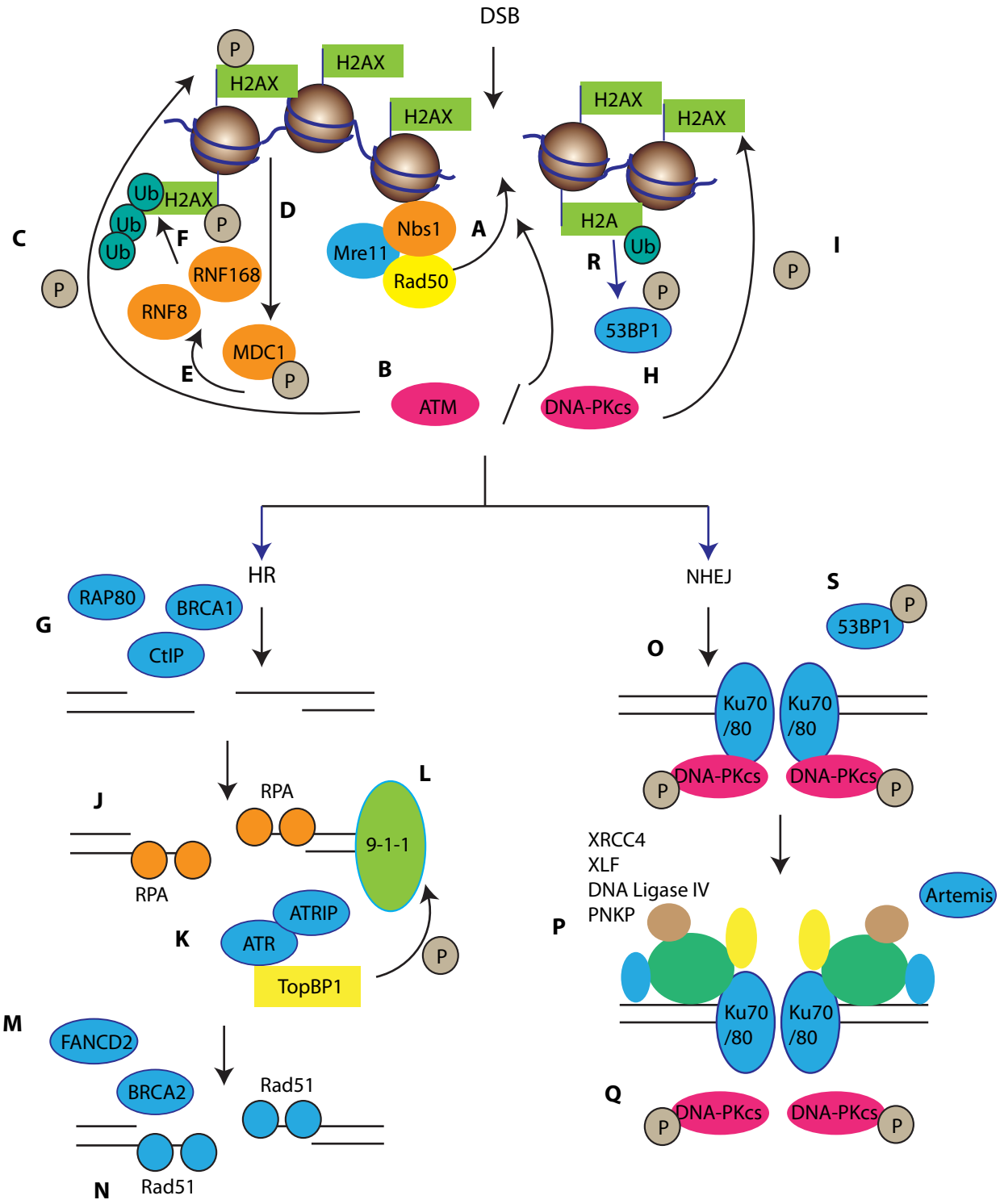

FIG. 1.1 **Schematic diagram shows the steps involved in repairing DNA DSBs.**

1.1.2.3.2 HR in DNA DSB repair

In S and G2 phases of the cell cycle, the homologous strand of the damaged DNA can be used for HR, which is considered as an 'error-free' way to repair DSBs. The activation of ATM-CHK2 pathway leads to the sequential activation of ATR-CHK1 pathway. However, in occasion of stalled DNA replication forks, the ATR-CHK1 pathway can also be activated independently of ATM. RPA binds ssDNA (step J), and interacts with ATR-interacting protein (ATRIP) (*30, 31*). ATR is then recruited through its interaction with ATRIP (*32*) (step K), and so is the RAD17-replication factor C (RFC) clamp complex, to load RAD9-RAD1-HUS1 (9-1-1) complex (*33*) (step L). The ATR activator topoisomerase-binding protein-1 (TopBP1) is recruited by the loading of the 9-1-1 complex (*34*). This event activates the ATR-CHK1 pathway and initiates DNA repair via HR (*28, 35*). Downstream repair proteins are then recruited, such as BRCA2 and FANCD2, etc. (step M). Through the interaction with BRCA2, Rad51 displaces RPA binding to ssDNA to promote strand invasion, enabling the HR repair (*36-38*) (step N).

1.1.2.3.3 NHEJ in DNA DSB repair

NHEJ is an efficient but considered as 'error-prone' pathway to repair DNA DSBs. It starts with the recognition of the DNA ends by Ku70/80 heterodimer (*39, 40*) (Fig. 1.1, step O). Ku70/80 recruits DNA-PKcs and other DNA repair proteins, such as XRCC4/DNA ligase IV, Artemis and MRN complex (*41-43*) (steps O&P). The molecules of DNA-PKcs at both DNA ends interact, and stimulate the auto-phosphorylation of DNA-PKcs, resulting in its dissociation to allow the binding of

XRCC4 and XLF proteins (*29, 44*). The final step of the repair is completed by the ligation activity of XRCC4/DNA Ligase IV (step Q). In addition, p53 binding protein-1 (53BP1) has been shown to be a downstream target of DNA-PKcs phosphorylation, and to function in the NHEJ pathway (*45*). 53BP1 is recruited to chromatin through its recognition of H2A K15 mono-ubiquitination by RNF168 (*46*) (step R). It is required for the NHEJ pathway, and it is epistatic with Ku proteins for DNA DSB repair in G1 phase (*47, 48*) (step S).

1.1.2.4 Translesion synthesis

TLS is a mechanism that can bypass the DNA lesion in the process of DNA replication, using TLS polymerases, including Rev1, Polξ, Polκ, Polη and Polι (*49*). Compared with normal DNA polymerases, they have a more open active site, which can accommodate bulky DNA templates. Given the intrinsic low fidelity of the specialized DNA polymerases involved, TLS is largely regarded as an 'error-prone' process. Another common feature of TLS polymerases is that most of them contain a PCNA-interacting protein (PIP) motif (*50*). Mono-ubiquitination of PCNA has been shown to be critical for TLS polymerase recruitment (*51*). Two pathways have been proposed to mono-ubiquitinate PCNA at Lys 164, either by Rad6/Rad18 or RNF8 (*52, 53*). Rad6/Rad18 through RPA interaction has been demonstrated to be required for PCNA mono-ubiquitination *in vivo*. The molecular mechanism of TLS is not yet completely understood. Currently, there are two models for the pathway. One is that when the complex of PCNA and replicative polymerase encounter a DNA lesion, the stalled replication fork triggers the mono-ubiquitination of PCNA, and the

polymerase is switched to a TLS polymerase to bypass the lesion. The second model is called 'post-replicative gap-filling' model, where the DNA synthesis is re-initiated downstream of the lesion when the previous synthesis is stalled by the lesion. Then PCNA is ubiquitinated to recruit the TLS polymerase to fill the gap (*49*).

1.1.2.5 DNA inter-strand cross-link (ICL) repair

Some chemical agents can create irreversible covalent linkage binding on DNA strands, causing DNA ICLs. ICLs are extremely toxic DNA leisions, which prevent the separation of DNA double helix, and can result in genome instability during DNA replication if left unrepaired. DNA ICL repair represents the collaboration of different repair pathways, including NER, TLS, and DSB repair pathways (HR and possibly NHEJ). Fanconi anemia patients are defective in repairing this type of DNA damage, and the ICL repair pathway is also known as the Fanconi anemia pathway. The details of the disease and the ICL repair pathway will be introduced in the following section (1.1.3).

1.1.2.6 Mismatch repair

In contrast to responding to DNA damage, Mismatch repair (MMR) is a proofreading process that corrects mismatches generated during DNA replication. Hereditary non-polyposis colon cancer is the most common form of hereditary colon cancer, and the majority of the mutations from the patients affect two genes that are involved in MMR, MutS protein homolog 2 (MSH2) and

MutL protein homolog 1 (MLH1) (*54*). The protein products of these two genes are essential for MMR. During DNA replication, some errors may be introduced such as base mismatches, insertions and deletions. MMR is required to correct these errors. It is also responsible to remove bases damaged by methylating and alkylating agents, such as methylnitronitrosoguanidine (MNNG). In MMR, the damages are detected by MSH2/MSH6 (also known as MutS-α) heterodimer or MSH2/MSH3 (MutS-β). The detection is stabilized through binding of MLH1-PMS1/PMS2 (MutL). Then the damage is removed by exonuclease I (ExoI), refilled by DNA Polδ and finally the ends are sealed by DNA ligase I (*55*).

1.1.3 Fanconi Anemia and DNA ICL repair

1.1.3.1 Background

Fanconi Anemia (FA) is a human recessive genetic disease. It is a rare genetic disorder and was first described by a Swiss pediatrician, Guido Fanconi. The patients are characterized by notable developmental defects, such as pancytopenia (a reduction of blood cells and platelets), skeletal malformations, hyperpigmentation and short statures (*56*). There is also a high rate of infertility among the FA patients. Patients commonly have an elevated susceptibility to cancer besides developmental defects at an early stage. The cells of FA patients are hypersensitive to DNA cross-linking damage. When treated with DNA cross-linking agents such as diepoxybutane (DEB) and mitomycin C (MMC), FA cells display an increased level of chromosomal breakage, leading to genome instability (*56*). This provides a unique marker for early and accurate diagnosis.

To be able to study a large number of patients with this rare genetic disorder, the International Fanconi Anemia Registry (IFAR) was established in 1982. Patients with one or more clinical features associated with FA, mostly diagnosed with DEB test, were assigned into complementation groups determined by phenotypes using somatic cell fusion method, as FA-A, B, C, D1, D2, etc. up to FA-N (*56*).

Besides DNA cross-linking agents, FA patients are sensitive to other types of DNA damage as well, underlying a complex DNA repair system defect. They are hypersensitive to nitrogen mustard, which alkylates DNA and produces cross-links, and monofunctional alkylating agent, e.g. MNNG (*57, 58*). Other alkylating agents, such as nitrosourea analogs (BCNU, CCNU and MeCCNU) are also toxic to some of the FA cells (*57*). The lymphoblastoid cells from FA complementation group H have increased sensitivity to ethylethane sulfonate (EMS) and methylmethane sulfonate (MMS) (*58*).

FA patient cells are more sensitive to DNA DSBs, caused by X-ray or bleomycin treatment, than normal cells in colony survival assays and micronucleus measurement (*58-60*). A recent study showed that FANCD2 deficient cells are hypersensitive to X-ray, and have a defect in S-phase checkpoint (*61*). Similar to Xeroderma pigmentosum cells, FA complementation group A cells are also sensitive to UV radiation, possibly reflecting a defect in the NER pathway (*58*).

Reactive Oxygen Species (ROS) can cause a large variety of DNA lesions, from base and sugar damage, to DNA breaks and DNA-protein cross-links. Oxygen and

oxidative stress have been suggested to be another factor to increase the sensitivity of FA cells to DNA damage. One study showed that dietary supplements with antioxidants (Tempol) could delay the age of onset of epithelial tumors in FA mouse models to some degree (*62*). Under oxygen tension, some FA cells present a tendency of increased chromosomal aberrations (*63*). Although the FA cells are not sensitive to hydrogen peroxide (H_2O_2) or potassium bromate ($KBrO_3$) which can activate the FA pathway, certain FA deficient cells suffer from S-phase checkpoint defects caused by the treatment (*64*). Recently, aldehydes have been identified as an endogenous genotoxin in Fanconi anemia, as a source of cellular environmental damages (*65*).

Another characteristic of the FA cells is that there is a pronounced G2/M arrest in response to DNA ICLs, although the mechanism is unclear (*66*). Moreover, as bone-marrow failure is one of the clinical markers of Fanconi anemia, its DNA repair defects are linked with stem-cell maintenance as well. Current studies suggest that disrupting the Fanconi anemia pathway leads to dysfunction of the haematopoietic stem cells and progenitor cells (*67*).

1.1.3.2 The FA pathway and FA proteins

Mutations have been identified in 16 genes, and these corresponding proteins are known as the FA proteins (listed in Table 2.2) (*67, 68*). There are also many interacting partners with the FA proteins that have been discovered. However, some of the FA patients have not yet been identified with a specific mutation.

These 16 proteins compose the FA pathway, and mostly known for their function in DNA ICLs repair.

Genes	Pathway and function	Other interacting proteins in FA pathway
FANCA (*69*)	FA core complex	FAAP20 (*70*)
FANCB (*71*)	FA core complex	
FANCC (*72*)	FA core complex	
FANCE (*73*)	FA core complex	
FANCF (*74*)	FA core complex	
FANCG (*75*)	FA core complex	
FANCL (*76*)	FA core complex, E3 ubiquitin ligase	Ube2t (*77*)
FANCM (*78*)	FA core complex	FAAP24 (*79*)
FANCD2 (*80*)	FA key marker protein	FAN1 (*81*)
FANCI (*82*)	FA key marker protein	FAN1
FANCD1 (*83*) (BRCA2)	FA, HR, loading RAD51 onto DNA	BRCA1
FANCJ (*84*) (BRIP1)	FA, HR, 3' to 5' helicase	BLM (*85*), BRCA1
FANCN (*86*) (PALB2)	FA, HR, promoting BRCA2 function	
FANCO (*87*) (RAD51C)	HR	
FANCP (*88*) (SLX4)	FA, Coordinating nucleases	XPF-ERCC1, MUS81-EME1, SLX1 (*89-91*)
XPF (*92*) (ERCC4)	NER, FA, nuclease	SLX4, ERCC1

Table 1.2 List of FA proteins, their function and interacting partners in the FA pathway.

FANCA-C, E-G, L and M compose the FA core complex, and FANCD2 and FANCI form an independent complex (*93*). Upon DNA damage, the core complex, which contains an E3 ubiquitin ligase FANCL, and accessory proteins such as FAAP20

and FAAP24, mono-ubiquitinate FANCD2 (*77, 94*) and FANCI (*93*). Failure in FANCD2/FANCI ubiquitination results in mis-localization of the complex and the defect in the repair process. The ubiquitinated heterodimer of FANCI/FANCD2 is then loaded onto chromatin, to recruit downstream repair proteins (*95*).

The structure of the mouse FANCD2/FANCI complex has been resolved, which overall reveals a pair of inverted saxophone-like shapes (*96*). Both FANCD2 and FANCI monomer and the heterodimer have been previously reported to possess some DNA binding activity, although whether they interact with DNA ICLs remains unclear (*96-98*). The phosphorylation of FANCD2 and FANCI is critical for DNA damage response, and is considered as the very first step of the FA pathway (*99, 100*). ATR has been proposed to be the acting kinase for the phosphorylation of both proteins (*99, 101*). However, the mechanisms of how the DNA ICLs are detected and the FA pathway is triggered are still not fully understood.

The repair of DNA ICLs by the FA pathway is generally believed to be DNA replication dependent, and the process is illustrated in Fig. 1.2 (*95*). As the replication proceeds, the ICL is detected through an unidentified mechanism, and FANCD2/FANCI heterodimer is activated by ubiquitination. This leads to the stall of replication fork before it reaches the ICL (Fig. 1.2, step B) (*67, 95*). One of the leading strand approaches to the site of damage and pauses again at -1nt position (step C). Then on the opposite parental strand, the ICL is incised by nucleases XPF, MUS81 and SLX1, coordinated by SLX4 serving as a scaffold protein (step D). Recent studies showed that FAN1 and SNM1A were important

for the ICL processing after the incision, although the mechanism is still under discussion (*102*). TLS polymerases are required to complete the leading strand synthesis bypassing the lesion (step E). The last step to resolve the damage involves NER and HR pathways, and the remaining FA proteins such as FANCD1 (BRCA2), FANCJ (BRIP1), FANCN (PALB2) and Rad51C are required.

1.1.3.3 The relationship between the FA and other DNA repair pathways

As described previously, resolving DNA ICLs requires the participation of several other signaling and repair pathways. For instance, SLX4 coordinates several nucleases to incise the cross-linked nucleotide, and the TLS pathway is responsible for filling the gap afterwards. In addition, the FA pathway acts together with ATR-dependent S phase checkpoint activation. In response to ICLs, the ATR-ATRIP complex phosphorylates NBS1 and CHK1 independently for S phase checkpoing activation. The complex also phosphorylates FANCD2 and FANCI, and the MRN complex re-localizes in response to MMC when the intact FA core complex is present (*103*). It is found that the FA deficient cells display a checkpoint defect similar to NBS1 or CHK1 deficient cells. Current data suggest that ubiquitinated FANCD2/FANCI participates in the ATR-NBS1-dependent checkpoint activation (*99*).

Fig. 1.2

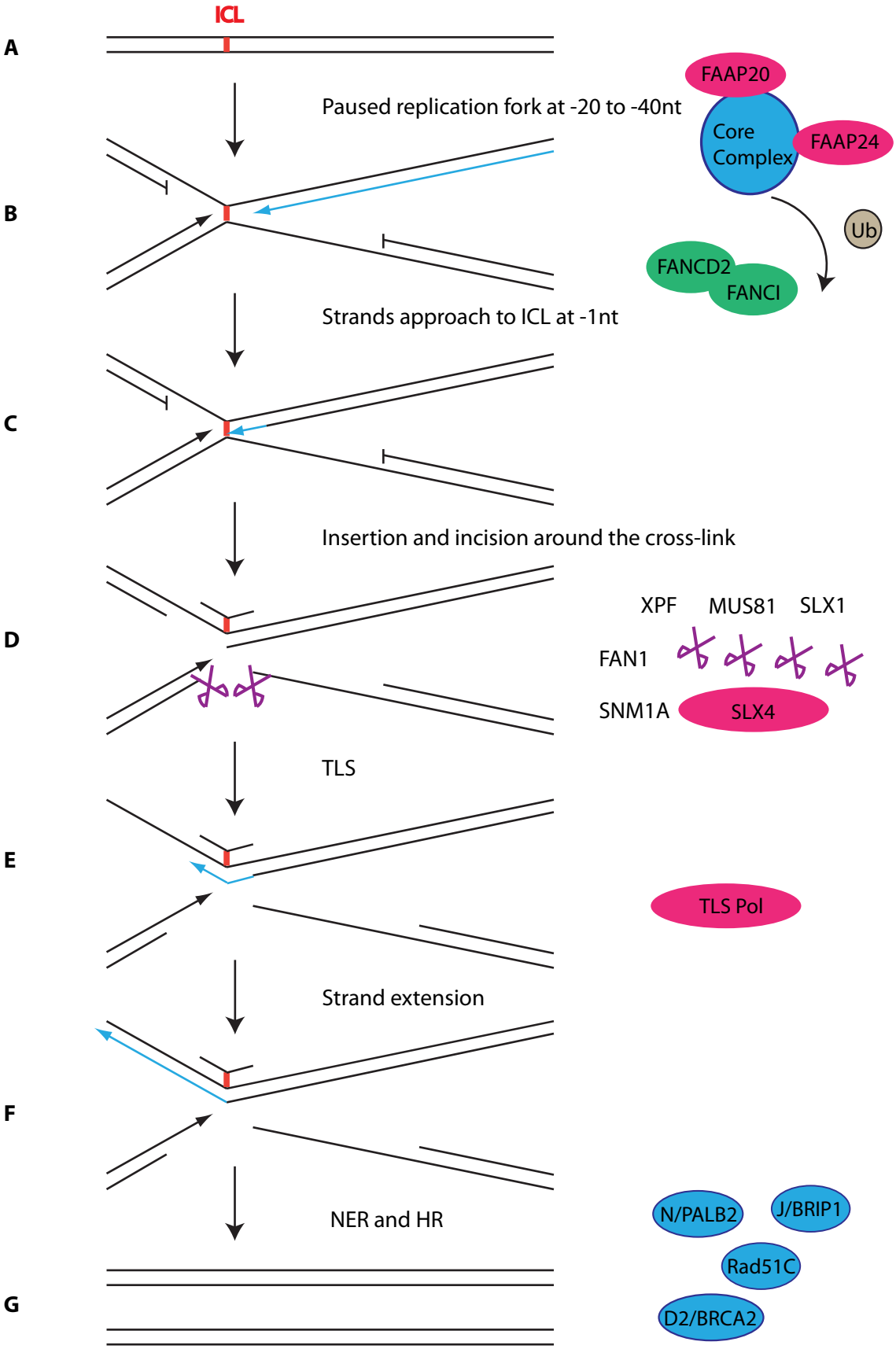

FIG. 1.2 **Schematic diagram shows the process of DNA ICL repair during DNA replication and the proteins participate in different steps. The illustration is adapted based on Knipscheer *et al.*, 2009 (95).**

The FA and BRCA pathways have long been studied for their function together in ICLs repair. FANCD1 is identical with BRCA2. From genetic studies, 18% of primary ovarian tumors have defective FANCD2 ubiquitination, and some have deficiency in certain FA proteins expression, whereas several FA patient-derived cell lines express mutations of BRCA2 (*83, 104*). Both FANCD2 and BRCA2 response to various types of DNA damage, including ICLs and DSBs. They co-localize in DNA damage-induced nuclear foci and pull-down assays have demonstrated their interaction (*105*). FANCD2 also participates in other DNA repair pathways. For example, it is mono-ubiquitinated under DNA replication stress and it is required for BRCA2 nuclear association in response to DSBs caused by IR (*106*). Moreover, it has been shown that besides promoting HR towards downstream function in the ICL repair, BRCA1 also facilitates the FANCD2 ubiquitination and localization in response to IR, possibly through its interaction with FANCD2 (*107, 108*).

It has been suggested that the FA pathway is important to promote HR over NHEJ in the cells to repair DNA damage. In fact, there is a speculation that NHEJ-mediated repair in the absence of the FA pathway causes the gross chromosomal abnormalities in FA deficient cells (*67*). It is believed that HR antagonizes NHEJ repair to some degree, especially in the repair of DNA DSBs during replication (*109*). FANCD2 has been shown to suppress the accumulation of DNA-PKcs at the stalled replication fork created by HU and MMC but not at DSBs created by IR (*110*). This suggests that the FA pathway promotes repair towards HR to preserve a high fidelity to the original DNA template during replication. Indeed, the reduction of NHEJ proteins such as Ku70/Ku80 and DNA-PKcs enhances HR

activity and partially rescue FA defect in DNA ICLs repair in HeLa and DT40 cells (*110, 111*). But in mouse embryonic fibroblasts, the depletion of NHEJ factors, such as 53BP1 and Ku80 in FANCD2 deficient cells exacerbates the genome instability, and the double knockout of Ku80 and FANCD2 is embryonic lethal (*108*). This indicates that FANCD2 provides additional functions during development that cannot be compensate by NHEJ factors.

However, whether DNA ICLs repair is strictly dependent of DNA replication is still controversial. For example, the recruitment of FANCJ/BACH1, and HR related FANCD1/RCA2 and FANCN/PALB2, is highly induced by DNA replication, but the core complex and FANCD2 can be recruited independently of DNA replication (*112*). Some research shows that ICLs can also be repaired independently of DNA replication (*112*).

Additionally, FANCD2 has been found to interact with MMR protein, MSH2, and the loss of MSH2 sensitizes cells to different types of DNA damages, including ICLs (*113*). Another example of the FA proteins collaboration with other pathways is the relationship with the Bloom syndrome protein (BLM) helicase. Mutations of the BLM helicase have been identified in Bloom syndrome, which is an autosomal recessive disease, characterized by growth retardation, immunodeficiency, UV sensitivity and cancer predisposition. BLM can unwind a variety of DNA structures. Together with DNA topoisomerase IIIα and other interacting proteins, it is able to remove the double Holliday junctions (HJ) which are formed during homologous recombination (*114*). FANCJ interacts with BLM helicase, and the disruption of the interaction results in hypersensitivity to DNA

replication stress (*85*). It was later discovered that FANCD2 is required for the full BLM complex assembly, and FANCD2 acts together with BLM to regulate replication restart and to suppress new origin firings (*115*). Overall, the FA pathway has emerged as a central player that is entwined with the DDR, and is engaged in almost all other classic repair pathways to preserve genomic integrity.

1.1.3.4 The existing questions in the FA pathway

With years of the advance in studies of the FA pathway, there are still many aspects of it that have not been understood thoroughly. For instance, although the importance of the ubiquitination of FANCD2 and FANCI has been well documented, the mechanistic consequence of the modification is still undiscovered. Also, the exact timing, order, and mechanism of some of the proteins' participation in the FA pathway are yet to be elucidated. Another pressing question is how the FA pathway is initiated, and in particular, how the DNA ICLs are detected. The discovery of such sensors of the damage is likely to bring us closer to understanding the assembly of the downstream repair pathway, and the interaction between different steps in the pathway.

We studied the DNA binding activity of two existing FA proteins, FANCD2 and FANCI. However, based on data from our DNA binding assay, the heterodimer did not seem to be a strong candidate for the recognition of DNA ICLs. Therefore, we designed a nuclear protein purification system, to isolate and identify proteins that could directly recognize DNA ICLs from human cells. The analysis

of our purification products identified that ubiquitin-like PHD and RING finger domain-containing protein 1 (UHRF1) may be the damage sensor that we had been searching for.

1.2 UHRF1 background

1.2.1 UHRF1 and its association with heterochromatin

Ubiquitin-like, containing PHD and RING finger domains protein 1 (UHRF1) is an 806aa protein, containing an N-terminal ubiquitin-like domain (UBL), a Tandem Tudor domain (TTD), a Plant-homeo domain (PHD), a SET and RING finger associated (SRA) domain, and a RING finger motif (Fig.1.3A). It is also known as ICBP90, and Np95 in mouse. It is mostly nuclear associated, and is most expressed in proliferating cells (*116*). In these cells, UHRF1 co-localize with PCNA, and the foci pattern is not altered by the presence of DNA DSBs (*117, 118*). UHRF1 has first been identified as an inverted CCAAT box binding factor in the topoisomerase IIα (TopoIIα) promoter and may regulate its expression (*119*). TopoIIα can cut both strands of DNA and separate the entangled daughter strand during replication. Studies have suggested that the expression of UHRF1 is regulated by cell cycle in non-cancerous cells, and coincides with TopoIIα expression (*120*). But in several cancer cell lines, the overall level of UHRF1 tends to be up-regulated and does not change with cell cycle progression (*118, 120*). In some cell lines, UHRF1 is related to the contact inhibition for the cell growth (*121*). One recent study with Xenopus egg extract even suggested that

UHRF1 is directly required for replication, although data from other research groups indicates that depletion of UHRF1 does not change the progression of DNA replication (*122, 123*).

UHRF1 is shown to be closely associated with heterochromatin activities, through its interaction with multiple histone modification markers. It binds histones, to H3 with the highest affinity, compared with H1, H2A and H2B (*124*). Proteins bearing the RING finger motif have long been reported with E3 ubiquitin ligase activity. *In vitro* auto-ubiquitination assay indicates that its RING domain carries E3 ligase activity, and it seems to undergo auto-ubiquitination during DNA replication in Xenopus egg extracts (*122, 124*). *In vivo* co-immuno-precipitation experiment suggests that UHRF1 can ubiquitinate histones, and H3 ubiquitination is observed from *in vitro* ubiquitination assay (*124, 125*). Reduction of UHRF1 leads to an increased level of histone H4 acetylation and a reduction in pericentromeric heterochromatin replication (*126*). It was later discovered that the reduction of UHRF1 caused a diffused pattern of the heterochromatin formation (*127*). Both TTD and PHD domains, and possibly SRA domain as well, are important for UHRF1 recognition of H3 Lys 9 di-and tri-methylation. However, whether it regulates heterochromatin formation through its interaction with H3K9 methylation remains a dispute (*125, 127-129*). It has been hypothesized that UHRF1 may have a role in regulating the opening and the stabilization of the dense chromatin structure during its replication.

Fig. 1.3

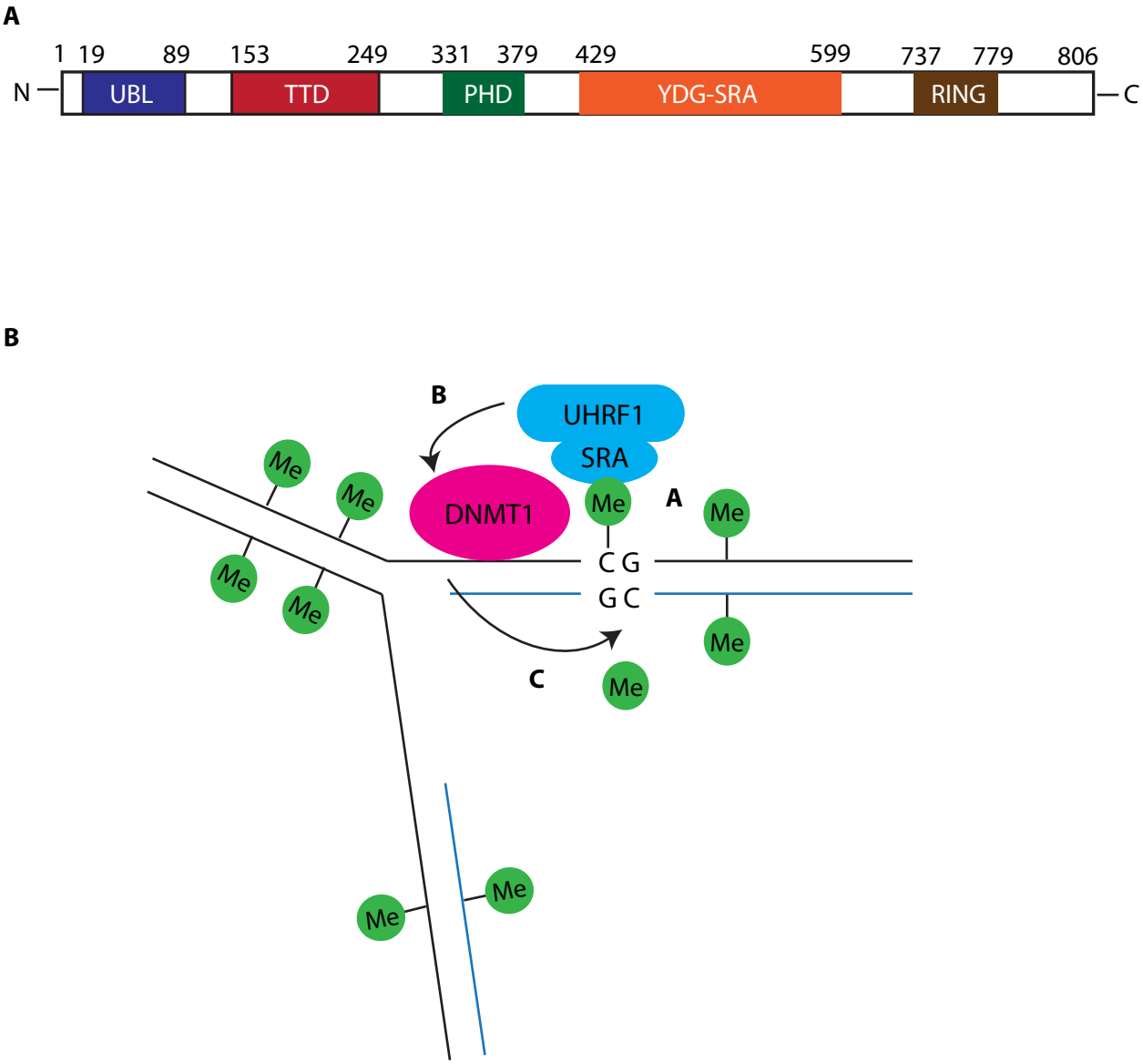

FIG. 1.3 **UHRF1 and its role in DNA methylation maintenance. A.** Schematic diagram shows different domains of UHRF1, including UBL, TTD, PHD, SRA and RING domains, and their coordinates; **B.** Schematic diagram shows UHRF1 recognizes hemi-methylated DNA through its SRA domain (step A) and recruit DNMT1 (step B) to methylate the opposite strand (step C) for the methylation maintenance during DNA replication.

1.2.2 UHRF1 in DNA methylation maintenance

There has been much focus on UHRF1's function in maintaining DNA methylation, and its involvement in epigenetic regulation. DNA methylation is critical in epigenetic gene silencing and the maintenance of genome stability. In vertebrates, the genomic DNA is almost exclusively methylated at CpG dinucleotides. CpG methylation is involved in various physiological processes, including embryogenesis, genome imprinting, etc. (*130*). UHRF1 was first discovered to recognize fully methylated DNA, and was recruited to several methylated promoter region (*121*). Later, from mESC works, UHRF1 was found to bind hemi-methylated DNA and the loss of UHRF1 greatly reduces genomic DNA methylation status (*131*). It is proposed that UHRF1's role in DNA methylation is probably achieved through its interaction with DNMT1. DNMT1, together with DNMT3a and DNMT3b, are the three important DNA methyl-transferases. DNMT1 methylates already hemi-methylated DNA alongside DNA replication, whereas DNMT3a and 3b are required for *de novo* DNA methylation (*132, 133*). UHRF1 has an impact in development as well. *Uhrf1* knockout is embryonic lethal in mice, and mutations in zebrafish also result in liver developmental defects and failure in liver-regeneration (*134, 135*).

The interaction of UHRF1 with DNMT1 is subsequently confirmed in human cells and it is endowed by UHRF1's SRA domain (*136*). The SRA domain has also been found in DNA methyltransferases in plants, such as SUVH5 (*137*). It is responsible for methyl-cytosine binding, and the SRA domain of UHRF1 binds to hemi-methylated DNA (*138-140*). It functions as an anchor of UHRF1 during

replication (Fig. 1.3, step A), and recruits DNMT1 (step B) to methylate the other strand (step C) (*141*). The crystal structure of a globular, saddle-like SRA domain of UHRF1 has been solved (*139, 140*), showing that the conserved residues in the SRA domain contribute to a positively charged nucleotide-binding site (Fig. 1.4A, the DNA binding pocket is marked in green). The DNA is bound to this inner surface, and the side chains of Arg 469 and Val 451 form van der Waals contacts to penetrate the center of the DNA helix (Fig. 1.4B, residues marked in red, V451, and magenta, R496). The methylated cytosine is then flipped out, and Val 451 occupies the original space of the nucleotide (Fig. 1.4, residue marked in red). The flipped-out methylated-cytosine is bound in a hydrophobic patch formed between two tyrosines (Fig. 1.4B, residues marked in cyan). The methylation of the cytosine on the other strand can cause a steric clash at the binding site and may explain the reduction of the binding of SRA domain to fully methylated DNA (*139*). Depletion of UHRF1 during DNA replication does not alter the localization of PCNA, but prevents the association of DNMT1 with chromatin, and causes hypomethylation of many genes (*131, 141*).

1.2.3 Potential UHRF1 function beyond DNA methylation

UHRF1 is highly conserved across different vertebrates. The species with conserved UHRF1 are listed below.

Fig. 1.4

A

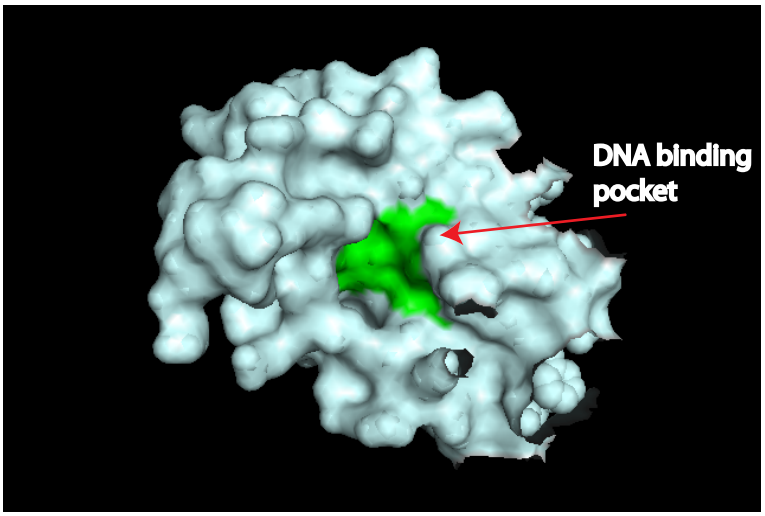

B

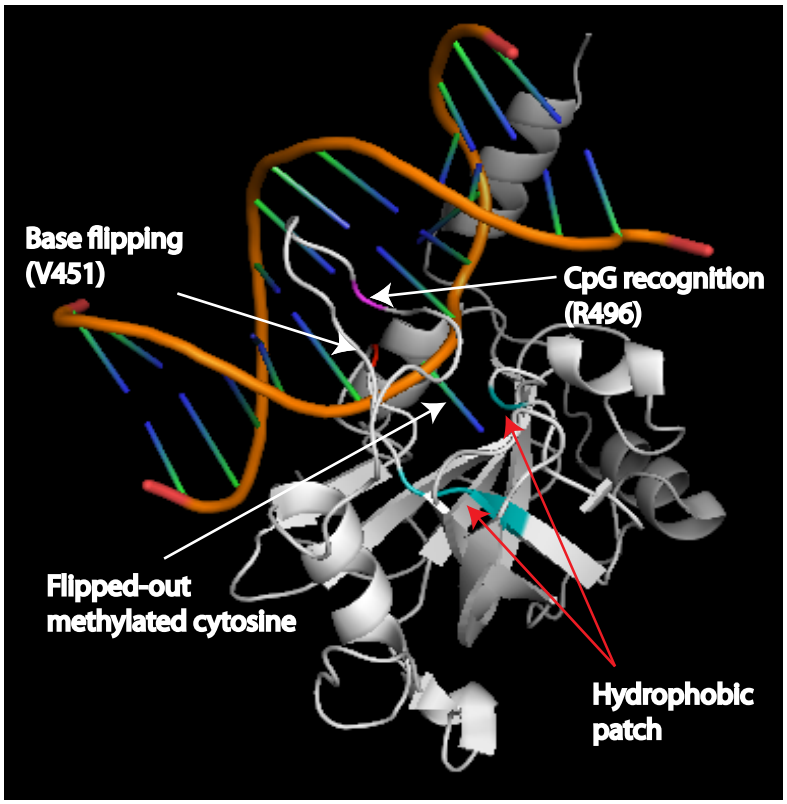

FIG. 1.4 **Structure of SRA domain and the SRA-DNA complex (images captured from the crystal stucture published in Protein Data Bank, and figures generated using PyMOL). A.** The surface illustration of the SRA domain from mouse (PDB ref. 2ZKG, isolated from the crystal structure of a tetramer). The conserved residues contributed to a negative-charged pocket (marked in green); **B.** The structure of the SRA domain bound to hemi-methylated DNA (PDB ref. 2ZO0). The side chains of R496 (marked in magentas) and V451 (marked in red) penetrate the centre of the DNA helix. The methylated cytosine is flipped out (marked with the arrow), and bound in a hydrophobic patch (marked in cyan).

Species	Latin	Coverage	Identical	CpG-me	FA Pathway
Human	*Homo sapiens*	100%	100%	+	+
Chimpanzee (predicted)	*Pan paniscus*	100%	99%	+	+
Cow	*Bos taurus*	98%	84%	+	+
Rat	*Rattus norvegicus*	99%	75%	+	+
Mouse	*Mus musculus*	98%	75%	+	+
Chinese hamster	*Cricetulus griseus*	98%	74%	+	+
Bat	*Myotis brandtill*	98%	74%	+	+
Sea turtle	*Chelonia mydas*	98%	74%	+	+
Frog	*Xenopus laevis*	98%	66%	+	+
Zebrafish	*Danio rerio*	98%	66%	+	+
Chicken	*Gallus gallus*	94%	64%	+	+

Table 1.3 Conservation of UHRF1 across species.

It has been discovered that the CpG methylation is nearly absent in lower species, for example, in *Drosophila melanogaster*, especially in adult flies, and the nucleotide sites of DNA methylation are significantly different from vertebrates (*142, 143*). In yeast and bacteria, cytosine methylation can only be found in RNA (*144*). UHRF1 is not present in these lower species, which coincides with the absence of CpG DNA methylation, suggesting that full length UHRF1 protein plays a conserved role in eukaryotic methylation (*145*). However, certain domains of the protein can be found in these organisms. For example, *Drosophila melanogaster* has small-sized proteins that are about 40% identical with human UBL, PHD, SRA and RING domains, respectively, some proteins in *Caenorhabditis elegans* are about 30% conserved compared to these four domains in human, and *Saccharomyces cerevisiae* has 20-30% conservation. There is a possibility that in these species, the smaller proteins may be homologues to the different

domains of UHRF1, which might potentially coordinate with each other, and perform a similar function as UHRF1 in higher species. While DNA CpG methylation is absent in these species, the presence of almost all the UHRF1 domains may hint for other functions in the cells.

1.2.4 UHRF1 in DNA repair

UHRF1 is shown to be required for the cellular response to different types of DNA damage. Depletion of the protein causes hyper-sensitivity to DSBs inducing agents, such as γ-irradiation; and hydroxyurea, which causes replication arrest that can transform into DSB; oxidative stress caused by base damaging agents, such as X-ray and UV light (*134, 146, 147*); as well as an increased frequency of chromosomal aberrations (*147*). It is recruited to the sites of damage in UV laser test (*148*). The increased level of UHRF1 seems to be common in cancer cells, and it has been proposed to be a diagnostic marker for several types of cancer, e.g. pancreatic cancer (*149*). There are a couple of mechanisms of UHRF1 function in DNA repair that have been suggested, but most of the studies still remain at observatory level. One study shows that in breast cancer cells, the up-regulation of UHRF1 expression is associated with BRCA1 down-regulation (*150*). It is found that the CCAAT box located in the BRCA1 promoter region is necessary for the relationship. Also, in these cells, there is an increase of H3 Lys 9 di-methylation (H3K9me2), but a decrease of H3 Lys 4 tri-methylation (H3K4me3) in the promoter region of BRCA1. Since UHRF1 has a much higher affinity to H3K9me2 than H3K4me3, it enables UHRF1 to bind to this region, and to suppress BRCA1 expression (*150, 151*).

In addition, it has been demonstrated that UHRF1 can be co-immuno-precipitated with Eme1, and it co-localizes with Eme1 following DNA DSBs created by camptothecin (*152*). The RING domain of UHRF1 has been proposed to be required for its function in response to different types of DNA damage (*153*). However, whether it is realized through its enzymatic activity remains unclear. For instance, UHRF1 RING domain mutant expression causes mis-localization of Eme1, but does not change the overall amount of Eme1 ubiquitination (*152*). Hence, insights into a well-defined mechanism of UHRF1 promoting DNA damage repair will be very important for developing novel cancer therapeutic targeting approaches.

1.3 Functional study of UHRF1 in the FA pathway

In the current model of the FA pathway, how the pathway is activated and what the sensor of the DNA ICL damage is remain unknown. Hence, we aimed to investigate if any human nuclear protein can detect the DNA ICL structure directly, as well as whether and how it is involved in the FA pathway. We examined the DNA binding activity of two key players in the pathway, FANCD2 and FANCI, and found that they did not have a specific interaction with DNA ICLs. Then we used a biochemical purification strategy to isolate nuclear protein(s) from HeLa cells that could recognize ICL DNA. UHRF1 was identified from our purification by mass-spectrometry.

To confirm that UHRF1 recognized DNA ICLs directly, we expressed and purified human UHRF1, and performed *in vitro* DNA binding assays. Data from these experiments showed that the UHRF1 directly interacts with DNA ICLs and has a higher binding activity to cross-linked DNA than non-cross-linked DNA. We then introduced KD of UHRF1 in several cell lines and found that UHRF1 was required for cells to tolerate ICL damage. By using epistasis analysis, we discovered that UHRF1 was epistatic with FANCD2, and participated in the FA pathway in response to MMC. To understand the function of UHRF1 in the FA pathway, we conducted a series of *in vivo* experiments to study the effect of UHRF1 KD on the activation of the FA pathway, i.e. the ubiquitination and recruitment of FANCD2 after DNA damage. We demonstrated that the main role of UHRF1 in response to DNA ICLs was to facilitate the localization of FANCD2 to the sites of damage, but not the ubiquitination.

To study the mechanism of the involvement of UHRF1 in the FA pathway, we also identified the domain that was required for the DNA binding activity of the protein, and showed that the mutation of the SRA domain caused the increased cell sensitivity and the defects in FANCD2 localization in response to MMC. Therefore, we propose that UHRF1 can function as a DNA ICL sensing protein. It is likely to recognize the damage in the cells, and participate in the FA pathway by recruiting FANCD2 to the sites of DNA damage.

Chapter 2 Materials and methods

2.1 Materials

2.1.1 DNA substrates and shRNA sequences

Name	Sequence
ICL1*	CTCTC GTCTG **T**ACAC CGAAG A
ICL2	GTCTG CTCGA GTCGA GTCGC TCTCG TCTG**T** ACACC GAAGA CTCGA CTGCA CTGCA GACTC
ICL3	GTCTG CTCGA GTCGA G**T**AGC TCTCG TCTG**T** ACACC GAAGC **T**ACGA CTGCA CGC**T**A GACTC
ICL4	CGCGAGAGCG CCAACAACCG CTTCTTGGTC GAAGGCAGCA AGCGCGATGA ATGTCT**T**ACT ACGGAGCAAG TTCCCGAGG**T** AATCGGAGTC CGGCTGATGT TGGGAG**T**AGG TGGC**T**ACGTC TCCGAACTCA CGACCGAAAA GATCAAGAGC AGCCCGCATG GATTTGACTT GGTCAGGGCC GAGCC**T**ACAT GTGCGAATGA TGCCCA**T**ACT TGAGCCACC**T** AACTTTGTTT **T**AGGGCGACT GCCCTGCTGC G**T**AACATCGT TGCTGCTGCG **T**AACATCGTT GCTGCTCCAT AACATCAAAC ATCGACCCAC GGCG**T**AACGC GCTTGCTGCT TGGATGCCCG AGGCA**T**AGAC TG**T**ACAAAAA AACAGTCA**T**A ACAAGCCATG AAAACCGCCA CTGCGCCGT**T** ACCACCGCTG CGTTCGGTCA AGGTTCTGGA CCAGTTGCGT GAGCGCA**T**AC GCTACTTGCA T**T**ACAGTT**T**A CGAACCGAAC AGGCT**T**ATGT CAACTGGGTT
ICL5	CGCGAGAGCG CCAACAACCG CTTCTTGGTC GAAGGCAGCA AGCGCGATGA ATGTCT**T**ACT ACGGAGCAAG TTCCCGAGG**T** AATCGGAGTC CGGCTGATGT TGGGAG**T**AGG TGGC**T**ACGTC TCCGAACTCA CGACCG
ICL8	CTCTC TGTC**T** AGTGA AAGAC G
CpG3	CTCTC TGTCC GGTGA AAGAC G

CpG3-me**	CTCTC TGTCC GGTGA AAGAC G
HJ1	CCGTA CCAGT GATCA CCAAT GGATT GCTAG GACAT CTTTG CCCAC CTGCA GGTTC ACCC
HJ2	GGGTG AACCT GCAGG TGGGC AAAGA TGTCC TAGCA ATCCA TTGTC TGTGA CGTCG AGCTC
HJ3	GAGCT CGACG TCACA GACAA TGGAT TGCTA GGACA TCTTT GCCGT CTTGT CAATA TCGGC
HJ4	GCCGA TATTG ACAAG ACGGC AAAGA TGTCC TAGCA ATCCA TTGGT GATCA CTGGT AGCGG
dsDNA (plus)	TTGATAAGAG GTCATTTGAA TTCATGGCTT AGAGCTTAAT TGCTGAATCT GGTGCTGGGA TCCAACATGT TTTAAATATG
ssDNA	TTGATAAGAG GTCATTTGAA TTCATGGCTT AGAGCTTAAT TGCTGAATCT GGTGCTGGGA TCCAACATGT TTTAAATATG
3'-OH	Plus: TTGATAAGAG GTCATTTGAA TTCATGGCTT AGAGCTTAAT TGCTGAATCT GGTGCTGGGA TCCAACATGT TTTAAATATG Minus: ATTAAGCTCT AAGCCATGAA TTCAAATGAC CTCTTATCAA
5'-OH	Plus: TTGATAAGAG GTCATTTGAA TTCATGGCTT AGAGCTTAAT TGCTGAATCT GGTGCTGGGA TCCAACATGT TTTAAATATG Minus: CATATTTAAA ACATGTTGGA TCCCAGCACC AGATTCAGCA
Y-fork	Plus: TTGATAAGAG GTCATTTGAA TTCATGGCTT AGAGCTTAAT TGCTGAATCT GGTGCTGGGA TCCAACATGT TTTAAATATG Minus: CATATTTAAA ACATGTTGGA TCCCAGCACC AGATTCAGCA TACGTTACCG ATCGTACGTT CGATGCTGGC TACTGCTAGC

Table.2.1 Sequences of DNA substrates used in this paper (only showing the plus strand, 5'-3', unless indicated otherwise). *the sites of cross-links are indicated in bold; **the methylated cytosine is marked with underline.

Name	Targeted Sequence	Note
sh2	AGATA TAACG TTAGG GTTT	This target sequence is also used for shUHRF1 in the inducible pSuperior.TetR vector and in the FA patient-derived cell lines
sh3	AGGAG ACGTT CCAGT GTAT	

Table.2.2 Targeted sequences for UHRF1 KD used in this study.

2.1.2 Antibodies

Antibody	Catelogue No.	Company
Primary		
HA (12CA5)	11583816001	Roche
UHRF1 (H8)	sc-373	Santa Cruz
FANCD2 (FI17)	sc-20022	Santa Cruz
α-Tubulin (DM1A)	5829	Millipore
BRCA1 (D9)	sc-6954	Santa Cruz
Lamin B	sc-6216	Santa Cruz
H3	Ab12079-100	Abcam
53BP1	MAB3802	Millipore
Penta(5X)-His	34660	Qiagen
Secondary		
α-mouse (HRP-conjugated)	NA9310V	GE Healthcare
α-rabbit (HRP-conjugated)	NA934V	GE Healthcare
α-goat (HRP-conjugated)	sc-2768	Santa Cruz
α-mouse (Alexa Fluor 488)	A21202	Life Technologies Inc.
α-rabbit (Alexa Fluor 568)	A11036	Invitrogen

Table. 2.2 List of antibodies used in this study.

DNA-PKcs antibody is a kind gift from Dr. Nicholas Lakin, University of Oxford.

Horseradish peroxidase (HRP)-conjugated secondary antibodies were used for Western blot, and the substrate was visualized by the enhanced chemiluminescence HRP substrate (Western Lightning Plus ECL, PerkinElmer). Alexa Fluor secondary antibodies were used for immuno-fluorescence microscopy.

2.2 Methods

2.2.1 Preparation of DNA substrates

ICL DNA: Two strands were annealed and were 5'-end radioactive labeled with [γ-^{32}P] ATP by T4 polynucleotide kinase (New England Biolabs). Psoralen (Trioxsalen, Sigma)/UVA cross-linking induction was described previously (*154*). The reaction was carried out with 10 μg/ml DNA in buffer containing 10 mM Tris, pH 7.6, 1 mM EDTA, 50 mM NaCl and 100 μg/ml of Trioxsalen (saturated Trioxsalen solution was prepared at 1 mg/ml in ethanol). After a 2 min incubation to allow for the equilibration of the Trioxsalen intercalation, DNA was irradiated on ice for 2 hr with a light intensity at 365 nm of 4000 μW/cm^2 using SpectroLinker XL-1500 UV Crosslinker. Subsequent additions of 1% saturated ethanol solutions of Trioxsalen were made at 15 min intervals; and the samples were equilibrated for 2 min before continuing the irradiation. The

cross-linking efficiency was confirmed by 20% 8 M Urea denaturing polyacrymide gel and 1% alkaline agarose gel (*155*).

HJ was made of synthesized HJ1, 2, 3 and 4, using the following steps: the single strands were annealed in 1x SSC buffer (15 mM Na-citrate at pH 7.0, 150 mM NaCl), at 95°C for 2min and 10min for each sequential step at 65°C, 37°C, 25°C, and 0°C. The HJ substrate was purified in a 2% agarose gel followed by gel extraction (Qiaquick Gel extraction kit, Qiagen). The HJ structure was then 5'-end radioactive labeled using [γ-^{32}P] ATP by T4 polynucleotide kinase (New England Biolabs).

2.2.2 Electrophoretic mobility shift assay (EMSA) and quantification

Binding reactions were composed of recombinant proteins as described in the figures, and 100counts-per-second radioactive DNA substrate in a volume of 10 μl. Reaction buffer contained 5 mM Tris, pH 7.9, 30 mM KCl, 1 mM dithiothreitol (DTT), 10 mM Hepes-KOH pH 7.9, 1 mM EDTA, 5% glycerol, 0.3 mg/ml bovine serum albumin (BSA, New England Biolabs), and 5 μg/ml salmon sperm DNA. Reactions were pre-incubated without radioactive labeled DNA substrate for 5min, and then incubated with the substrate at 30°C for 15 min. The reaction products were analyzed by electrophoresis on a 4% 0.4x TBE polyacrylamide gel (1x TBE buffer: 0.1 M Tris, 0.1 M Boric acid; 1 mM EDTA, pH 8.0). The gels were dried onto Whatman paper and exposed to either X-ray film or PhosphorImager (imaged and analyzed by FujiFilm FLA-7000).

For EMSA quantification, total amount of free DNA was defined as the intensity of an area S of free DNA probe in the control lane where no protein was added, R_{total} (Fig. 2.1, lane 1). The area S of a shifted band in a lane where the protein was added was selected and the measurement of the intensity was collected, e.g. R_1, R_2, and R_3 (lanes 2-4). An area of the same size as S was selected in the same lane away from the band and the measurement of the intensity was collected as background, e.g. $R_{1'}$, $R_{2'}$ and $R_{3'}$. The control was collected as R_0 and $R_{0'}$ (lane 1). The percentage of protein-bound DNA was calculated as $[(R_{1/2/3}-R_{1'/2'/3'})-(R_0-R_{0'})]/(R_{total}-R_{0'})$.

2.2.3 Cell culture and nuclear extract preparation

HeLa cells were grown in DMEM (D5796, Sigma) supplemented with 2.5% fetal bovine serum (FBS, F7524, Sigma). HeLa S3 cells were grown in cell culture spin flasks (BELLCO, Glass, Inc.) and cultured in CO_2 independent Joklik's medium (adapted from the formulation from Sigma), supplemented with 2.5% FBS, 1x MEM non-essential amino acids (M7145, Sigma), 2 mM L-glutamine (G7513, Sigma) and penicillin (10 unit/ml)/streptomycin (10 μg/ml) (P4333, Sigma). The cells were maintained in a 37°C incubator (SANYO MIR-162). 160 ng/ml Mitomycin C (Sigma, M0440) was used for *in vivo* DNA inter-strand cross-link damage 16 hr prior to nuclear extraction. Nuclear proteins were extracted as described (*156*).

Figure 2.1

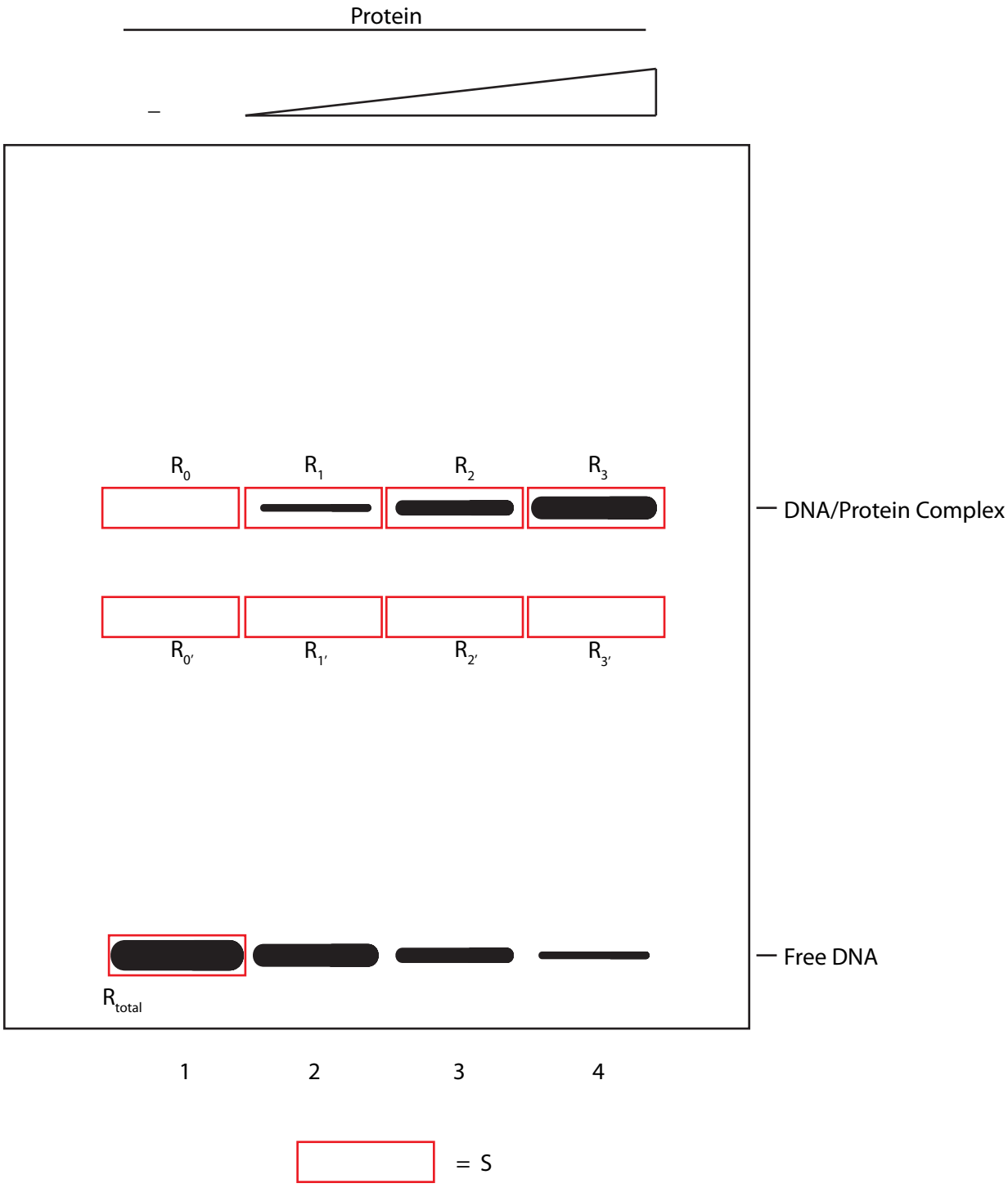

Fig. 2.1 Cartoon illustrating the measurements collected for EMSA quantification.

293T, Phoenix A and FA patient-derived cells were cultured in DMEM, supplemented with 10% FBS. mESCs were cultured in GMEM (G5154, Sigma), supplemented with 15% FBS, 1x MEM non-essential amino acids, 2 mM L-glutamine, 57.2 μM β-mercaptoethanol (M7154, Sigma), penicillin (10 unit/ml)/streptomycin (10 μg/ml) and 10^3 units/ml LIF (ESGRO mLIF, ESG1107, Millipore).

Sf9 insect cells were cultured in Sf-900 II SFM (Gibco, Life Technologies Inc.), and maintained in a 26°C incubator (Innova, Eppendorf) on an orbital shaker platform rotating at 120 rpm. Sf9 culture caps were loosened to allow for oxygenation/aeration. When used for protein purification, cells were plated at $2.4x10^7$/dish in 15 cm tissue culture dishes, and kept for protein expression for 72hr after transduction before harvest.

2.2.4 Nuclear Protein Purification and UHRF1 *in vitro* DNA binding

10μg nuclear extract or 200 ng recombinant UHRF1/FANCL from Sf9 cells were incubated with 25 pmol biotin labeled DNA substrates (ICL1 and ICL1-XL were used for nuclear protein purification; ICL2 and ICL2-XL were used for UHRF1/FANCL *in vitro* binding test). Binding buffer is as described for EMSA. The protein and DNA probe mix was incubated at 30°C for 15 min, and mixed with 10 μl 50% Streptavadin sepharose (GE Healthcare). The matrix with streptavadin beads was washed and proteins were eluted in 20 μl elution buffer (30 mM KCl, 10 mM Hepes-KOH pH7.9, 5 mM Tris-HCl pH7.9, 1.5 mM $MgCl_2$ and 25% glycerol) containing 12 unit benzonase (Sigma). For nuclear protein

purification, after denaturing at 70°C for 10 min, the proteins were analyzed by electrophoresis on 4-12% NuPage Bis-Tris gradient gel (Life Technologies). Gels were silver stained for detection of proteins (Silver Quest staining kit, Invitrogen). For UHRF1 and FANCL *in vitro* DNA binding, the proteins were analyzed by electrophoresis on 10% SDS-PAGE gel followed by Western blot.

2.2.5 Protein expression, purification and site-directed mutagenesis

HA-epitope tagged FANCD2 and monoubiquitinated FANCD2 (FANCD2-Ub) were purified as described (*157*). UHRF1, FANCL, Uba1, UbcH5b and ubiquitin cDNA were cloned from HeLa total RNA, using standard cloning methods (*155*). Flag-HA tagged UHRF1 was expressed in HeLa and FA patient-derived cells using the pOZ-N plasmid (*158*). UHRF1, FANCL, Uba1 and UbcH5b were expressed using the pFastBac vector (Invitrogen) with an engineered Flag and HA tag and purified as described (*157*), and purified from Sf9 cells. 6xHis-tagged ubiquitin was expressed in bacteria BL21 cells using pET28c construct. The expression was induced using 0.5 mM IPTG for 3hrs and purified by affinity chromatography using Ni-NTA agarose (Qiagen). Ubiquitin was cloned and purified by former students Jean Tian and Maarten van der Velden.

To generate the mutants of UHRF1, the pOZ-N-UHRF1 and pFastBac-Flag-HA-UHRF1 were subject to PCR amplification with the primers to incorporate the mutations. PCR products were digested with the methylation sensitive restriction enzyme *Dpn1* to eliminate any original plasmid. UHRF1 mutants

were cloned and purified from Sf9 cells by Chih-Chao Liang (DPhil student in our laboratory).

2.2.6 *In vitro* ubiquitination assay

Ubiquitination reactions were carried out in a buffer containing 30 mM Tris-HCl pH 7.9, 5 mM $MgCl_2$, 100 mM NaCl, 2 mM $ZnSO_4$, 2 mM DTT and 2 mM ATP. Recombinant proteins were added at 0.84 μM of purified UHRF1 protein, 0.33 μM of Uba1, 4.4 μM of UbcH5b, and 147 μM of 6xHis-Ub in 20 μl. The mixture was incubated at 37°C for 1 hr, and the reaction was stopped by the addition of 1x LDS loading buffer (Invitrogen). The reaction mixture was resolved by SDS-PAGE, and visualized by Western blot.

2.2.7 Plasmid transfection and transduction

Constitutive UHRF1 Knock-down (KD) was introduced in 293T cells using pSuper.retro plasmid containing shRNA sequence targeting human UHRF1. Two-plasmid method was used for retroviral packaging of pSuper.retro.shUHRF1 construct, where Gag and Pol are encoded on one plasmid and Env on the other plasmid (*159*). Gag is a polyprotein that comprises the viral nucleoprotein core particle, Pol is the reverse transcriptase that integrates the RNA genome to DNA and Env forms the envelope protein for the virus. Phoenix A cells were cultured and transfected transiently using two-plasmid method for retroviral packaging by FuGENE6 Transfection (12743400, Roche). For one 9 cm tissue culture dish, cells are transfected using 1.5 μg pGag/Pol and 1.5 μg pEnv,

and 3 μg of either pSuper.puro containing shRNA targeting the human UHRF1 (sh2 and sh3), or pOZ-N containing UHRF1 sequence.

After 72 hr, the supernatant containing retroviral particles was collected and sterile filtered using 0.45mm filter (MILLEX.GP, Millipore). HeLa and FA patient-derived cells were transduced using the supernatant with 4 μg/ml polybrene. For pSuper.puro expressing cells, positive cells were selected using 5 μg/ml puromycin (P8833, Sigma). For pOZ-N expressing cells, positive cells were sorted and selected using magnetic beads (goat-anti-mouse, S1431S, New England Biolabs) conjugated with α-IL2 receptor antibody.

293T cells expressing inducible UHRF1 KD pSuperior.TetR construct were generated by transfection using electroporation device: Gene Pulser II (Bio-Rad) connected to the Pulse Controller (Bio-Rad) and Capacitance Extender *Plus* (Bio-Rad). Electroporation was carried out using with 5μg plasmid DNA (250 V, capacitance 750 μF). The KD was induced by the addition of 10 μg/ml doxycylin (Sigma).

For Sf9 cell protein purification, recombinant bacmids were generated using DH10Bac cells transfected with pFastBac plasmids containing cloned protein sequence. Sf9 cells were transfected by bacmids using Cellfectin II (10362-100, Invitrogen). After 48 hr, the supernatant containing baculovirus was collected, sterile filtered and stored as P1 virus. Fresh Sf9 cells were then transduced using P1 virus to generate new virus of a higher titer, i.e. P2 and P3 (150 μl viral supernatant for $2.4x10^7$ cells in 15 cm tissue culture dish). Sf9 cells were finally

transduced using P3 virus for protein expression and purification.

2.2.8 Clonogenic assay

Cells were seeded in 6-well plate at fixed number overnight before being treated with different concentration of MMC. For HeLa and FA patient-derived cells, 500 cells/well were used for 0 and 0.5 ng/ml MMC, 1000 cells/well for 1 and 2 ng/ml and 2000 cells/well for 4 and 8 ng/ml. For 293T and mESCs, 1000 cells/well were used for 0 and 1 ng/ml MMC, 2000 cells/well for 2 and 4 ng/ml and 4000 cells/well for 8 and 16 ng/ml. After the treatment of MMC, cells were kept for growth for 2 weeks. Once cell colonies were formed, they were fixed in solution containing 10% methanol and 10% acetic acid for 10 min at room temperature (RT), and stained with crystal violet solution (10 mg/ml in methanol) for 5 min at RT. After the excess crystal violet was washed away, the numbers of the colonies were counted and the percentage of survived colonies was calculated. The percentage of live colony at 0 ng/ml MMC treatment was normalized as 100%.

2.2.9 Preparation of cell lysate and fractionation

To prepare whole cell lysate for Western blot (WB), the cells were detached using trypsin (0.25% Trypsin-EDTA, T4049, Sigma), and collected in equal volume of the cell pellet of benzonase buffer (2 mM $MgCl_2$; 50 mM Tris, pH8.0; 10% glycerol; 1% Triton X-100, 0.2 mM PMSF and 2 mM β-mercaptoethanol) containing 12.5 units/ml benzonase. The DNA in the cells was digested by using

vortex gently, and incubated on ice for 30 min. The cells were then lysed with the addition of equal volume of 2% SDS to reach a final concentration of 1%. Samples were heated at 95°C degree for 10 min. The protein concentration was calculated by measuring the absorbance of the protein sample and BSA standard at 595 nm using Bradford solution (Bio-Rad Life Science).

To separate cells into cytoplasmic and nuclear fractions, the cells were pre-extracted using twice of the cell pellet volume of CSK solution (10 mM PIPES, pH7.3; 100 mM NaCl; 300 mM sucrose; 1 mM $MgCl_2$; 1 mM EDTA, pH8.0; 1 mM DTT and 1% Triton X-100) and incubated on ice for 5 min. The CSK containing cytoplasmic fraction was collected by centrifugation at 3000 rpm for 5 min. The remaining nuclear pellet was digested in benzonase buffer as described for whole cell lysate.

2.2.10 Immuno-fluorescent (IF) microscopy

10mm cover slips were sterilized using 70% ethanol and put in 24-well plate. Cells were seeded in the wells with the cover slips at 40% confluent and kept overnight with 500 μl medium for experimentation the following day. After the experiment, the medium was removed and the cells were washed once with phosphate buffer saline (PBS). Cells were pre-extracted with cold 1% Triton X-100/PBS on ice for 10 min, and fixed in 4% paraformaldehyde/PBS at room temperature (RT) for 10 min. After washed with PBS, the cells were blocked with 5% BSA/0.1% sodium azide in PBS containing 0.1% Tween-20 (PBS-T) for 1 hr at RT (BSA, A7906, Sigma). Primary antibodies were diluted at 1:100 in 5%

BSA/0.1% sodium azide/PBS-T, and incubated on the cells overnight at 4°C. Secondary antibodies (Alexa Fluor-conjugated 488/568) were diluted at 1:1000 in 5% BSA/0.1% sodium azide/PBS-T, and incubate on the cells for 1 hr at RT. After washed in PBS, the cells were fixed again with 4% paraformaldehyde/PBS for 5 min at RT. Fixing solution was washed away using PBS, and the samples were mounted in Vectra Shield (containing DAPI) on a microscopic slide and sealed with nail polish.

Imaging was carried out using DeltaVision System (Applied Precision) installed with Resolve3D SoftWoRx-Acquire Version 4.0.0. 60x optic objective was selected (Olympus 60x/1.42, PlanApo, N). Fluorescent images were captured by camera (CoolSNAP_HQ / ICX285).

2.2.11 Fluorescence-activated cell sorting (FACS)

Cells were detached using trypsin, and collected in 1 ml cold PBS. The cells were fixed by adding in 100% ethanol slowly by drops on vortex and incubated on ice for 30 min (ethanol final concentration: 50%). Cells were collected by centrifugation at 1000 rpm/min for 5 min and re-suspended for staining in PI/PBS buffer at 37°C for 15 min (50 μg/ml propidium iodide, 0.1% Triton X-100, 5% Glycerol, and 50 μg/ml RNase). Samples were analyzed on flow cytometre FACS Calibur (BD Biosciences).

Chapter 3 FANCD2 and FANCI DNA binding activity

3.1 Introduction

When cells are treated with DNA damage inducing agents, such as MMC and cisplatin, the FANCD2 and FANCI are activated by phosphorylation and ubiquitination (*95, 99*). Then the heterodimer of FANCD2/FANCI is loaded onto chromatin to initiate the downstream repair pathway (*95*). As the two key players in the Fanconi Anemia pathway, FANCD2 and FANCI have been long suspected to interact with DNA and function as a sensor of the damage to activate the pathway. Both FANCD2 and FANCI have been previously reported to possess some DNA binding activity and affinity to certain DNA structure (*96-98*). However, it is unclear whether FANCD2 and FANCI can recognize DNA ICLs directly. Therefore, we aimed to investigate whether FANCD2/FANCI can interact with ICL DNA directly.

We used recombinant FANCD2 and FANCI to conduct EMSA with different DNA structures, including cross-linked DNA. In the lab, we have previously purified flag-HA-tagged FANCD2 and ubiquitinated FANCD2 from HeLa cells (Dr. Martin Cohn), flag-HA-tagged FANCD2 and FANCI monomers, and FANCD2/FANCI complex from Sf9 cells (Chih-Chao Liang). We studied if FANCD2 could recognize ICL directly, and whether ubiquitination or the complex formation with FANCI could enhance the interaction.

3.2 Results

3.2.1 Introducing site-specific DNA ICLs

Psoralens have been widely used for medical purpose, to treat certain skin disorder in combination with UVA. Psoralens are compounds that are formed by linear fusion of a furan ring and a coumarin, giving a tricyclic planar structure. This structure allows it to intercalate between the stacked bases of DNA, and once irradiated with light of wavelength 320nm-400nm, it can form covalent bonds between adjacent pyrimidines in opposite strands of the DNA (*160*). It has been shown that psoralens cross-link 5'-TA site preferentially, 12-fold more efficient than cross-linking 5'-AT site, and barely introduces any change to other sequence combinations (*154*).

We took advantage of photochemistry property of psoralens, and used trioxsalen, a derivative of psoralen, to create site-specific ICLs in the DNA substrates. We designed a pair of substrates containing only one -TA- site in the sequence (Fig. 3.1A). The method to introduce ICLs using psoralen and UVA was based on a published study and adapted as described in chapter 2 (*154*). By using denaturing urea polyacrylamide gel, we could analyze the formation of cross-links, that the uncross-linked DNA substrate would be denatured to single-stranded DNA (Fig. 3.1B, lane 1), whereas the two strands of the cross-linked DNA could not be separated and therefore would give a shift from the single-strand DNA. We optimized the condition using UVA source of 365nm wavelength, with irradiation time up to 2hr. After 15min of UVA activation,

some of the DNA was cross-linked and the migration of the cross-linked DNA was greatly retarded, forming an upper band (Fig. 3.1B, lane 2). As the duration of the activation increased, the population of DNA that was cross-linked also increased, and the majority of the radioactive labeled DNA shifted to the upper band after 120min, with very low level of mono-adduct product (Fig. 3.1B, lanes 3&4). We increased the scale of the reaction and carried out the experiment in a 6-well plate to achieve a more uniformed irradiation surface than in a microcentrifuge tube. The cross-linking efficiency increased to 100% using this set-up (Fig. 3.1C). We also extended the length of the substrate to 60bp with a single cross-linking site, ICL2, and with 4 sites, ICL3. ICL4 and ICL5 are two DNA fragments generated from a plasmid DNA containing 19 and 5 -TA- sites, respectively, mimicking endogenous -TA- sequence occurrence in the genome (Fig. 3.1D). The cross-linking of ICL2, ICL3, ICL4 and ICL5 are analyzed by denaturing agarose gel, which provides a better separation of the larger-sized DNA substrates than the polyacrylamide gel (Fig. 3.1E).

We also designed a 27bp DNA substrate, ICL8, which contains a single -TA- site but with stronger adhesion of the two strands because of the high GC content at the two ends. Similar to the other substrates, using this method, we could cross-link ICL8 at approximate 100% efficiency as well, and on a native polyacrylamide gel, we excised the corresponding bands and purified the radioactive labeled DNA substrates (Fig. 3.1F).

Figure 3.1

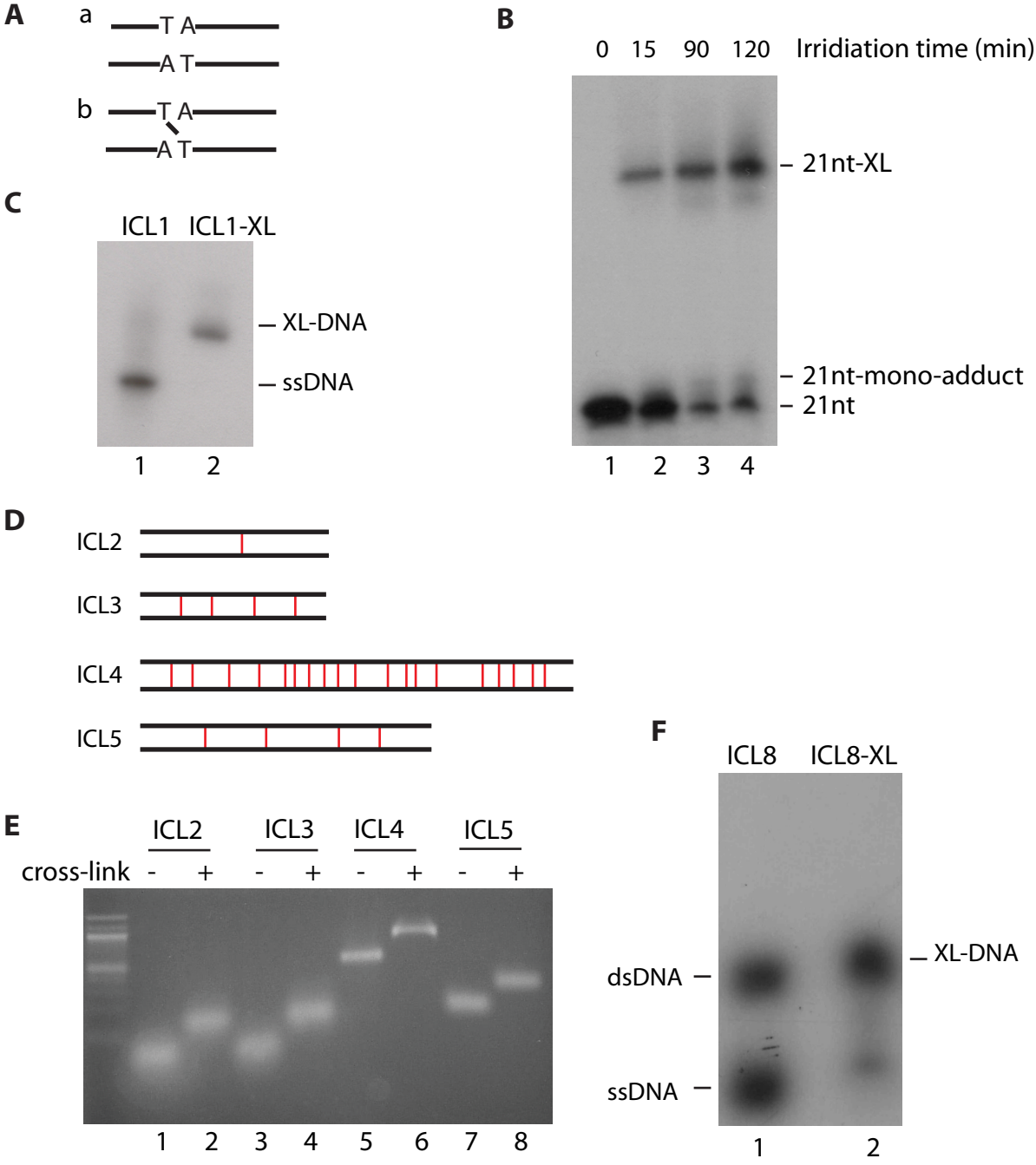

FIG. 3.1 **Introduction of site-specific DNA ICLs. A.** Schematic diagram shows: a. normal dsDNA; and b. Psoralen and UVA cross-linked DNA at -TA- site; **B.** Optimization of the cross-linking condition using end-labeled ICL1 with 32P; treated with trioxsalen and 365nm light for the indicated length of time; **C.** 100% cross-linked ICL1, shown on a 20% urea polyacrylamide gel; **D.** Schematic diagrams show the cross-linking sites of ICL2, ICL3, ICL4 and ICL5 (marked in red); **E.** Test of cross-linking condition for ICL2, ICL3, ICL4 and ICL5, shown on a 2% alkaline agaroase gel; **F.** Radioactive labeled ICL8 and ICL8-XL on a native polyacrylamide gel for purification.

3.2.2 FANCD2/FANCI complex has higher DNA affinity than each monomer

FANCD2 and ubiquitinated FANCD2 were purified from HeLa cells (purification was performed by Dr. Martin Cohn). The protein amount was balanced by quantitative Western blot (WB) (Fig. 3.2A). The purified protein was loaded to the gel according to dilution of 1:9 (9x) (Fig. 3.2A, lanes 1&4), 1:3 (3x) (lanes 2&5) and undiluted (1x) (lanes 3&6). The intensity of the blot of FANCD2 and FANCD2-Ub was compared to balance the amount of proteins to be used for the subsequent experiment. The DNA affinity of these two types of protein was tested by electrophoretic mobility shift assay (EMSA). When a protein molecule is bound to the radioactive labeled DNA substrate, the migration of the DNA will be retarded in the gel, and therefore be separated from the unbound free DNA, which will be accumulated at the bottom of the gel (Fig. 3.2B, marked as free DNA). The degree of retardation depends on the size of the protein. Using increased amount of FANCD2 (Fig. 3.2, lanes 1-3) and FANCD2-Ub (lanes 4-6), we did not observe any DNA binding activity of the protein to the 21bp double-stranded DNA substrate, ICL1.

We then studied whether the FANCD2/FANCI heterodimer formation increased the DNA affinity compared to the two proteins alone. The protein complex, as well as FANCD2 and FANCI monomers, was purified from Sf9 cells (purification was performed by Chih-Chao Liang) (Fig. 3.3A). ICL8 and cross-linked ICL8 (ICL8-XL) were used for the EMSA (Fig. 3.3B, lanes 1&2). We did not see any DNA binding activity from FANCD2 (lanes 3-6) or FANCI monomer (lanes 7-10).

However, the FANCD2/FANCI complex can bind to the double-stranded DNA substrate, and the binding is slightly reduced when a cross-link is introduced (Fig. 3.3, lanes 11-14). We suspect that FANCD2/FANCI complex prefers a normal DNA double helix, and therefore the binding was lost when using ICL DNA, which has a distorted structure.

To confirm the interaction of FANCD2/FANCI with dsDNA, we went on to test if it binds to other DNA substrates, by using ICL1 (Fig. 3.4A, lanes 1-4), ICL2 (lanes 5-8), ICL3 (lanes 9-12), and ICL5 (lanes 13-16). FANCD2/FANCI binds stronger to uncross-linked ICL1 than ICL1-XL (Fig. 3.4A, lanes 3&4), which is similar to the result we observed with ICL8. But the complex seemed to interact with the other substrates regardless of the presence of the cross-link. This could be explained that as the size of the DNA increases, the proportion of affected area by the cross-linking distortion to the DNA substrate is reduced, and therefore the complex could still bind to the rest of the unaffected double helix of the substrate. To verify that the protein-DNA interaction was specifically originated from the recombinant protein, anti-HA antibody was used to conduct a super-shift assay, which can bind to the recombinant FANCD2 and cause a further retardation of the protein-DNA complex. The anti-HA antibody showed no binding activity to the radioactive labeled 80bp double-stranded DNA substrate when incubated alone with the DNA (Fig. 3.4B). Then we added 800ng anti-HA antibody into the binding reaction with FANCD2/FANCI. As shown in Figure 3.4C, the shifted band of protein bound DNA is further shifted in the presence of the antibody (lanes 2 to 3), which indicates that the complex formed between protein and DNA in lane 2 is specific.

Figure 3.2

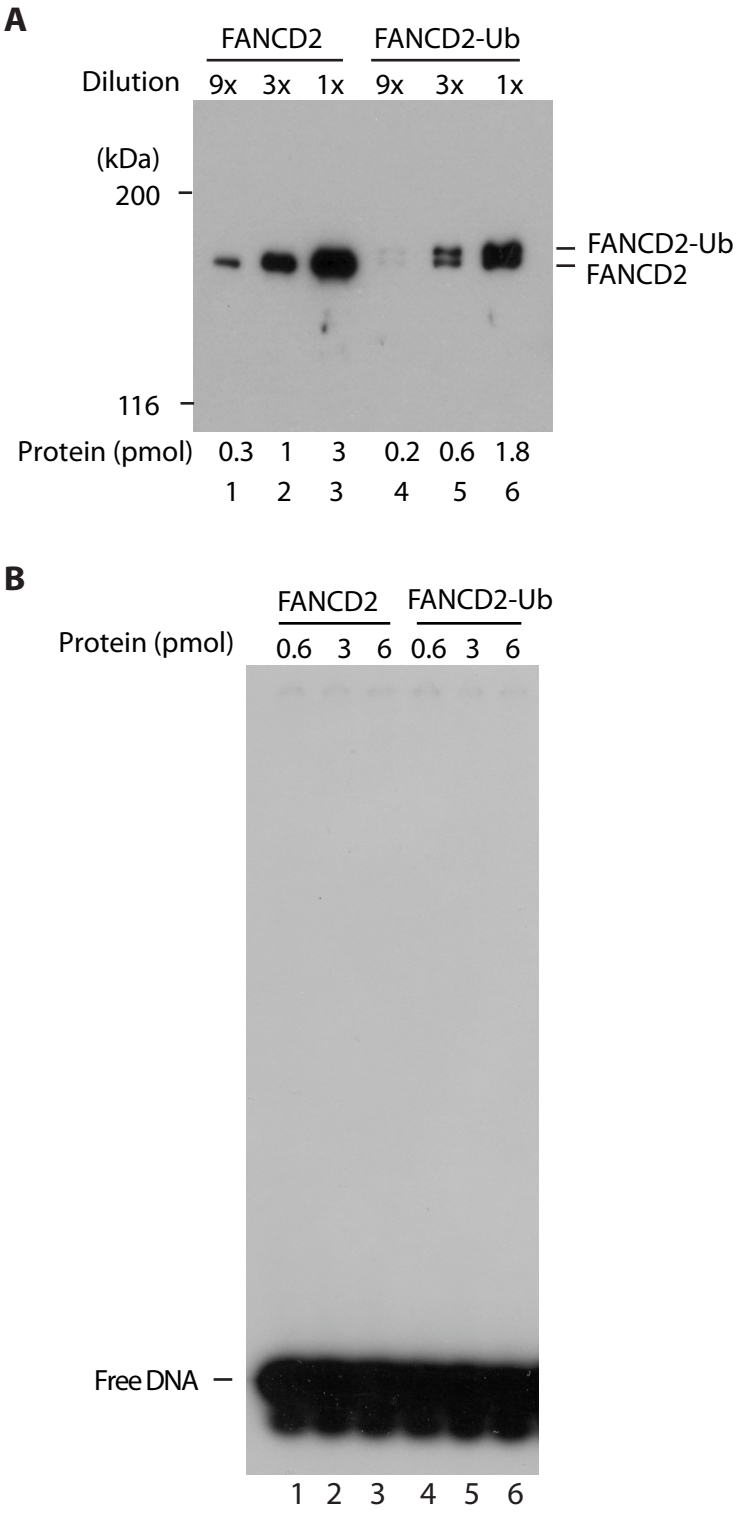

FIG. 3.2 **The DNA binding activity of FANCD2 and ubiquitinated FANCD2 from HeLa cells. A.** Quantification of FANCD2 and ubiquitinated FANCD2 purified from HeLa cells by WB (α-FANCD2: FI17); **B.** EMSA of ICL1 using proteins FANCD2 and FANCD2-Ub. No binding of FANCD2 (lanes 1-3) to ICL1 was observed, and the ubiquitination of FANCD2 (lanes 4-6) did not enhance its DNA binding activity.

Figure 3.3

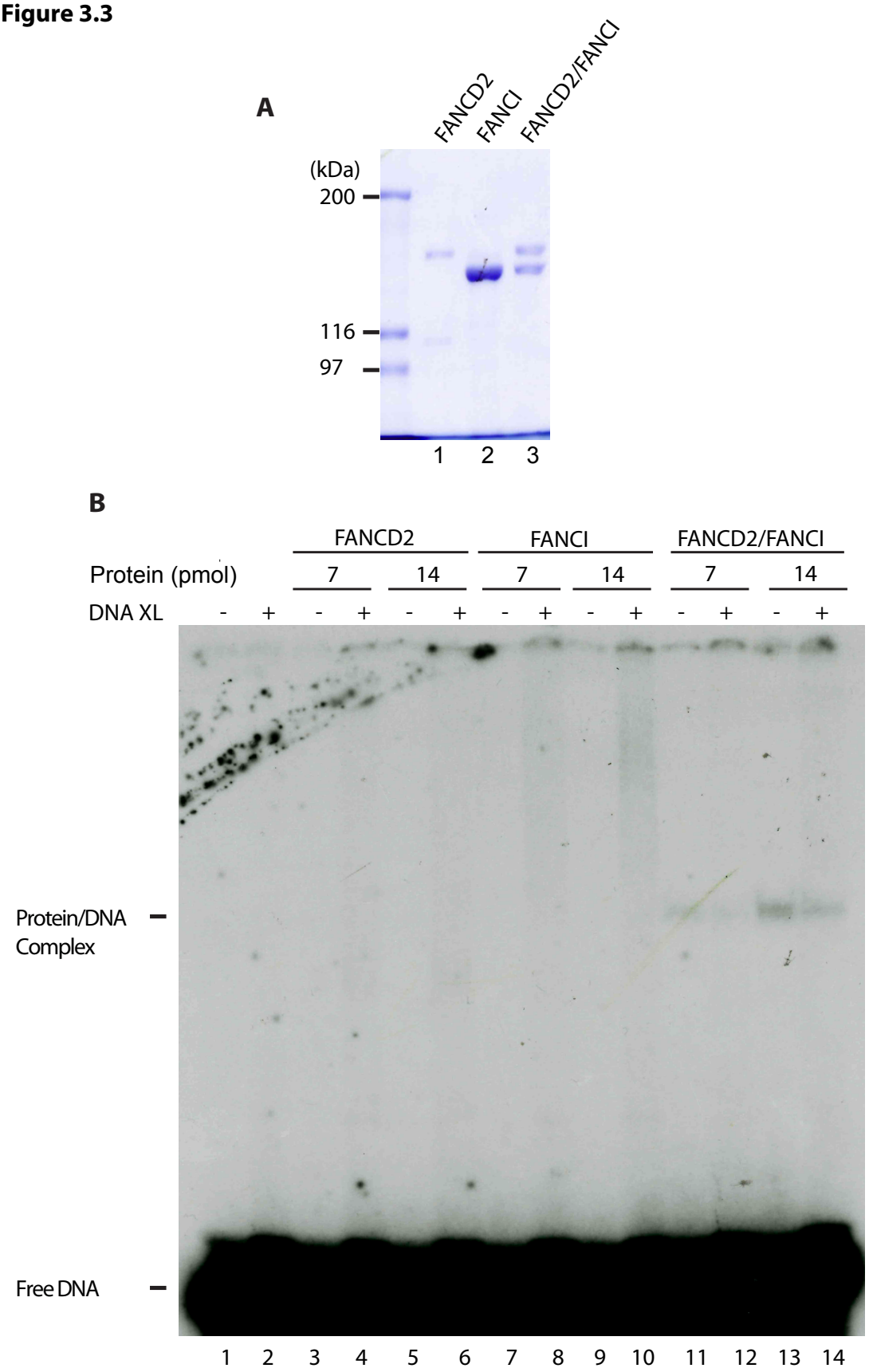

FIG. 3.3 **FANCD2/FANCI heterodimer binds DNA. A.** Coomassie blue staining shows FANCD2, FANCI and FANCD2/FANCI complex purified from Sf9 cells (proteins purified by Chih-Chao Liang); **B.** EMSA of ICL8 and ICL8-XL using FANCD2, FANCI, and FANCD2/FANCI heterodimer. No DNA affinity was observed from the monomers (lanes 3-10). The FANCD2/FANCI complex could bind to ICL8 (lanes 11&13), and the binding was stronger to than ICL8-XL (lanes 12&14).

Figure 3.4

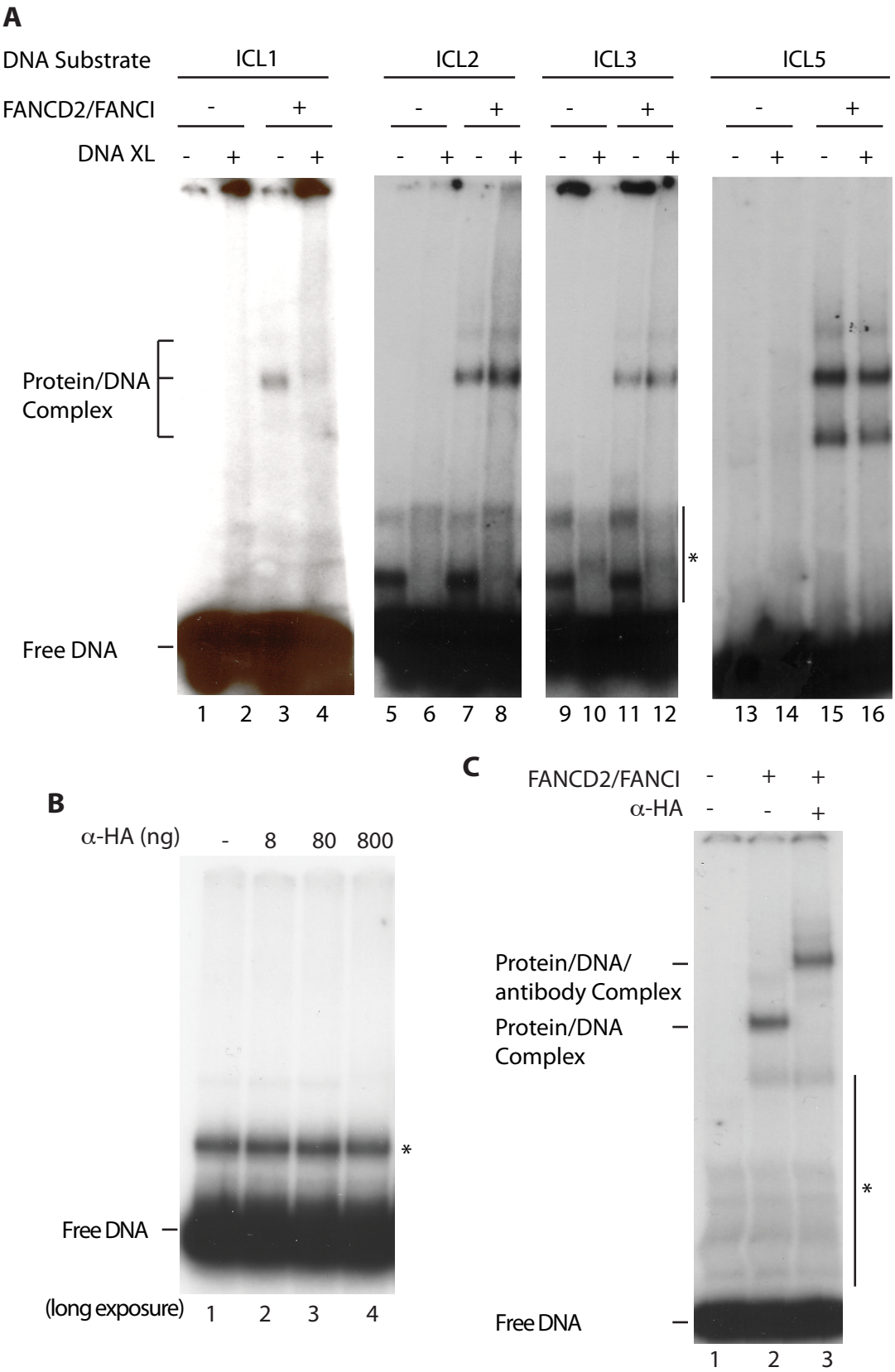

FIG. 3.4 **FANCD2/FANCI heterodimer binds dsDNA but does not recognize DNA ICLs specifically. A.** EMSA shows that FANCD2/FANCI heterodimer interacted with ICL1, ICL2, ICL3 and ICL5 (lanes 3, 7, 11 and 15). Except to ICL1-XL (lane 4), the complex also interacted with other substrates with ICLs as with dsDNA (lanes 8, 12 and 16); **B.** Increasing amount of α-HA antibody (12CA5) was incubated with DNA, and no binding of the DNA was observed; **C.** α-HA (added-in in lane 3) could further shift the retarded DNA band bound by FANCD2/FANCI complex. *unspecific DNA signal.

3.2.3 FANCD2/FANCI has lower binding activity to HJ and Y-fork than other DNA structures

Since the FANCD2/FANCI heterodimer is recruited to chromatin and forms nuclear foci in response to DNA damage, we aimed to investigate if the complex recognizes other DNA structures, which could potentially represent the intermediate DNA products during repair (*161*). Hence, we tested FANCD2/FANCI DNA affinity towards ssDNA, dsDNA, 3'-overhang (OH), 5'-OH, Holliday Junction (HJ) and replication fork (Y-fork) (Fig. 3.5A). With the increased amount of protein, all six DNA substrates had an increased population that was bound by the complex (Fig. 3.5B and Fig. 3.6). We found that while FANCD2/FANCI could bind to ssDNA, dsDNA, 3'-OH and 5'-OH, its bindings to HJ and Y-fork are weaker (Fig. 3.5B, lanes 9-12, and Fig. 3.6, lanes 9-12). The interactions of the complex with dsDNA, 5'-OH and 3'-OH were comparable. This is consistent with the reported FANCI DNA binding activity (*98*). Hence, we believe that the heterodimer of FANCD2/FANCI possesses intrinsic DNA affinity, but may not specifically recognize certain DNA structure.

Figure 3.5

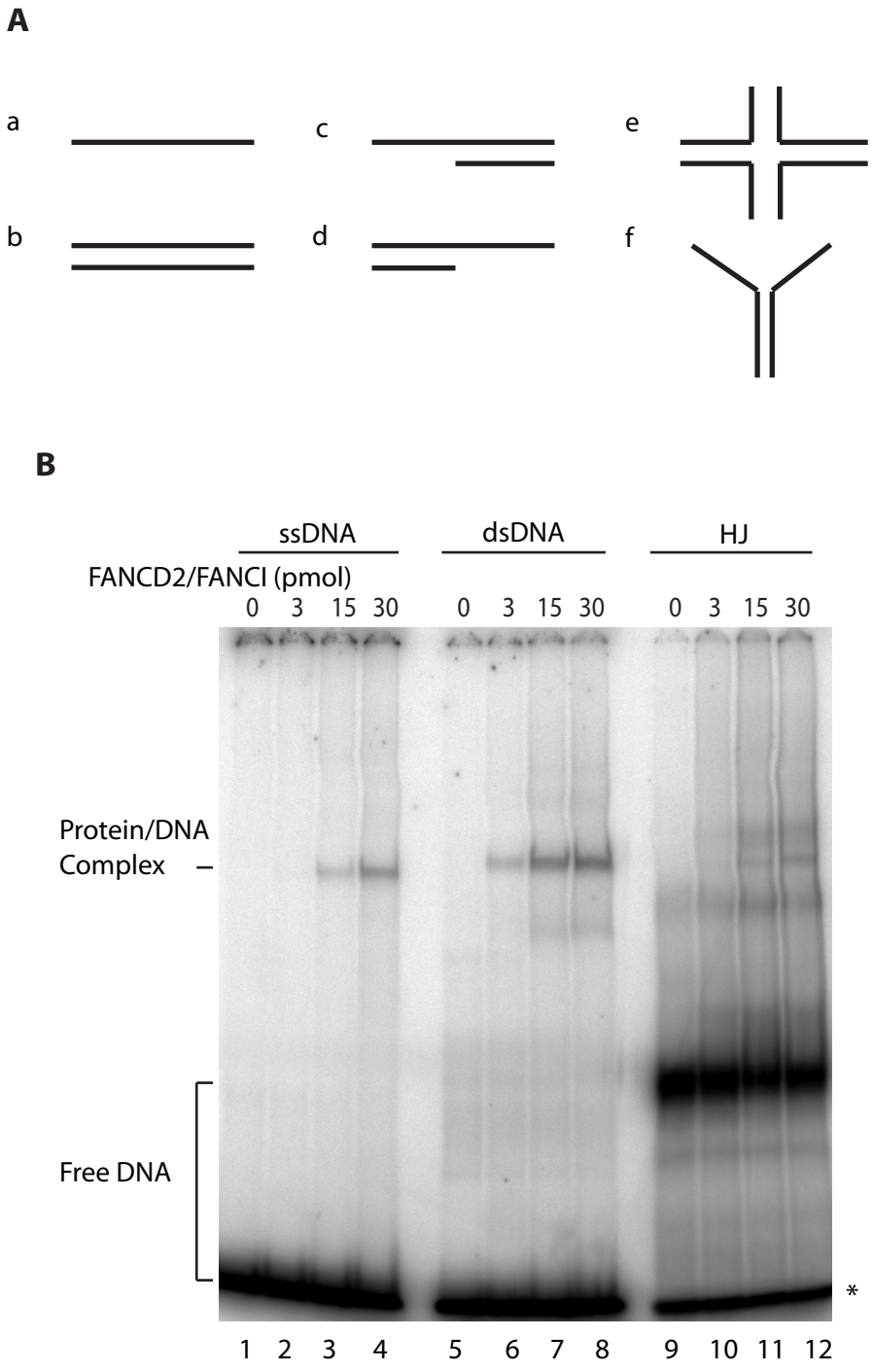

FIG. 3.5 **FANCD2/FANCI interacts with different DNA structures. A.** Schematic diagrams show the different DNA structures used in the following experiments: a. ssDNA; b. dsDNA; c. 5′-OH; d. 3′-OH; e. HJ; f. Y-fork; **B.** EMSA shows the binding of FANCD2/FANCI to ssDNA (lanes 1-4), dsDNA (lanes 5-8) and HJ (lanes 9-12), with the amount of protein as indicated; * in lanes 9-12: denatured DNA strands from HJ.

Figure 3.6

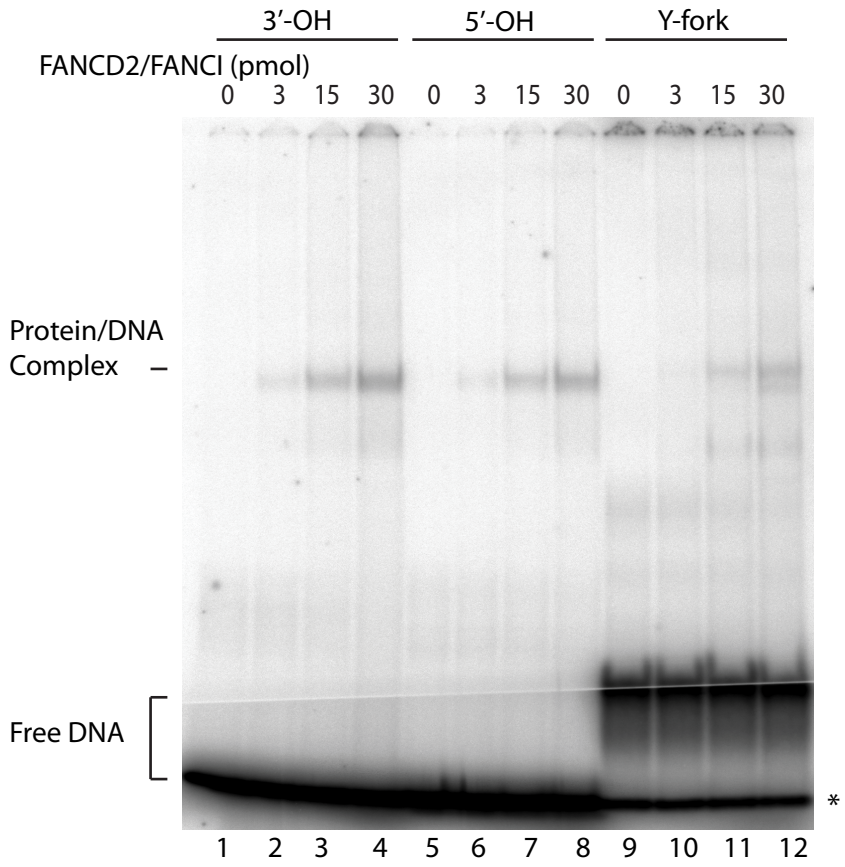

FIG. 3.6 **FANCD2/FANCI interacts with different DNA structures (cont'd). A.** EMSA shows the binding of FANCD2/FANCI to 3′-OH (lanes 1-4), 5′-OH (lanes 5-8) and Y-fork (lanes 9-12), with the amount of protein as indicated; * in lanes 9-12: denatured DNA strands from Y-fork.

3.3 Discussion

The photochemistry of psoralen is rather versatile. The cross-link is formed through the initial formation of a monoadduct (*160*). The ratio between the formation of mono-adducts and cross-links can be controlled by the wavelength and the delivery time of the light (*162*). The method described in this study of creating site-specific inter-strand cross-links in DNA gives high efficiency and only generates a minor population of the mono-adduct product.

A previous study has shown that FANCI could bind to different DNA structures, including dsDNA, overhangs, Y-fork and HJ, but prefers Y-fork and HJ structure (*96*). Also, using comparable conditions as in this study, FANCD2 has been reported to bind to these four structures as well, and preferably binds to ssDNA (*96, 163, 164*). Based on our data, FANCD2 and FANCI monomers do not display significant dsDNA binding activities. Since the series of DNA binding assays performed in the structural study of FANCD2/FANCI heterodimer used mouse protein, the difference between our results and the previous data may reflect the difference between the proteins from difference species (*96*). However, it is also likely that the FANCD2 or FANCI binding of dsDNA in our experiment was attenuated by the presence of non-radioactive labeled DNA competitors (salmon sperm DNA), which was added to differentiate the binding with a structural specificity from the general nucleic acid affinity of the protein. To study the binding of FANCD2 or FANCI to normal dsDNA in future, the non-radioactive DNA competitors can be removed. Nevertheless, we observed that the heterodimer formation of FANCD2/FANCI increased the DNA binding activity of

the two proteins, and could generate a relatively stable complex with dsDNA.

Although it is understood that monoubiquitination of FANCD2/FANCI is critical step for its chromatin recruitment (*105, 106*), the exact timing of FANCD2 and FANCI heterodimer formation is still unclear, in relation to ubiquitination and chromatin association. Based on our *in vitro* data, it is possible that the FANCD2/FANCI complex binds to DNA better than the monomers. Therefore, it is more likely that FANCD2 and FANCI form heterodimer first and then locate onto chromatin. This is in line with the structural study of FANCD2/FANCI complex, showing that the heterodimer has a lower dissociation constant with DNA than FANCD2 or FANCI (*96*). The DNA structural preference of FANCD2/FANCI complex is mild from our observation. However, upon ubiquitination, there could be potential conformational change of the complex, to increase DNA affinity of the heterodimer, and perhaps the structural specificity could also be more pronounced. Finally it is likely that the recognition of ICL DNA requires other protein factors, with their recruitment closely associated with FANCD2/FANCI complex.

Chapter 4 Detection, purification and identification of nuclear proteins that are able to recognize DNA ICLs

4.1 Introduction

The two key components of the FA pathway, FANCD2 and FANCI are activated by ubiquitination upon DNA damage and localize to the sites of damages (*107, 161*). The loss of ubiquitination results in failure of chromatin recruitment and defects in downstream repair (*95, 107*). Studies have shown that the FA core complex is required for the FANCD2/FANCI heterodimer monoubiquitination and its chromatin recruitment (*78, 98, 165*). Among the core complex, FANCA and FANCM have been reported to possess nucleic acid affinity (*166, 167*), but neither has been linked to the binding to inter-strand cross-links. The molecular mechanism of the precise recruitment of the ubiquitinated FANCD2/FANCI complex to the inter-strand cross-links remains elusive. It seems unlikely that FANCD2 or FANCI could localize to the sites of damages directly prior to ubiquitination as described in the previous chapter, therefore, other protein factor(s) may act as the upstream initiator(s) of the pathway, by binding to the cross-linked DNA to initiate the ubiquitination of FANCD2 and FANCI.

In order to discover proteins that can associate with DNA ICLs in human cells, we designed a strategy to use biotin-labeled DNA substrate as a bait, to purify components that interact with DNA from a pool of nuclear proteins extracted from HeLa cells. By comparing the purification products from non-cross-linked

DNA with the cross-linked DNA, we could isolate the proteins that recognize the cross-linked DNA directly. The purification process utilized the interaction between biotin and streptavidin, which is the strongest non-covalent biological interaction known (*168*). Streptavidin is a protein secreted by *Streptomyces avidinii*. It interacts with biotin of high affinity and generates very low unspecific binding (*169, 170*). Streptavidin sepharose beads captured the proteins bound to the biotin-labeled cross-linked DNA. Then the DNA was digested by benzonase to allow the elution of the protein. Finally, the purification product was analyzed by mass-spectrometry protein identification.

4.2 Results

4.2.1 Preparation of nuclear extract from HeLa cells

It has been shown that upon DNA damage, some protein localization can be changed, and certain post-translational modifications can take place. For instance, FA proteins are recruited to chromatin (*112*), and NBS1 is phosphorylated in response to DNA damage (*99*). In some FA deficient cells, certain protein expression levels are altered in the presence of DNA damage. For example, cyclin-dependent kinase inhibitor 1 (p21) is up-regulated in FANCC or FANCA deficient cells (*171*). These changes of nuclear proteins may be important for the initiation of DNA ICL repair. Therefore, we used the nuclear extracts from cells treated with MMC to incubate with biotin-labeled DNA substrate to purify ICL interacting proteins. This may enhance the abundance

and the specificity of the proteins, and hence the detection of them as the damage sensors.

We tested the activation of the DDR using MMC. After 6hr of MMC treatment, FANCD2 was ubiquitinated and BRCA1 was shifted, possibly due to phosphorylation in response to DNA damage (Fig. 4.1A, lanes 3). The ubiquitination of FANCD2 and phosphorylation of BRCA1 continued following the time course, suggesting that these cells were going through DDR, although the 24hr treatment only showed marginal increase from 9hr (lanes 4&5). Therefore, to purify nuclear extract from cells experiencing an active DDR, we treated HeLa S3 cells with 160ng/ml MMC for 16hr prior to cell harvesting. Using the method described previously (*156*), we obtained nuclear extract from these cells. We separated most of the cytoplasmic protein from the nuclei, as α-Tubulin was only detected in the cytoplasmic fraction of the extracts but not in the nuclear fraction (Fig. 4.1B). We also retained the nuclei integrity, as DNA-PKcs was largely preserved in the nuclear fraction (Fig. 4.1C, lanes 1&2 and lanes 4&5). The extract of the nuclear protein was also efficient, that only a minor population of DNA-PKcs remained in the chromatin pellet (lanes 3&6). We noticed that there was slightly less DNA-PKcs left in the cytoplasmic fraction after the treatment with MMC than before (lane 4 compared with lane 1). This may reflect the nuclear recruitment of DNA-PKcs in response to DNA damage.

Figure 4.1

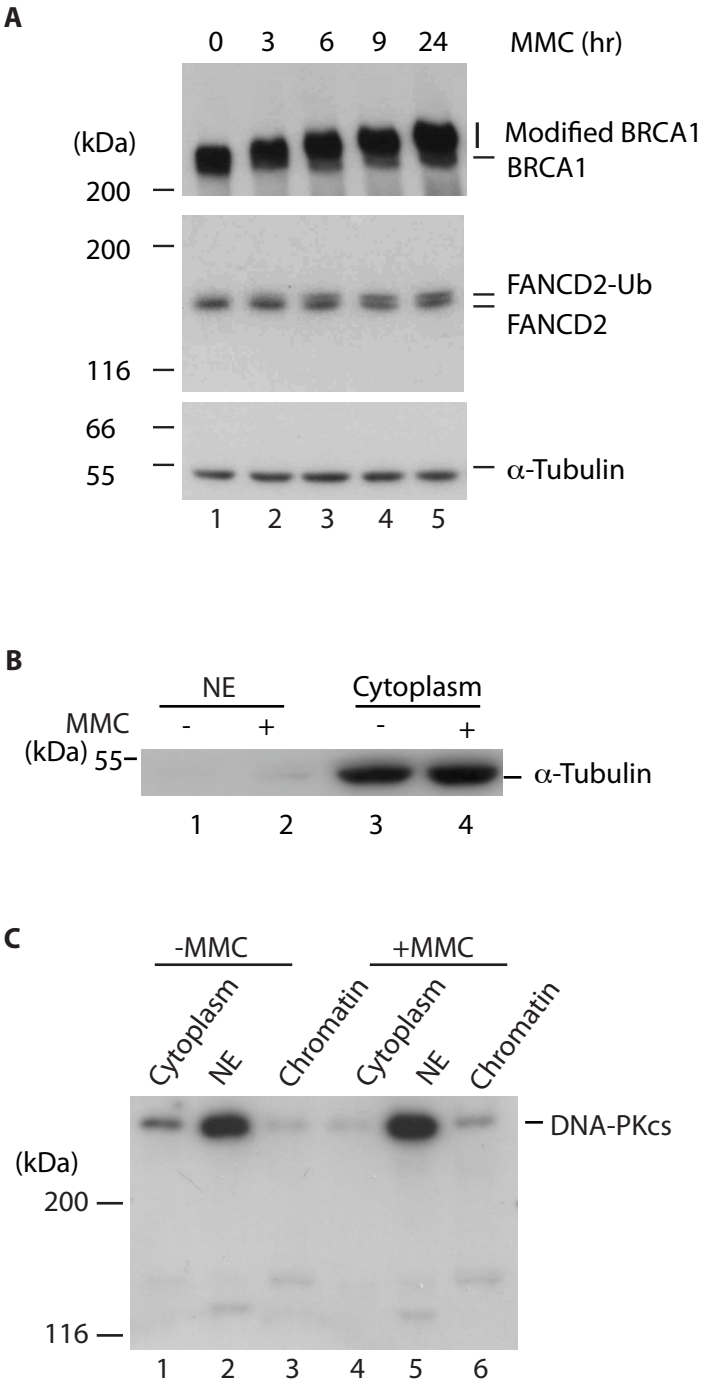

FIG. 4.1 **The preparation of nuclear extracts from HeLa cells. A.** HeLa S3 cells were treated with 160ng/ml MMC for indicated amount of time. WB shows that in the whole cell lysate BRCA1 (α-BRCA1: D9) was shifted, possibly due to phosphorylation upon DDR activation and FANCD2 (α-FANCD2: FI17) was monoubiquitinated; **B.** Fractionation of cells treated with or without MMC, into nuclear extract and cytoplasmic population using Western blot of tubulin (α-α–tubulin: DM1A) as control; **C.** From the same cell fractionation, DNA-PKcs (antibody is a gift from Dr. Lakin) is shown in WB as a control of efficient extraction from the chromatin and the preservation of the in the nuclear extract.

4.2.2 Purification of nuclear proteins that recognize DNA ICLs

To purify the proteins bound specifically to the cross-linked DNA, we designed a strategy using biotin-streptavidin affinity purification. Biotin-labeled ICL1 and ICL1-XL were incubated with nuclear extracts treated with MMC (in buffer containing 5 mM Tris, pH 7.9, 30 mM KCl, 1 mM DTT, 10 mM Hepes-KOH pH 7.9, 1 mM EDTA, 5% glycerol, 0.3 mg/ml BSA, and 5 μg/ml salmon sperm DNA), captured by streptavidin sepharose beads and eluted by benzonase digestion (Fig. 4.2A). The eluates were analyzed on a gradient polyacrylamide gel to obtain the best separation and the visualization of proteins of variable sizes. In the mock purification (Fig. 4.2B, lane 1), no DNA substrate was added. Most of the bands were identical from the purification with non-cross-linked (lane 2) or cross-linked (lane 3) DNA, and some proteins may interact better with non-cross-linked DNA than cross-linked DNA (lane 2, Bands 1, 2 and 3). These bands may contain proteins that interact with normal dsDNA, and when a cross-link is introduced, the DNA double helix structure was distorted, resulting in a loss of binding from the protein. We found that a band at a position around 97kDa (Band 4) was stronger in the sample purified with ICL1-XL than ICL1 (Fig. 4.2B, indicated with an arrow), suggesting that it may comprise proteins that have a tighter association with cross-linked DNA than with non-cross-linked DNA. Hence, we hypothesized that this band potentially contained protein(s) that could recognize inter-strand cross-linked DNA specifically.

Figure 4.2

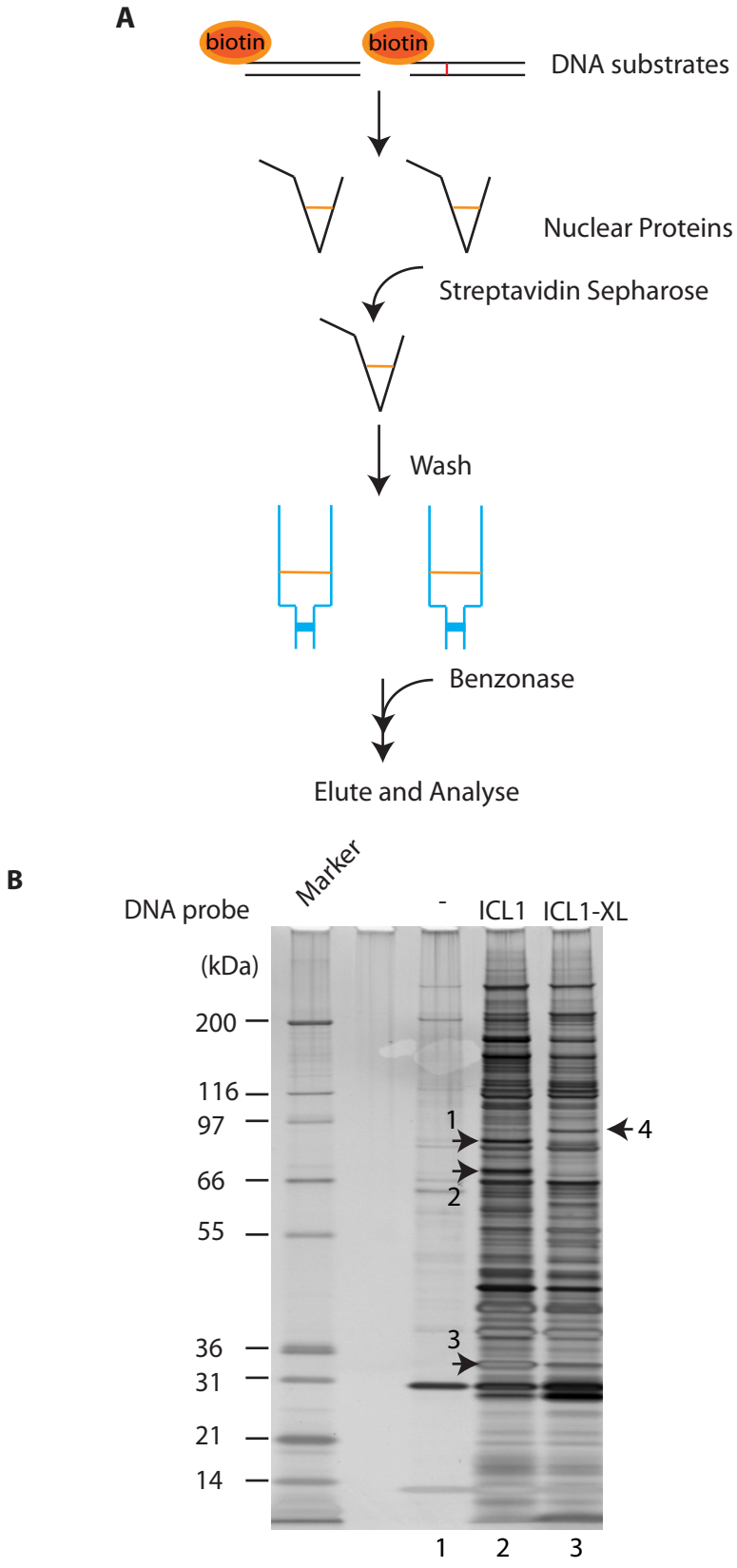

FIG. 4.2 **Purification of proteins recognizing DNA inter-strand cross-links. A.** Schematic diagram shows the purification strategy. Biotinylated ICL1 and ICL1-XL were incubated with nuclear extract treated with MMC. Streptavidin sepharose beads were added to capture the biotin-labeled DNA. After washing, the DNA substrates were digested with benzonase and the proteins were eluted; **B.** The purification products were analyzed by electrophoresis followed by silver staining: lane 1, mock; lane 2, nuclear extract with biotinylated ICL1; lane 3, nuclear extract with biotinylated ICL1-XL. The band indicated by an arrow in lane 4 was cut out, processed and identified by mass-spectrometry.

4.2.3 Identification of nuclear proteins that recognize DNA ICLs

Mass-spectrometry was used to identify those proteins by measuring and analyzing the peptide components of the proteins. It is known that the thiol group of cysteines of a protein is highly susceptible to oxidization, which generates disulfide derivative cystine. These side reactions give rise to heterogeneous protein modificiations that complicate mass-spectrometry data analysis. Iodoacetic acid is an alkylating agent that can react with and form irreversible block of the free thiol group, preventing undesired modification of the protein during analysis (*172*). Separated alkylation of the samples can generate uniformed and quantitative cysteine modification. Thus, it becomes an important step before mass-spectrometry identification to avoid the complexity of protein analysis (*173*). We excised Band 4 from the silver-stain gel, and de-stained, dehydrated and alkylated the sample using iodoacetic acid.

The sample was analyzed by mass-spectrometry (in collaboration with Prof. Steve Gygi, Harvard Medical School). 354 unique peptides were identified (Fig. 4.3A). The most prominent hits from the identification were UHRF1 and UHRF2, present with 76 and 11 peptides, respectively. UHRF1 was clearly the most dominant species over common contaminations, e.g. keratins. The peptide coverage of UHRF1 is 48.8% and of UHRF2 is 16.6% (Fig. 4.3B&C). Both proteins belong to the UHRF family, composed by structural domains including an ubiquitin-like domain, a planthomeodomain (PHD), SRA domain and RING domain. Human UHRF1 is an 806aa protein, with a molecular weight of 95kDa, whereas UHRF2 has 802aa, and the two proteins are of 52.6% identical (*174*).

Figure 4.3

A

Protein
(354 unique, 690 total, 94 total protein)

Unique	Total	AVG	Gene Name	MW (kDa)
39	76	4.2381	UHRF1	95
33	79	3.5044	KRT1	66
26	117	5.4927	KRT9	64
26	45	4.1946	KRT10	56
25	42	4.1763	KRT2	65
16	23	3.277	KRT5	58
9	11	3.5121	UHRF2	90
7	8	2.8194	AZGP1	34
7	7	3.46	DSG1	150
6	6	3.0455	EXOSC10	100
5	9	3.1493	KRT6B	60
5	9	2.6848	CAPRIN1	78
5	8	4.7448	KRT14	52

B

UHRF1

MGVFAVPPLSADTMWIQVRTMDGRQTHTVDSLSRLTKVEELRRKIQELFHVEPGLQRLFYRGKQM
EDGHTLFDYEVRLNDTIQLLVRQSLVLPHSTKERDSELSDTDSGCCLGQSESDKSSTHGEAAAET
DSRPADEDMWDETELGLYKVNEYVDARDTNMGAWFEAQVVRVTRKAPSRDEPCSSTSRPALEEDV
IYHVKYDDYPENGVVQMNSRDVRARARTIIKWQDLEVGQVVMLNYNPDNPKERGFWYDAEISRKR
ETRTARELYANVVLGDDSLNDCRIIFVDEVFKIERPGEGSPMVDNPMRRKSGPSCKHCKDDVNRL
CRVCACHLCGGRQDPDKQLMCDECDMAFHIYCLDPPLSSVPSEDEWYCPECRNDASEVVLAGERL
RESKKKAKMASATSSSQRDWGKGMACVGRTKECTIVPSNHYGPIPGIPVGTMWRFRVQVSESGVH
RPHVAGIHGRSNDGAYSLVLAGGYEDDVDHGNFFTYTGSGGRDLSGNKRTAEQSCDQKLTNTNRA
LALNCFAPINDQEGAEAKDWRSGKPVRVVRNVKGGKNSKYAPAEGNRYDGIYKVVKYWPEKGKSG
FLVWRYLLRRDDDEPGPWTKEGKDRIKKLGLTMQYPEGYLEALANREREKENSKREEEEQQEGGF
ASPRTGKGKWKRKSAGGGPSRAGSPRRTSKKTKVEPYSLTAQQSSLIREDKSNAKLWNEVLASLK
DRPASGSPFQLFLSKVEETFQCICCQELVFRPITTVCQHNVCKDCLDRSFRAQVFSCPACRYDLG
RSYAMQVNQPLQTVLNQLFPGYGNGR

C

UHRF2

MWIQVRTIDGSKTCTIEDVSRKATIEELRERVWALFDVRPECQRLFYRGKQLENGYTLFDYDVGL
NDIIQLLVRPDPDHLPGTSTQIEAKPCSNSPPKVKKAPRVGPSNQPSTSARARLIDPGFGIYKVN
ELVDARDVGLGAWFEAHIHSVTRASDGQSRGKTPLKNGSSCKRTNGNIKHKSKENTNKLDSVPST
SNSDCVAADEDVIYHIQYDEYPESGTLEMNVKDLRPRARTILKWNELNVGDVVMVNYNVESPGQR
GFWFDAEITTLKTISRTKKELRVKIFLGGSEGTLNDCKIISVDEIFKIERPGAHPLSFADGKFLR
RNDPECDLCGGDPEKKCHSCSCRVCGGKHEPNMQLLCDECNVAYHIYCLNPPLDKVPEEEYWYCP
SCKTDSSEVVKAGERLKMSKKKAKMPSASTESRRDWGRGMACVGRTRECTIVPSNHYGPIPGIPV
GSTWRFRVQVSEAGVHRPHVGGIHGRSNDGAYSLVLAGGFADEVDRGDEFTYTGSGGKNLAGNKR
IGAPSADQTLTNMNRALALNCDAPLDDKIGAESRNWRAGKPVRVIRSFKGRKISKYAPEEGNRYD
GIYKVVKYWPEISSSHGFLVWRYLLRRDDVEPAPWTSEGIERSRRLCLRLQYPAGYPSDKEGKKP
KGQSKKQPSGTTKRPISDDDCPSASKVYKASDSAEAIEAFQLTPQQQHLIREDCQNQKLWDEVLS
HLVEGPNFLKKLEQSFMCVCCQELVYQPVTTECFHNVCKDCLQRSFKAQVFSCPACRHDLGQNYI
MIPNEILQTLLDLFFPGYSKGR

FIG. 4.3 **The results from mass-spectrometry identification. A.** The list of peptides found in the purification sample, showing the total and unique number of peptides detected, and the proteins identified; **B.** The peptide coverage of UHRF1; **C.** The peptide coverage of UHRF2, green underlined letters showing the amino acids detected from the sample.

4.3 Discussion

The observation of BRCA1 phosphorylation with MMC treatment of the cells is consistent with previous studies, that FANCD2 and BRCA1 are co-localized at the sites of DNA damage upon activation, and the two proteins function as a link between the FA pathway and the downstream repair process (*106, 107*).

To differentiate the protein binding to cross-linked DNA versus undamaged or other DNA structures, we experimented with different types of non-specific DNA competitors, including poly(dI:dC), plasmid DNA and salmon sperm genomic DNA. In this study, we found that with the addition of sheared genomic DNA from salmon sperm, while the interaction of many proteins with the DNA substrates was reduced, certain protein complexes with DNA ICL persisted. It is likely that potential endogenous DNA damage in salmon sperm generates different species of DNA structures, resembling DSBs, oxidative adducts, etc. As a result, salmon sperm genomic DNA became a better competitor than the others to enhance the detection of proteins with direct interaction with DNA ICLs.

Previously, attempts have been made to purify ICL-interacting protein using cisplatin cross-linked DNA, and several proteins have been identified, including poly(ADP-ribose) polymerase 1 (PARP-1), MutSβ, etc. (*175, 176*). Photo-cross-linking of proteins and the DNA has been used prior to purification in these studies, which helped to preserve the interaction between proteins and DNA, but may also increase the risk of unspecific DNA binding of a protein due to the

artificial cross-linking. Although PARP-1 and MutSβ have been shown to be required for DNA repair, the direct and specific interaction of with ICL DNA has not been verified. Also, in contrast to our purification, non-specific DNA competitors were not included in the previous studies, which may potentially result in obtaining proteins that recognize damaged DNA but not specifically inter-strand cross-linked DNA.

Using individual protein bands from silver-stain gel for identification provides a set of clean and straightforward mass-spectrometry results for the subsequent analysis. However, we could possibly have over-looked some potentially interesting candidates due to the low abundance in the sample, as they may not be clearly visible from the gel. It may help to overcome this limitation in our strategy in future by using the entire purification product for identification, in addition to analyzing individually isolated protein bands.

Chapter 5 *In vitro* characterization of UHRF1: UHRF1 recognizes DNA ICLs directly

5.1 Introduction

UHRF1 contains an N-terminal ubiquitin-like domain, a tandem tudor domain (TTD), a plant homeodomain (PHD), an SET and RING associated (SRA) domain, and a RING finger motif (Fig. 1.3A). It is a nuclear protein and was initially identified as an inverted CCAAT box binding factor of the topoisomerase IIα promoter to regulate its expression (*119*). Subsequent studies have demonstrated that UHRF1 can affect DNA methylation (*131, 141*), histone deacetylation (*121*), histone methylation (*177*), and histone ubiquitination (*123, 124*). Therefore UHRF1 has been long believed to be very important for regulating gene expression epigenetically.

Its interaction with the DNA methyltransferase DNMT1, histone and hemi-methylated DNA has been studied in depth. The crystal structure of the SRA domain of UHRF1 has been presented in complex with DNA containing a hemi-methylated CpG site (*139*). It is believed that when the SRA domain of UHRF1 binds to hemi-methylated DNA, it creates an access for DNMT1 to methylate the complementary DNA strand (*178*). Multiple regions, including PHD, TTD and SRA, are suggested be responsible for its histone binding activity, and different histone markers recognition, e.g. methylation and acetylation (*125, 128, 141*).

Possibly due to its important function in the maintenance of DNA methylation and the regulation of gene expression during development and DNA repair, knockout of *Uhrf1* in mice causes embryonic lethality (*134, 141*). As UHRF1 is also required for genome stability in the cells, the disruption of UHRF1 in mouse embryonic stem cells results in an increased sensitivity to DNA damage inducing agents (*134*). Other studies reported a critical role for human UHRF1 in the cellular response to different types of DNA damages, e.g. γ-irradiation, X-ray, UV light, base damaging agents and hydroxyurea (*134, 147*), suggesting a possible dual-function or link of UHRF1 in DNA methylation and DNA damage repair.

Based on the design and result of our purification, as well as the previous literature, we hypothesized that UHRF1 may participate in the DNA ICL repair through its direct binding to ICLs. To confirm UHRF1's direct interaction with DNA ICLs, we expressed and purified UHRF1, and tested its binding activity to ICL DNA by DNA pull-down assay and EMSA.

Ubiquitination is a common post-translational modification, which plays an important role in regulation of many aspects of cell physiology, and RING domain proteins have been widely demonstrated to mediate ubiquitin ligase activity (*179, 180*). The auto-ubiquitination activity of UHRF1's RING domain has been studied, and the RING domain possibly interacts, as well as ubiquitinates core histones (*123, 124*). Besides histones, DNMT1 and PML have also been proposed as substrates of UHRF1 (*181-183*). We confirmed the E3 ubiquitin ligase activity of UHRF1 by auto-ubiquitination assay. In collaboration with Chih-Chao Liang, we also identified the domains that were important for its recognition of ICLs

and ubiquitination activity, to investigate whether there was any interplay between the two functions.

5.2 Results

5.2.1 Cloning, expression and purification of UHRF1

Full length human UHRF1 (Ref. Seq. NP_037414.3) (Fig. 1.3A) was cloned by reverse transcription PCR from human total RNA. We used Invitrogen Baculovirus Expression Vector System for protein expression in Sf9 cells (Fig. 5.1A). The cDNA of UHRF1 was digested by XhoI and PspOMI, and inserted into a pFastBac vector containing the Flag and HA epitope tags. The pFastBac.UHRF1 vector was then transfected into DH10Bac cells to generate recombinant bacmids. Sf9 cells were subsequently transfected by the bacmids for 48hr to produce baculovirus. This transfection step was repeated three times to generate virus of high titre, determined by expression level. Finally, the Sf9 cells were infected by the baculovirus for 72hr and the cells were harvested for the purification of expressed UHRF1.

Expressed UHRF1 was purified by column chromatography using α-Flag M2 agarose beads. The protein was eluted by competition with excess Flag peptide. The purification product was then analysed by electrophoresis on a polyacrylamide gel followed by Coomassie staining (Fig. 5.1B).

Figure 5.1

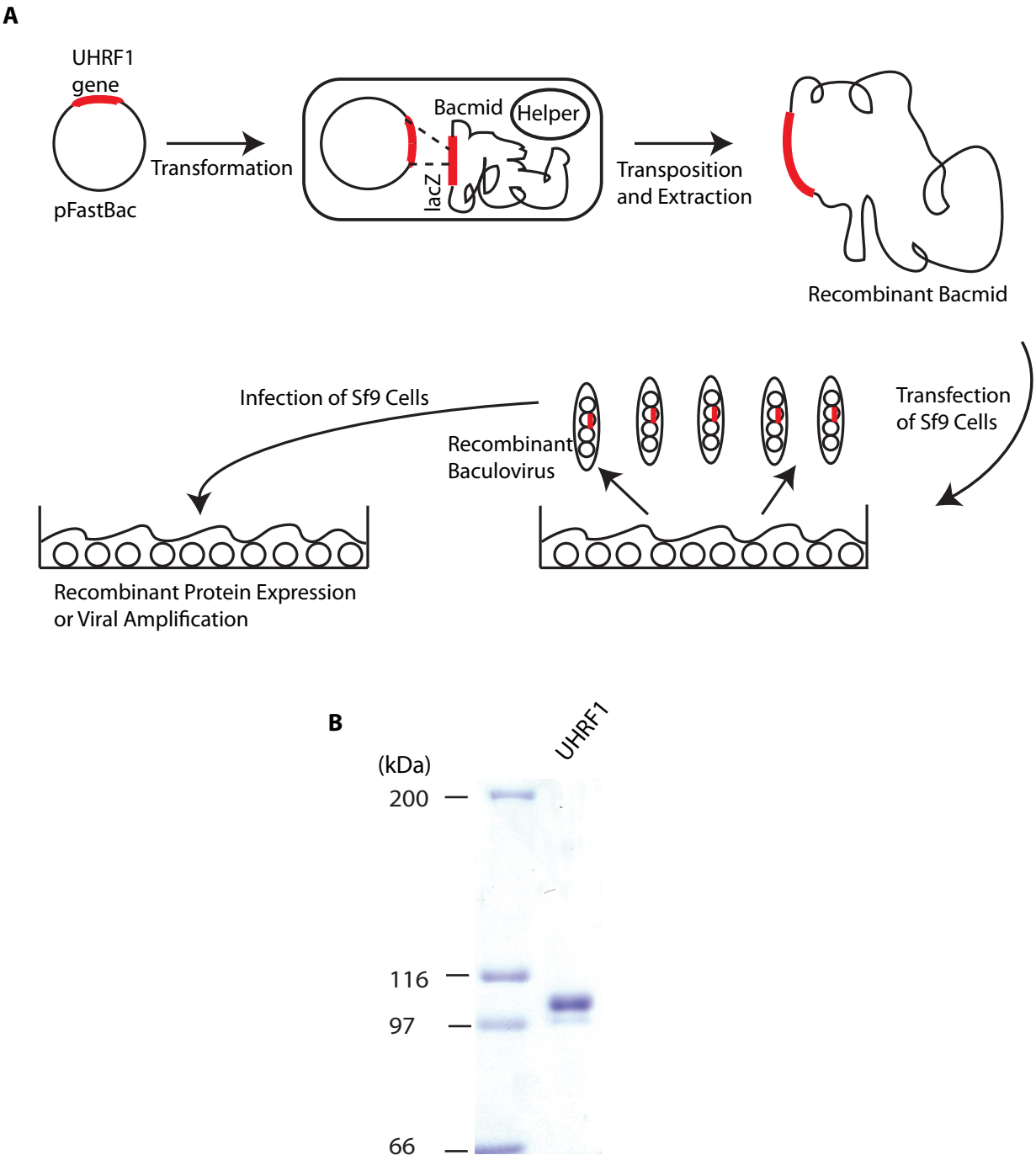

FIG. 5.1 **Expression and purification of UHRF1**. **A.** Schematic diagram shows the procedure of the baculovirus protein expression system; **B.** Purified Flag-HA-tagged UHRF1 from Sf9 cells, stained by Coomassie blue.

5.2.2 UHRF1 binds to DNA ICLs and hemi-methylated CpG preferentially

To test whether UHRF1 interacts with DNA ICLs directly, we used the purified recombinant UHRF1, and as a negative control FANCL, to perform the DNA pull-down assay that is similar to the purification strategy described in the chapter 2 (Fig. 4.2A). Biotin-labeled ICL2 (Fig. 5.2A) and cross-linked ICL2-XL (cross-link shown in red) were incubated with UHRF1 or FANCL. FANCL is also an E3 ubiquitin ligase, and it is a part of the FA core complex (*77*). There is no evidence showing that it binds to DNA, hence it was introduced as a negative control. After DNA capture and protein elution, the protein bound to DNA was analyzed by Western blot. No protein was pull-down in the absence of DNA substrate (Fig. 5.2A, lanes 2&6). There was more UHRF1 pull-down by ICL2-XL than with non-cross-linked ICL2, indicating a stronger interaction with cross-linked DNA (lanes 3&4). As expected, there was no detectable FANCL protein bound to either of the DNA substrate (lanes 7&8). This result indicates that UHRF1 can recognize ICL DNA *in vitro* specifically and directly.

Since hemi-methylated DNA has already been reported as a preferred substrate of UHRF1, we sought to compare UHRF1's binding specificity to ICLs and to hemi-methylated CpGs. Four DNA substrates were designed with mostly identical sequence, except the site where -TA- site was introduced for cross-link substrates, i.e. ICL8 and ICL8-XL (Fig. 5.3A), while -CG- site was introduced for hemi-methylation probes, i.e. CpG3 and CpG3-me (Fig. 5.3B). We could see that there was more protein/DNA complex formation for UHRF1 with both ICL8-XL

and CpG3-me than with ICL8 and CpG3 (Fig. 5.3C, lanes 5-8). Using α-HA antibody, we could see a further retardation in the gel of the complex, confirming that the complex is indeed formed with DNA by UHRF1 (Fig. 5.3C, lanes 10&11). Quantification by phosphor-imager showed that there was about 1.5 fold increased interaction with either cross-linked or hemi-methylated DNA (Fig. 5.3D). These data suggest that the protein preferential recognition to these two types of DNA structures is at a comparable level.

5.2.3 UHRF1 has E3 ubiquitin ligase activity through its RING domain

To study UHRF1's E3 ubiquitin ligase activity, we expressed and purified E1 ubiquitin activating enzyme, i.e. Flag-HA tagged Uba1, and 6xHis-tagged ubiquitin (Uba1 was cloned by Jean Tian, and ubiquitin was cloned and purified by Jean Tian and Maarten van der Velden). We also cloned, expressed and purified UbcH5b in Sf9 cells, an E2 ubiquitin conjugating enzyme, which has been shown to function together with UHRF1 to perform ubiquitination (*124*) (Fig. 5.4, A-C).

We established an in vitro ubiquitination assay using these components. E1 and E2 were shown in the HA blot in Fig. 5.4D, lane 1. After the addition of ubiquitin (lane 2) and ATP, both proteins were activated and E2 was ubiquitinated to form mono- and di-ubiquitination products (lane 3). It may be unusual to have ubiquitination without E3, however, E3-independent substrate ubiquitination have been reported previously in ubiquitin-binding domains (UBD) containing protein (*184*). As UbcH5b has an ubiquitin-binding interface (*185*), it is possible

Figure 5.2

A

5′–GTCTGCTCGAGTCGAGTCGCTCTCGTCTG**TA**CACCGAAGACTCGACTGCACTGCAGACTC–3′

3′–CAGACGAGCTCAGCTCAGCGAGAGCAGAC**AT**GTGGCTTCTGAGCTGACGTGACGTCTGAG–5′

B

5′–GTCTGCTCGAGTCGAGTCGCTCTCGTCTG**TA**CACCGAAGACTCGACTGCACTGCAGACTC–3′

3′–CAGACGAGCTCAGCTCAGCGAGAGCAGAC**AT**GTGGCTTCTGAGCTGACGTGACGTCTGAG–5′

C

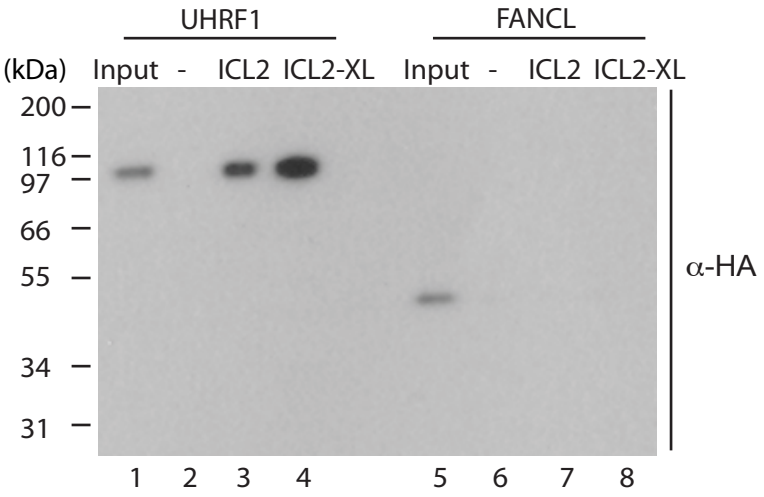

FIG. 5.2 **Confirmation of UHRF1 direct interaction with inter-strand cross-linked DNA. A.** Sequence of ICL2. The potential site of cross-link is shown in bold; **B.** Sequence of ICL2-XL. The site of cross-link is shown in bold and the cross-link is represented by a red line; **C.** The interaction of Flag- and HA- tagged UHRF1 and FANCL with ICL2/ICL2-XL was tested by biotinylated DNA pull-down experiment. 10% of each protein for input was loaded in lanes 1 and 5. Mock pull-down (no DNA) was loaded in lanes 2 and 6. More UHRF1 was bound to ICL2-XL than ICL2, as shown in lane 3 and 4, whereas no FANCL interacted with either of the DNA substrate. α-HA: 12CA5.

Figure 5.3

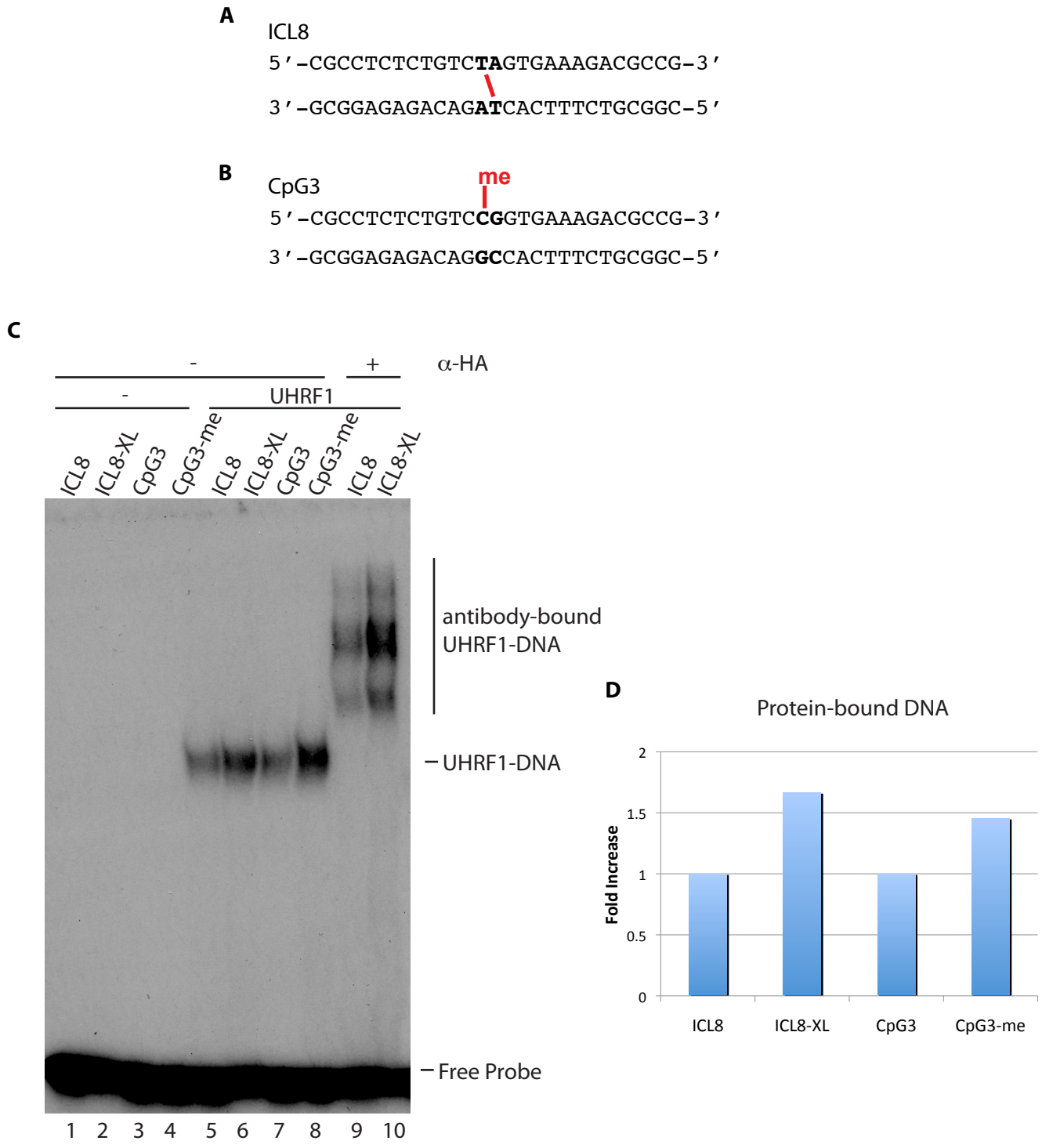

FIG. 5.3 **Comparison of UHRF1 binding to DNA ICLs and DNA hemi-methylation. A.** Sequence of ICL8 and ICL8-XL. The site of cross-link is marked in bold and the cross-link is represented by a red line; **B.** Sequence of CpG3 and CpG3-me. The site of hemi-methylated CpG is marked in bold and the methyl group is in red; **C.** EMSA shows UHRF1 interacted stronger with cross-linked DNA (ICL8-XL) and hemi-methylated DNA (CpG3-me) than with ICL8 or CpG3-me, in lanes 5 to 9. α-HA (12CA5) antibody interacted with the complex in lanes 6 and 7, causing a super-shift, indicating that the complex was formed specifically by UHRF1; **D.** Quantification of the EMSA in C, lanes 5-9, comparing the increase from lane 5 to 6 and 7 to 8. The percentage of shifted DNA substrate of ICL8 or CpG3 is normalized to 1.

that when at high concentration of ubiquitin, the protein carries out auto-ubiquitination activity in the absence of E3 or a substrate.

We then used this protocol to introduce E3, UHRF1 to perform ubiquitination assay, and analyzed the products by WB using anti-His tag antibody. In the presence of ATP, UHRF1 and ubiquitin were incubated in the reaction as negative control (Fig. 5.4E, lane 1). When only E1 and ubiquitin were incubated with ATP, we could see the charging of E1 with one or two ubiquitin molecules (lane 2). With E1, E2, ubiquitin and ATP, we observed a minor ubiquitination activity (lane 3), likely originated from E2 ubiquitination as we saw previously (Fig. 5.4D, lane 3). Finally, we introduced all components, and we could see a pronounced mono- and di-ubiquitination of UHRF1 (Fig. 5.4E, lane 4, bands pointed by arrows). Also, there were poly-ubiquitin products forming above the position of mono-and di-ubiquitinated UHRF1, indicating a robust auto-ubiquitination activity of UHRF1 (Fig. 5.4E, lane 4).

We then questioned that whether the RING domain entailed UHRF1's E3 ligase activity. Chih-Chao Liang designed and purified several mutants of UHRF1, including ubiquitin-like domain deletion (ΔUBL), SRA deletion (ΔSRA), RING deletion (ΔRING), TTD point mutation (F165A) (*128*) and PHD double-point mutation (D347A/E348A) (*186*) (Fig. 5.5A). It has been demonstrated that in TTD domain, Phe-165 contributes to an aromatic cage and interacts with trimethylammonium moiety of H3K9me3, and its mutation to Ala destroys the binding pocket (*128*). In PHD domain, Asp-347 and the adjacent Glu-348 form

Figure 5.4

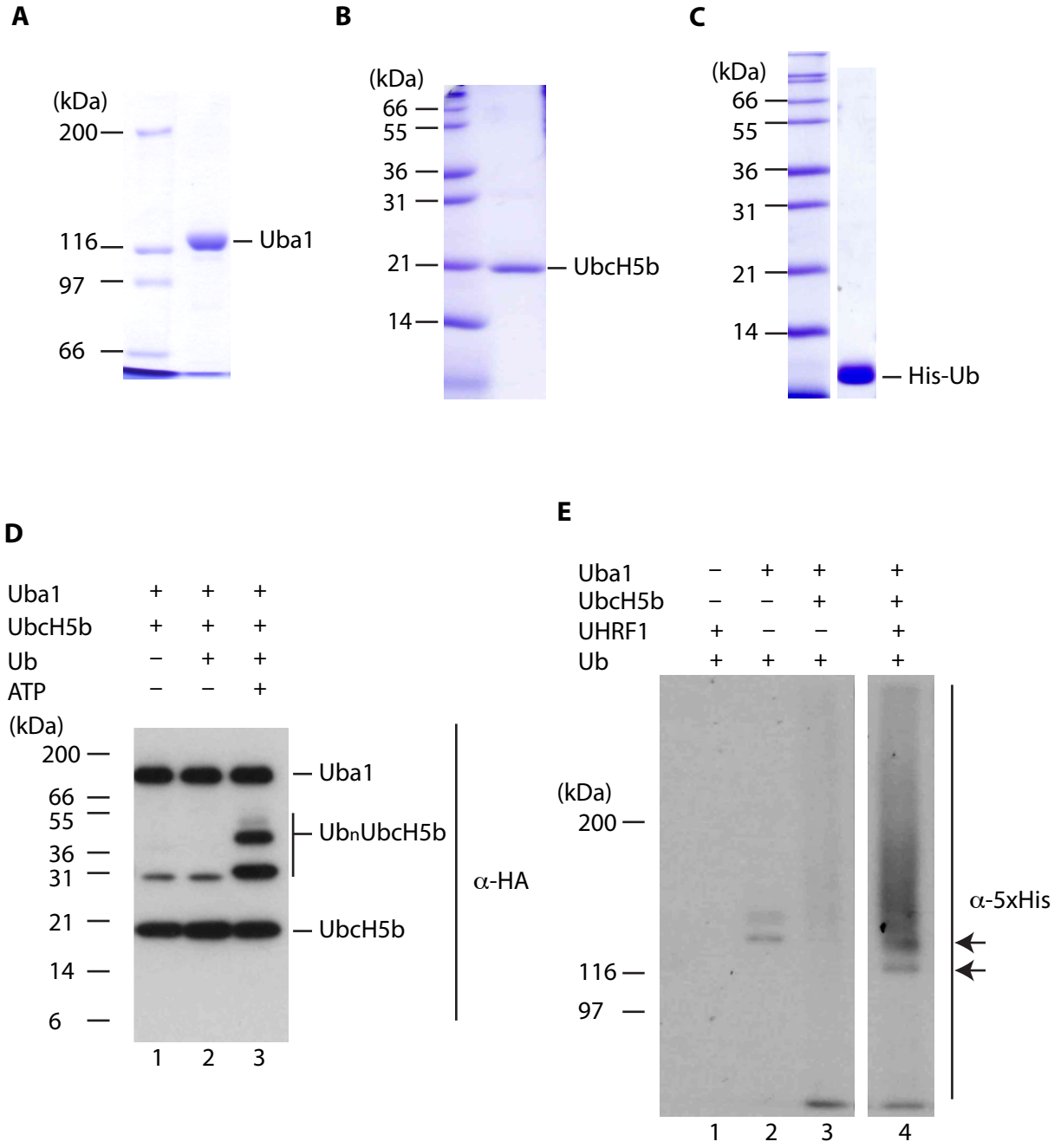

FIG. 5.4 **UHRF1 has E3 ubiquitin ligase activity. A.-C.** Coomassie stains show purified Uba1 (A), UbcH5b (B) and His-tagged ubiquitin (purified by Maarten van der Velden, C); **D.** Uba1, UbcH5b (lane 1), ubiquitin (lane 2) and ATP (lane 3) were incubated in ubiquitination mixture at 37°C for 1hr. E2, UbcH5b, ubiquitin conjugation is shown from the α-HA (12CA5) blot in lane 3; **E.** UHRF1 auto-ubiquitination assay (lane 4), using UHRF1+ubiquitin (lane 1), Uba1+ubiquitin (lane 2) and Uba1+UbcH5b+ubiquitin (lane 3) as control. The ubiquitination product is shown in α-His-tag (34660, for ubiquitin) blot.

hydrogen bonds with guanidinium group of H3 Arg 2, and when they are mutated to Ala, the PHD domain loses binding to H3 peptide (*187*). These mutants were used in the ubiquitination assay as described previously (Fig. 5.5B). We found that only in the reaction with ΔRING mutant, the auto-ubiquitination activity was abolished (Fig. 5.5B, lane 6), which is consistent with previous literature on RING domain's function in UHRF1 (*124, 153*). We also noticed that there was an increased level of auto-ubiquitination, possibly di- and tri-ubiquitination in the ΔUBL mutant (lane 4). UBL domain has been reported to be important for protein-protein interactions in many examples (*188, 189*). Its presence may actually hinder the protein's auto-ubiquitination activity, or multi-ubiquitination conjugation at certain regions of the protein, to therefore enhance the specific interaction with ubiquitination substrates.

5.2.4 Both SRA and RING domains may be required for UHRF1's recognition of DNA ICL*s*

It has been demonstrated that the SRA domain is responsible for UHRF1's interaction with hemi-methylated DNA. We raised the question whether UHRF1 recognized cross-linked DNA using the same domain and mechanism. ΔUBL did not alter the DNA binding activity and specificity of UHRF1 compared with the WT protein, and neither did the mutations in TTD and PHD domains (Fig. 5.6, lanes 1-8 and lanes 17-28). As expected, the deletion of SRA domain caused the loss of specific binding to ICL8-XL and CpG3-me (lanes 9-12).

Figure 5.5

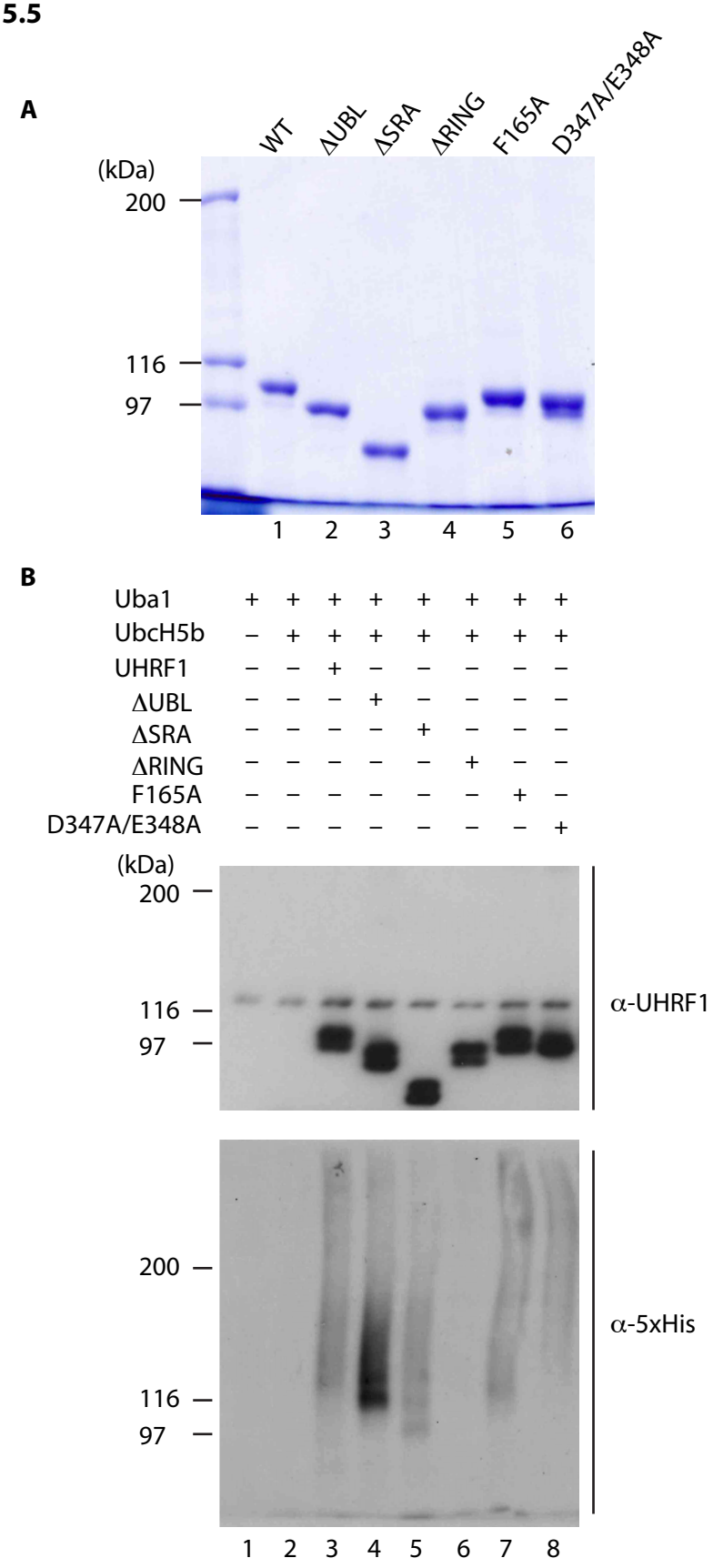

FIG. 5.5 **RING domain is required for UHRF1 auto-ubiquitination activity. A.** Coomassie stain shows purified multiple mutants of UHRF1 (mutants are purified by Chih-Chao Liang); **B.** UHRF1 auto-ubiquitination assay using WT (lane 3) and the mutants (lanes 3-8) as indicated. Uba1 (lane 1) and Uba1+UbcH5b (lane 2) were used as negative controls. The protein amount of different mutants is shown in α-UHRF1 (H8) blot, and the ubiquitination product is shown in α-His-tag (34660, for ubiquitin) blot.

Based on the previous study, SRA domain is sufficient to bind to DNA, and to provide specificity to the hemi-methylated DNA (139). Since the SRA domain is dispensable for UHRF1 E3 ubiquitin ligase activity (Fig. 5.5B, lane 5), UHRF1 ICLs interaction should be independent from its enzymatic activity. However, DRING mutant also had a similar defect in specific binding, although overall binding to DNA was better preserved than DSRA (Fig. 5.6, lanes 13-16). It is possible that the RING domain may be important for the overall protein folding, which may enhance the protein/DNA interaction in the full-length UHRF1. It could be more physiological to study the DNA binding activity of the RING domain by introducing point mutations than deleting the entire domain in future. Finally, it is possible that there can be a difference between in vitro and in vivo DNA recognition. It will be important to study whether both domains are required for its function in DNA repair in vivo.

5.3 Discussion

Baculovirus expression system in Sf9 cells enables us to express and purify proteins of relatively high molecular weight, and it is easy to generate high yield from the cell culture (*190*). We purified UHRF1 to a high degree of homogeneity, which facilitates the subsequent biochemical assays.

Figure 5.6

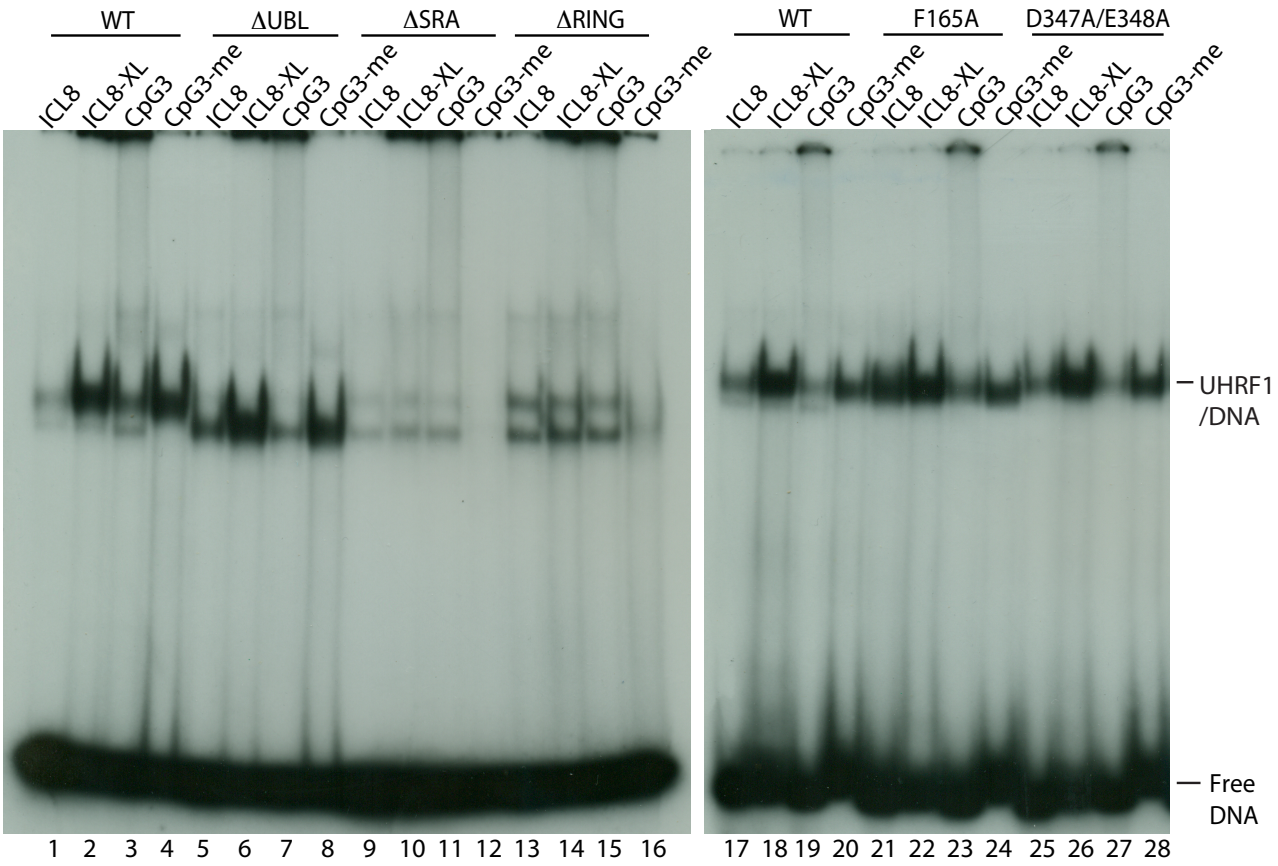

FIG. 5.6 **Identification of domains that interact with DNA ICLs.** EMSA shows that WT UHRF1 preferentially bound to ICL8-XL and CpG3-me, as well as mutants ΔUBL, TTD F165A and PHD D347A/E348A, but the specificity was lost in mutants ΔSRA and ΔRING. The experiment was performed by Chih-Chao Liang.

This is the first report on a protein that interacts directly and preferentially with inter-strand cross-linked DNA *in vitro*. UHRF1 could potentially function as the missing link between the DNA ICL damages and the current Fanconi Anemia pathway. Its direct DNA binding activity and association with heterochromatin region (*125, 127*) could promote DNA repair in both replication independent and dependent manner.

Our results demonstrate that UHRF1 recognizes DNA ICLs, similar to its recognition to hemi-methylated DNA. From *in vitro* DNA binding assay, UHRF1 binds to hemi-methylated DNA with about 2-fold increase compared with non-methylated DNA or fully methylated DNA (*131, 139*). However, the knockout of *Uhrf1* in mESCs results in a significant decrease in genomic methylation and up to 70% decrease of methylation in individual genes (*131*). This suggests that its *in vivo* association with DNA ICLs may be much higher than what we can observe from the biochemical experiments *in vitro*. Hence, we have reasons to believe that its recognition DNA ICLs is potentially sufficient to support its function in the damage repair.

We confirmed that UHRF1 possesses E3 ubiquitin ligase activity, however, its specific substrate remains a question. DNMT1 and histones have all been proposed to be the substrate of UHRF1 (*123, 124, 181-183*). In a previous study, the RING domain mutant of UHRF1 creates a dominant negative DNA repair defect phenotype (*153*). Therefore, it can be very useful to determine UHRF1 substrate in DNA repair pathway. We have not yet been able to isolate and identify any UHRF1 ubiquitination substrate *in vitro*. However, based on a very

preliminary *in vivo* IP data, H2AX ubiquitination may be affected by the KD of UHRF1 (data not shown). H2AX ubiquitination is a critical marker in signaling transduction and DNA repair (*191-193*), which could be a meaningful substrate of UHRF1. It is important to study whether UHRF1 E3 ligase activity is required in DNA ICLs repair, as well as its mechanism.

Consistent with UHRF1's binding to hemi-methylated DNA, the SRA domain is also required for the interaction with cross-linked DNA. The mechanism of UHRF1 binding to hemi-methylated DNA has been well documented (*139, 140*). The overall structure of the SRA domain is globular, which looks like a saddle, composing a concave on the open side. The conserved residues in the SRA domain contribute to a positively charged surface in the inner concave. Hemi-methylated DNA fits in the concave, the DNA binding causes a change in the structure the region. The methylated cytosine is therefore flipped out, and inserted into the inner concave of the domain. We suspect that the SRA interaction with DNA ICLs does not use the same flipping-out mechanism, as the structure of psoralen/UVA cross-linked DNA is quite different from the hemi-methylated DNA. The psoralen cross-link causes unwinding at the -TA- site and the neighboring 3 base parings are distorted (*194*). However, the increased flexibility of the sugar-phosphate backbone of the DNA could provide amino acid contact area, which might fit into the concave of the SRA domain.

It is quite surprising to us that the RING domain deletion caused a similar DNA binding defect as the SRA domain deletion. On the other hand, although the SRA domain has been shown to be sufficient to recognize hemi-methylated DNA

(*139*), published data indicate that the deletion of the RING domain may reduce the overall binding activity (*121*). RING finger domains are specialized Zn-finger motifs, which are involved in DNA and RNA binding (*195, 196*). It is possible that the RING domain of UHRF1 inherites some of the nucleic acid affinity, and therefore facilitates the overall binding to DNA of the protein. Also, the RING domain may affect UHRF1's heterochromatin association (*124*) and H3K9me3 interaction (*125*), which may imply an alteration of the DNA association of the protein. It would be interesting to study the individual SRA and RING domains DNA binding activity to understand if the defect in ΔRING is a result of direct DNA interaction of the RING domain, or the effect on the change of the full-length protein structure/multiple-domain interaction. Given the distinct *in vitro* characteristics of the two domains, it is important to discover whether there is any cross talk of DNA binding and ubiquitination activity in the FA pathway.

Chapter 6 *In vivo* characterization of UHRF1 (Part 1): UHRF1 is required for cells to repair DNA ICLs

6.1 Introduction

Several studies have suggested a critical role for UHRF1 in the cellular response to different types of DNA damage. It has been shown that UHRF1 is up-regulated in certain cancer cell lines, such as MCF7 (*153*), and it is required for cell cycle checkpoint regulation upon DNA damage although the mechanism remains controversial (*148, 197*). The reduction of the protein (by knock-out in mESCs and by knock-down in human cell lines) causes hyper-sensitivity to γ-irradiation, X-ray, UV light, base damaging agents (e.g. MNNG), and replication inhibitors (e.g. hydroxyurea) (*134, 147*). Other phenotypes include reduction of γH2AX foci formation, as well as an increased frequency of chromosomal aberrations (*147*).

To date, there has not been any report on UHRF1's function in the FA pathway or its involvement in the DNA ICL repair. Given UHRF1's recognition of DNA ICLs *in vitro*, and its role in general DNA repair process, we hypothesized that it was also required in the FA pathway. DNA ICLs inducing agents, e.g. MMC and cisplatin, have been used to diagnose FA patients. FA cells demonstrate much higher sensitivity to DNA ICLs, and after damage has occurred, the cells have much more chromosomal breaks and chromatids exchange radials than aplastic anemia cells or healthy cells (*198, 199*). Hence, we decided to use the same

approach to measure the survival of cells when UHRF1 expression was reduced and to study whether UHRF1 is required for the FA pathway.

6.2 Results

6.2.1 Down-regulation of UHRF1 increases cellular sensitivity to MMC

To understand UHRF1's involvement in the FA pathway, we wanted to test the cell sensitivity to MMC when UHRF1 expression was reduced. We found that the KD of UHRF1 in 293T cells was generally not stable, probably due to its role in regulating cell contact inhibition. It has been discovered that when UHRF1 expression is disrupted, cell proliferation stops when cells are in contact with each other (*119*), which is a feature not present in normal 293T cells. As a result, the growth of cells with large degree of UHRF1 reduction was probably inhibited, while cells with higher amount of UHRF1 grew into dominance. Hence, we decided to use an inducible KD system in these cells.

We designed a single-plasmid tetracycline-controlled transcriptional activation (Tet-On) KD vector to introduce UHRF1 KD shRNA, based on the pSuperior (Oligoengine) vector system. In the pSuperior Tet-On system, the transcription of the shRNAs follows a Tet-response element. When pSuperior.shUHRF1 vector is transfected into tetracycline repressor (TetR) expressing cells, TetR binds to its Tet-response element, and the shRNAs transcription is blocked. Tetracycline or its derivative, doxycyline, when added onto the cells, will bind to TetR protein and release it from the Tet-response element, thus the transcription of shRNAs

can progress. Traditionally, TetR is generated from cells expressing a TetR expressing vector, and the pSuperior.puro construct will be transfected into those cells as a second step. Cells need to go through two rounds of antibiotic selection before forming a stable cell line for this purpose. To simplify the system, we cloned the TetR gene, together with its CMV promoter from pcDNA6/TR vector and inserted them into pSuperior.puro vector (Fig. 6.1). Therefore, through a single-step transfection and puromycin selection, we can obtain the cells that express both TetR and the shRNA construct.

Using this vector system, we established UHRF1 KD in HEK293T cells. Two shRNA sequences were introduced, sh2 and sh3. After the addition of doxycycline, the shRNA expression was activated. Cells were treated with or without doxycycline for 72hr before harvested for WB to test for the level of UHRF1. Both shRNA sequences reduced UHRF1 protein level efficiently (Fig. 6.2A, lane 2 compared with lane 1, and lane 4 compared with lane 3). We then performed survival assay using these cells, where the KD cells were maintained in doxycyline at the time of DNA damage treatment. Cells were seeded in a fixed amount in 6-well tissue culture plates. Different dosages of MMC were added after 24hr when the cells had adhered, and the colony formation was evaluated after 2 weeks. In all cell lines, the survival rate was gradually reduced as the dose of MMC increased. However, between 1-8ng/ml of MMC, both cell lines treated with doxycycline, sh2+Dox and sh3+Dox (Fig. 6.2B, the red and the purple curves) had about 20% lower survival than the control cells, sh2-Dox and sh3-Dox (Fig. 6.2B, the blue and the turquoise curves).

Figure 6.1

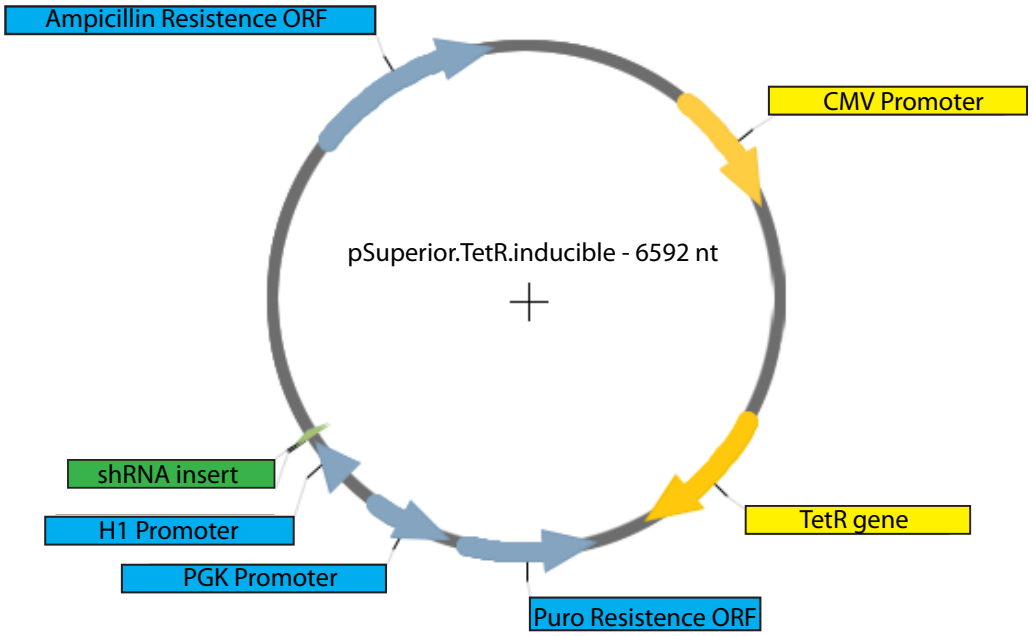

FIG. 6.1 **Generation of pSuperior.TetR inducible shRNA vector.** Schematic diagram shows the map of constructed pSuperior.TetR.inducible vector. TetR gene and CMV promoter were cloned from pcDNA6/TR vector and inserted into pSuperior.puro vector. shRNA sequence was to be inserted at position indicated, using HindIII and BglII sites.

Figure 6.2

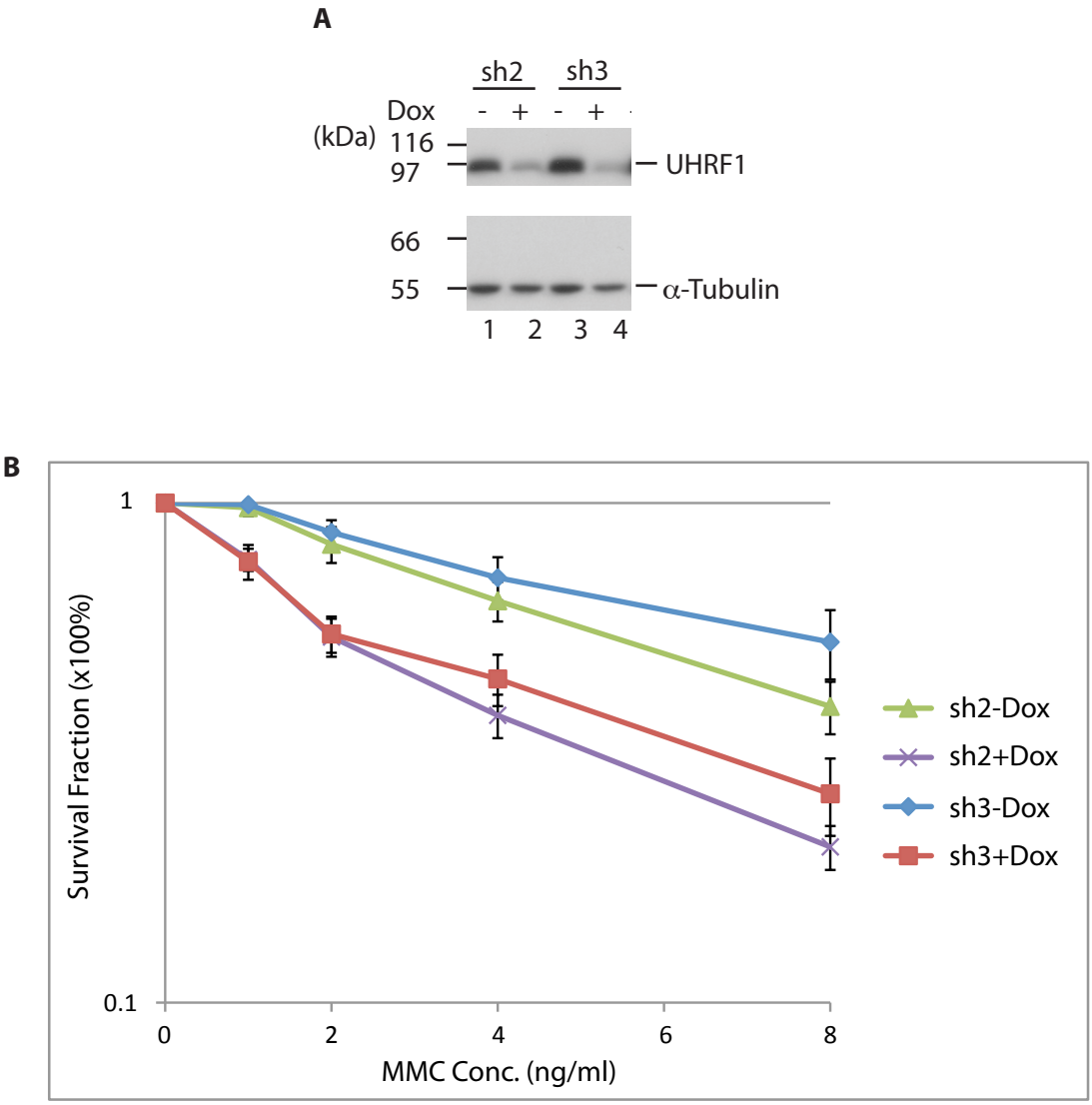

FIG. 6.2 **Inducible KD of UHRF1 in 293T cells leads to hypersensitivity to MMC. A.** WB shows the inducible KD (α-UHRF1: H8) using two shRNA sequences in 293T cells. Cells transfected with sh2 (lanes 1 and 2) and sh3 (lanes 3 and 4) vectors were grown with (lanes 2 and 4) or without (lanes 1 and 3) 10μg/ml doxycyline for 72hr before being harvested. Tubulin (α-α-Tubulin: DM1A) blot was used for a loading control; **B.** After the doxycyline treatment to reduce the protein level, cells (sh2±Dox, the blue and red curves, and sh3±Dox, the turquoise and the purple curves, as labeled) were seeded in a fixed amount in 6-well plates. Different dose of MMC, up to 32ng/ml was added into the culture after 24hr, and the cells were maintained for about 2 weeks. Then the survived colonies were counted and the survival rate was calculated. The survival percentage at 0ng/ml MMC treatment was normalized as 100%. The experiments were repeated three times with triplicates. Error bars indicate stand error.

To confirm this phenotype and to test if UHRF1 was sufficient for cells to endure DNA ICL damages, we repeated the experiment using a different cell line, HeLa, and introduced WT UHRF1 (tagged with Flag and HA) expression in the sh2 (target sequence in the untranslated region, 3'-UTR) KD cells (to see if it could reverse the hypersensitivity. This was also an additional test in case of any off-target effect generated by using shRNA KD. We were able to reduce UHRF1 expression constitutively using sh2 sequence in HeLa cells stably (Fig. 6.3A, lanes 1&2), and complemented with the WT protein to the endogenous level (Fig. 6.3A, lane 3). We noticed that HeLa control cells were generally more sensitive to MMC than HEK293T cells, which is probably due to the intrinsic characteristics between cell lines. We also observed a ~20% reduction of survival between the control and KD cells (Fig. 6.3B, the blue and the red curves). The survival rate was elevated back to the control level when the addition of WT protein complemented the UHRF1 expression (Fig. 6.3B, the green curve). Hence, we believe that UHRF1 is required for cells to tolerate DNA ICL damage.

6.2.2 UHRF1 can support DNA ICL tolerance independently from its function in DNA methylation

The maintenance of methylation is critical for normal protein expression, cell cycle progression, etc., and UHRF1 has been proposed as a link between DNA methylation and DNA repair (*148*). It is not clear if UHRF1 bears separate functions in both epigenetics and DNA repair, or if UHRF1 affecting DNA repair is a result of its effect on DNA methylation.

Figure 6.3

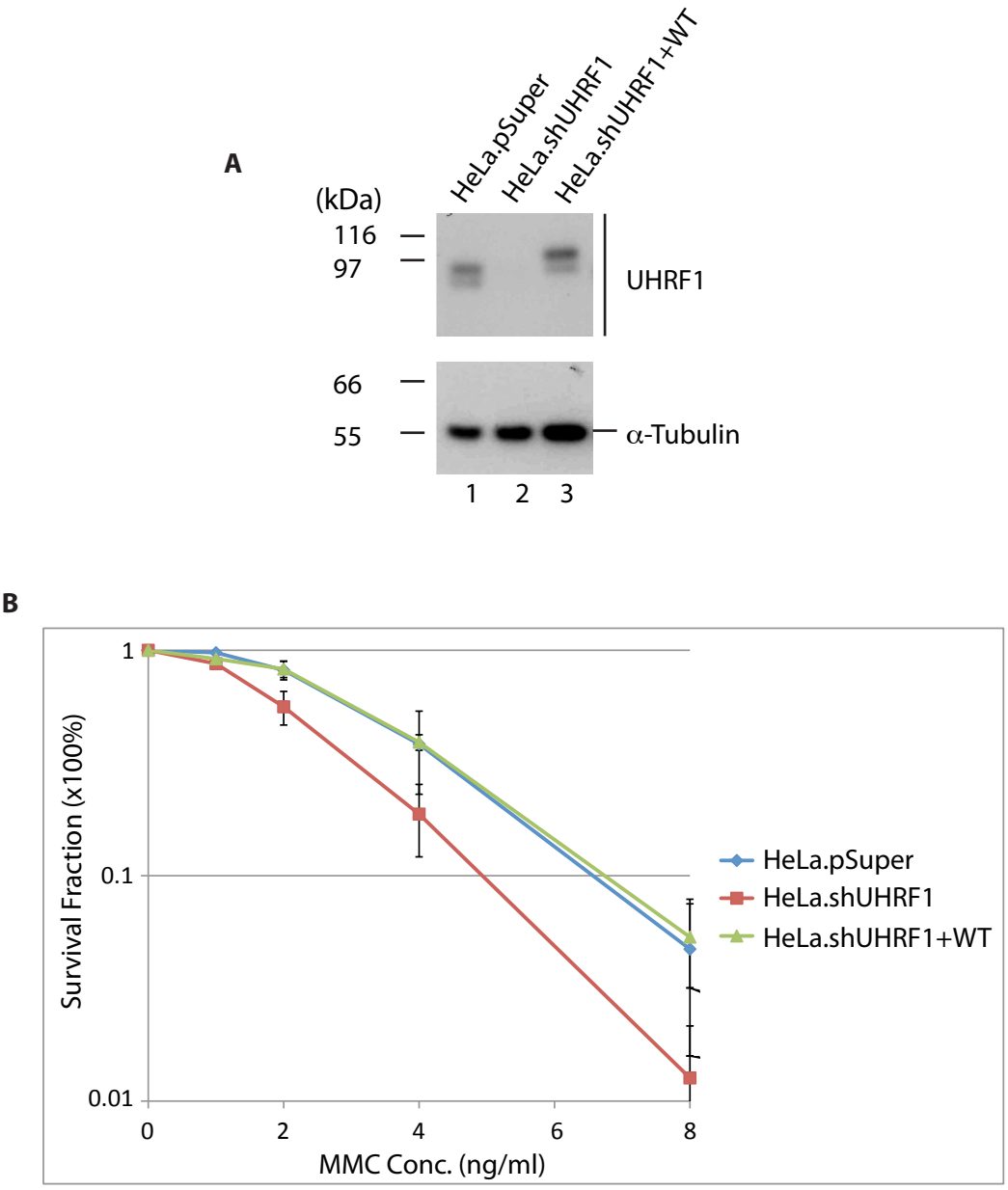

FIG. 6.3 **Constitutive KD of UHRF1 in HeLa cells leads to an increased sensitivity to MMC.** A. WB (α-UHRF1: H8) shows control cells with empty vector, HeLa.pSuper (lane 1), KD cells using sh2 sequence, HeLa.shUHRF1 (lane 2), and WT complemented cells, HeLa.shUHRF1+WT (lane 3). The complemented WT exogenous protein in lane 3 had Flag-HA tag, thus the shift from endogenous protein showing in lane 1. Tubulin (α-α-Tubulin: DM1A) blot was used as a loading control; **B.** The clonogenic assay shows the survival rates of HeLa.pSuper (the blue curve), HeLa.shUHRF1 (the red curve) and HeLa.shUHRF1+WT (the green curve) cell lines treated with different dosages of MMC. The experiment was repeated three times with triplicates within each experiment. Error bars indicate stand error.

We took advantage of two pairs of established cell lines: E14 (control) and *Uhrf1* knock-out mESCs, UKO (a generous gift from Dr. Haruhiko Koseki, RIKEN Institute of Allergy and Immunology, Yokohoma, Japan); as well as JI (control) and *Dnmt1*, *Dnmt3a* and *Dnmt3b* knock-out cell lines, TKO (a generous gift from Dr. Masaki Okano, RIKEN Centre of Developmental Biology, Kobe, Japan). UKO cells have normal level of DNMT1, but largely reduced genome-wide DNA methylation (*141*). They are hypersensitive to a series of DNA damage inducing agents (*134*). TKO cells have all three *Dnmt*s knocked out, but with UHRF1 expression unaffected. They have greatly lost DNA methylation genome-wide, but maintain the global chromatin structure (*130*). We could therefore compare the two pairs of cells survival rates under DNA damage stress, and determine whether the loss of methylation causes an increased sensitivity to ICL-inducing agents.

To investigate whether UHRF1's requirement in DNA ICLs repair is a secondary effect of its function in DNA methylation, we compared the sensitivity to MMC between the cells lack of UHRF1 expression and the cells lack of DNA methylation. The upper panel of the WB in Fig. 6.4A confirmed the normal UHRF1 expression in E14 cells and the loss of expression of UHRF1 in UKO cells. The WB in Fig. 6.4B showed the normal level of UHRF1 expression in both control J1 and DNMTs KO cells, TKO.

Figure 6.4

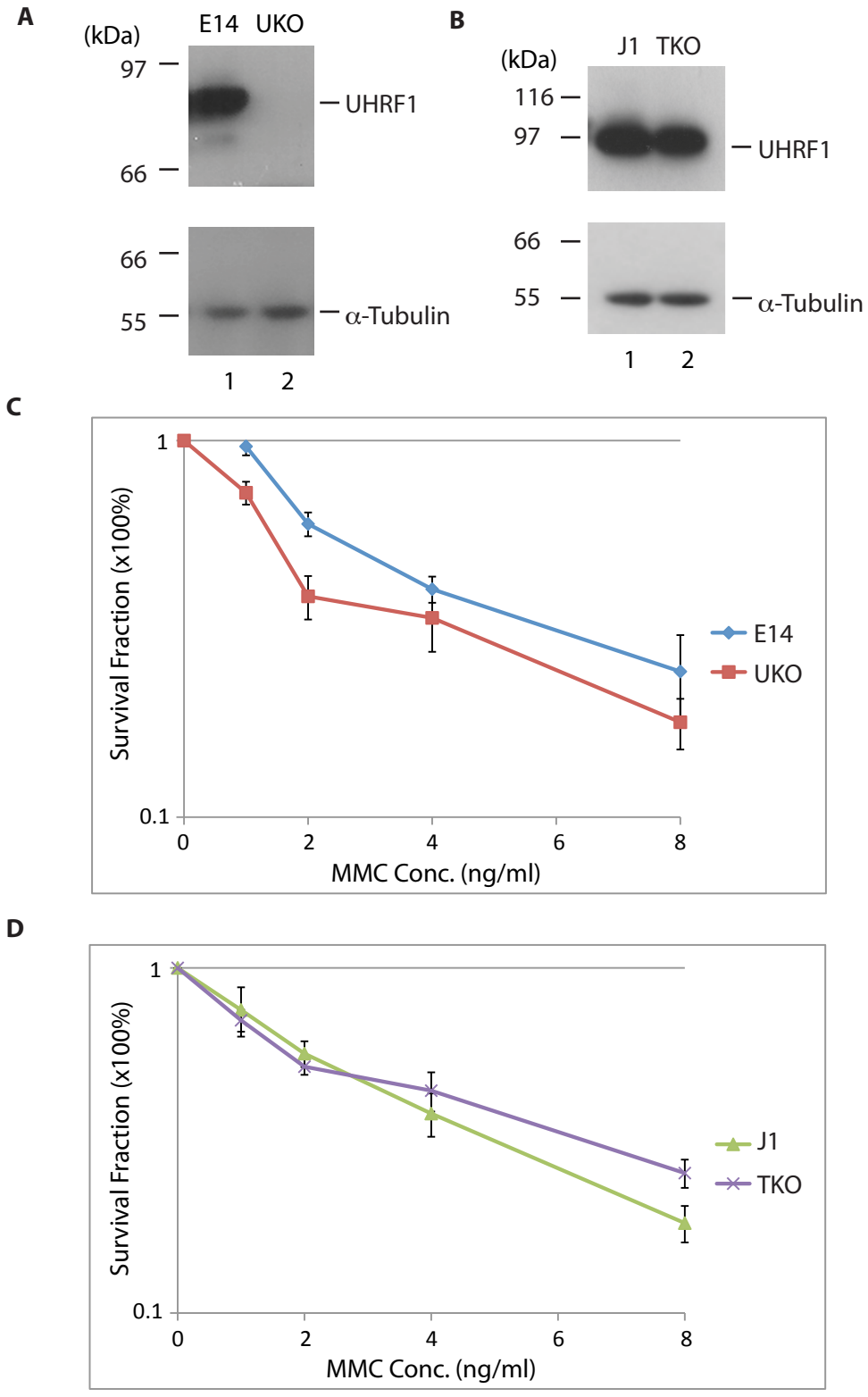

FIG. 6.4 **The loss of UHRF1 causes MMC hypersensitivity in cells independent of methylation defects. A.** WB shows the UHRF1 (α-UHRF1: H8) level of control, E14 cells, and UHRF1 KO, UKO cells. Tubulin (α-α-Tubulin: DM1A) blot was used as a loading control; **B.** WB shows no change of UHRF1 level in control, J1 cells, and DNMTs KO, TKO cells; **C.** The clonogenic assay shows that the survival rates of E14 and UKO cells, indicating that the loss of UHRF1 in mESCs sensitized the cells to MMC treatment; **D.** The clonogenic assay shows the survival curve of J1 and TKO cells, indicating that there was no major difference in MMC sensitivity when DNA methylation was defective. Experiments were repeated three times with triplicates within each experiment. Error bars indicate standard errors.

We used the same method to measure the MMC sensitivity of these two pairs of cell lines. UKO cells were more sensitive, i.e. ~20% reduction in survival, than E14 cells at 1 and 2ng/ml of MMC concentration (Fig. 6.4C). On the other hand, there was no difference on the survival rate between J1 and TKO cells at most of the MMC concentration tested. Towards the very high dose of MMC treatment, when both survival rates dropped below 20%, there may even be a slight increase of survival of the TKO cells (Fig. 6.4D). Since the genome-wide DNA methylation is significantly reduced in the TKO cells (*130*), we conclude that in these mESCs, the loss of DNA methylation did not result in hypersensitivity to DNA ICLs. Therefore, although UHRF1 has a significant role in maintaining genome-wide DNA methylation, it is likely to facilitate DNA ICL repair in a methylation independent manner. In future, it can be also important to introduce UHRF1 KD in TKO cells, to conduct epistasis analysis between UHRF1 and DNA methylation in response to DNA damage.

6.2.3 UHRF1 is epistatic with FANCD2 in the DNA ICL repair pathway

Although we think UHRF1 is required for DNA ICL repair, it is unclear whether it functions as part of the FA pathway. In the lab, we obtained two FA patient-derived cell lines, PD20, an immortalized patient derived FANCD2 deficient fibroblast cell line (*80*) and EUFA1421 (a kind gift from Dr. Johan de Winter, VU University Medical Center, Amsterdam, the Netherlands). PD20 cells have normal UHRF1 expression but are defective in FANCD2 expression (Fig. 6.5A, lanes 1&4), and the same is observed for EUFA1421 cells (Fig. 6.5B, lane 1).

Figure 6.5

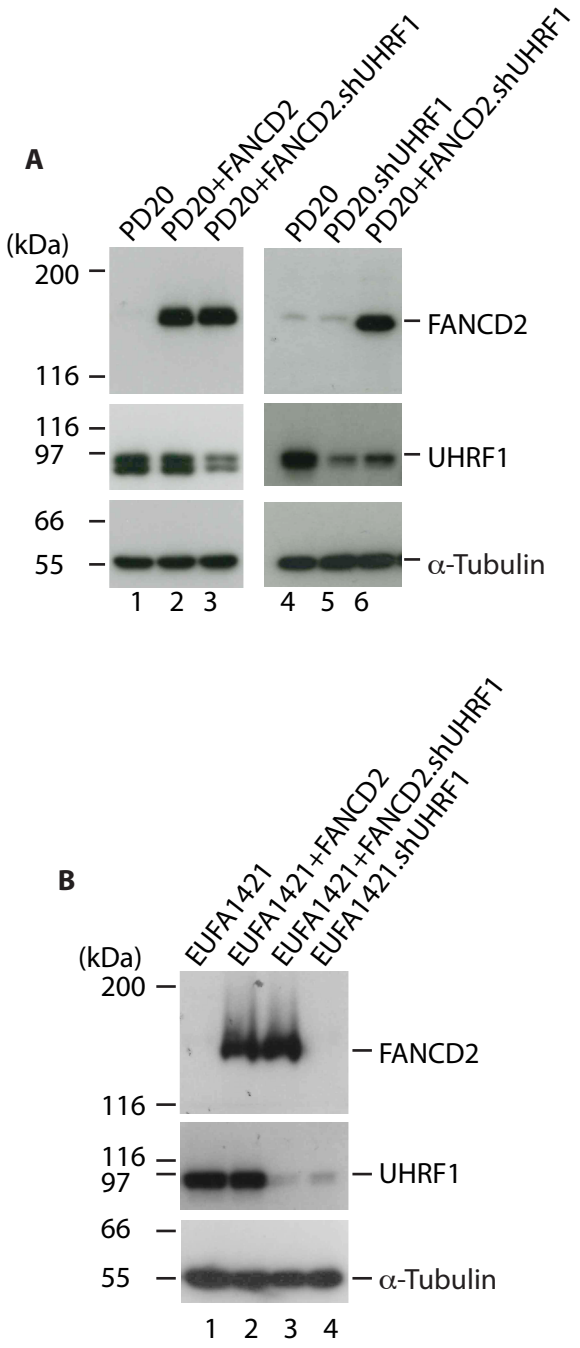

FIG. 6.5 **Complementation of FANCD2 and KD of UHRF1 in the FA patient-derived cell lines. A.** WB shows the expression level of FANCD2 (α-FANCD2: FI17) and UHRF1 (α-UHRF1: H8) in the patient derived FANCD2 deficient cells, PD20 (lanes 1 and 4), FANCD2 corrected cells, PD20+FANCD2 (lane 2), UHRF1 KD using sh2 sequence in FANCD2 corrected cells, PD20+FANCD2.shUHRF1 (lane 3 and 6), and UHRF1 KD in FANCD2 deficient cells, PD20.shUHRF1 (lane 5); **B.** WB shows the expression level of FANCD2 and UHRF1 in the patient derived FANCD2 deficient cells, EUFA1421 (lane 1), EUFA1421+FANCD2 (lane 2), EUFA1421+FANCD2.shUHRF1 (lane 3) and EUFA1421.shUHRF1 (lane 4). Tubulin (α-α-Tubulin: DM1A) blots were used as controls.

We expressed fully functional WT FANCD2 in PD20 and EUFA1421 to be used as control cells, where UHRF1 was at normal level and the FANCD2 expression was restored (Fig. 6.5A, lane 2, and Fig. 6.5B, lane 2, FANCD2 blot). UHRF1 KD vector, pSuper.UHRF1.sh2, was transduced into these control cells, and the UHRF1 level was reduced, as shown in PD20+FANCD2.shUHRF1 (Fig. 6.5A, lane 3) and EUFA1421+FANCD2.shUHRF1 (Fig. 6.5B, lane 3). Cells had disrupted expression for both proteins when pSuper.UHRF1.sh2 was introduced into PD20 and EUFA1421 cells (Fig. 6.5A, lane 5, and Fig. 6.4B, lane 4). Then we conducted epistasis analysis, measuring cell sensitivity to MMC using control cells, PD20+FANCD2 and EUFA1421+FANCD2, FANCD2 deficient cells, PD20 and EUFA1421, UHRF1 deficient cells, PD20+FANCD2.shUHRF1 and EUFA1421+FANCD2.shUHRF1, and FANCD2/UHRF1 double deficient cells, PD20.shUHRF1 and EUFA1421.shUHRF1 (the cell lines described above were generated by Dr. Martin Cohn).

In the presence of MMC, the survival of the FANCD2 deficient cell lines, i.e. PD20 and EUFA1421, was dramatically reduced (Fig. 6.6A&B, the blue and the red curves). The UHRF1 deficient cells were more resistant to the damage than PD20 and EUFA1421, but were more sensitive than the control cells (Fig. 6.6A&B, the green curves). We noticed that when treated with 0.5ng/ml of MMC, EUFA1421+FANCD2.shUHRF1 and EUFA1421.shUHRF1 cells are more sensitive than PD20+FANCD2.shUHRF1 and PD20.shUHRF1, whereas EUFA1421+FANCD2 cells are more resistant than PD20+FANCD2 cells. This could be a result of an increased level of KD of UHRF1 in the EUFA1421 cells, or PD20 cells had an alternative pathway to repair the damage, which was independent of UHRF1.

The double deficiency of FANCD2 and UHRF1 did not augment the extent of hypersensitivity to MMC. PD20.shUHRF1 and EUFA1421.shUHRF1 had a similar survival level as PD20 and EUFA1421 cells (Fig. 6.6A&B, the purple curves). This suggests that in cellular response to MMC, UHRF1 is epistatic with FANCD2, making it very likely to function within the FA pathway.

We noticed that there was still a fraction of UHRF1 remaining in the PD20+FANCD2.shUHRF1 and EUFA1421+FANCD2.shUHRF1 cells, in contrast to the FANCD2 expression in PD20 and EUFA1421 cells which was nearly absent (Fig. 6.5A, lane 1 vs. lane 3, and lane 4 vs. lane 6; and Fig. 6.5B, lane 1 vs. lanes 3/4). This might explain why there was less sensitivity of UHRF1 KD cells to MMC than the FANCD2 deficient cells, although they were epistatic. However, it is also possible that after the activation of FANCD2, there could be a repair pathway of ICLs that is independent of UHRF1, and therefore UHRF1 KD would lead to a less severe phenotype than FANCD2 deficiency.

6.2.4 UHRF1 SRA domain is required for its function in the FA pathway

Since UHRF1 specifically binds to DNA ICLs, and it is required in the FA pathway, we hypothesize that it facilitates repair by recognizing the ICLs as the first step. To test this hypothesis, we attempted to mutate regions that were responsible for DNA binding, and to study whether these mutations could cause DNA ICLs repair failures.

Figure 6.6

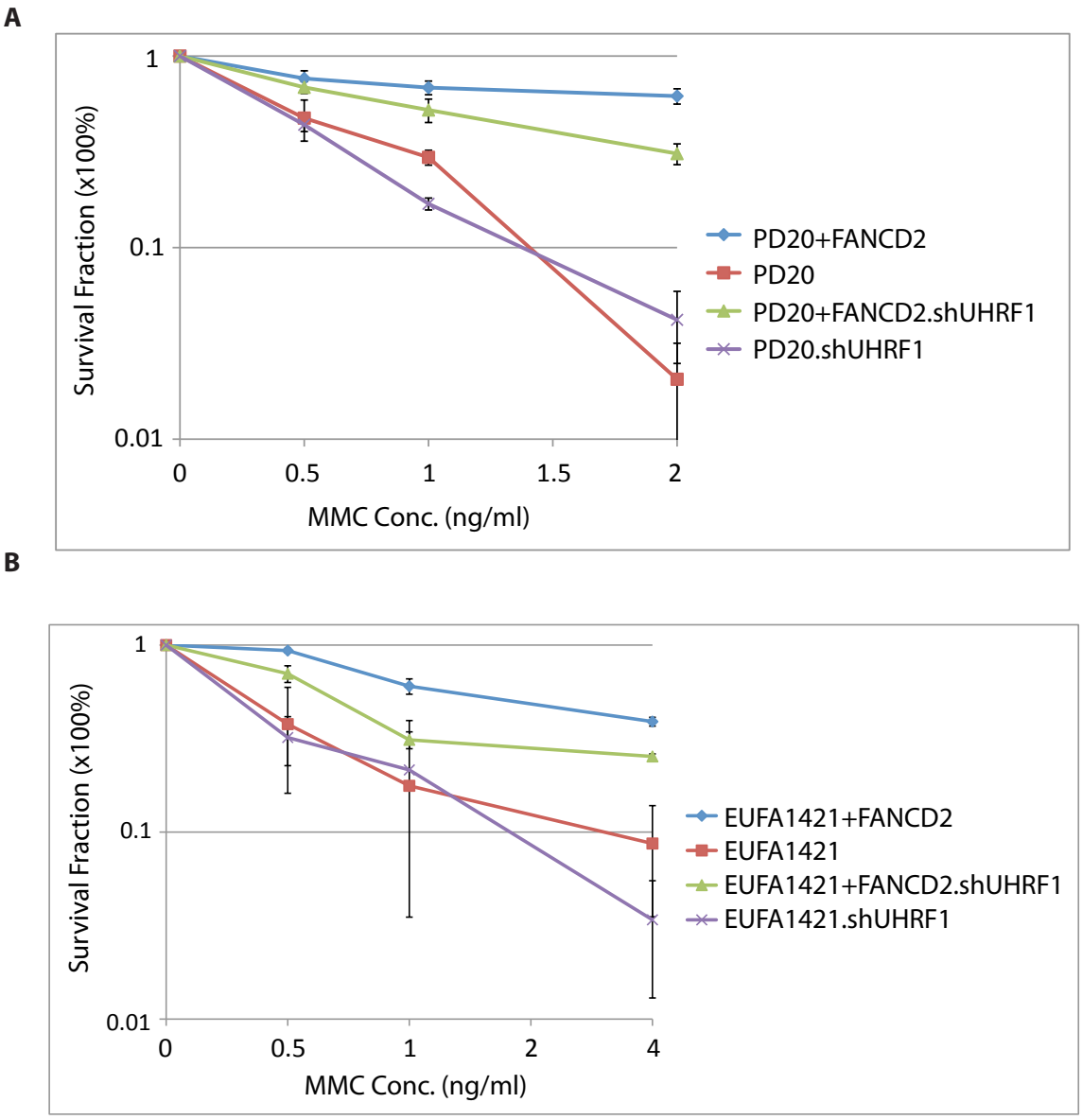

FIG. 6.6 **UHRF1 is epistatic with FANCD2 in DNA ICLs repair. A&B.** Epistatic survival assay shows that UHRF1 KD in FANCD2 corrected cells were more sensitive to MMC than the control cells (PD20+FANCD2 and EUFA1421+FANCD2), but less sensitive than FANCD2 deficient cells (PD20 and EUFA1421). The double-deficiency in the cells did not increase the sensitivity further (PD20.shUHRF1 and EUFA1421.shUHRF1). Experiments were repeated for three times in triplicates, and the representative data is shown here. Error bars indicate standard deviation.

In collaboration with Chih-Chao Liang, we introduced two SRA domain mutants, D482G and R504A (both were tagged with Flag and HA), with point mutations on the amino acid sites that are believed to be important for DNA binding based on the structure study of the SRA domain (*139, 140*). It has been confirmed that both of the mutations reduced UHRF1's interaction with DNA and abolished the specificity to hemi-methylated DNA (Chih-Chao Liang, Fig. 6.7A), but do not affect its auto-ubiquitination activity compared with the WT (Fig. 6.7B, lanes 4&5).

We expressed these two mutants into the UHRF1 KD cells in HeLa cells to a physiological level (Fig. 6.8A, lanes 4&5), and the two mutants were slightly more abundant in the cells than the WT complemented (Fig. 6.8A, HA blot, compared to lane 3). Survival assay was performed in parallel with the experiment described previously (Fig. 6.3B). UHRF1 KD cells were about 20% more sensitive to MMC treatment than control cells when using low dosage (Fig. 6.8B, the blue and the red curves). SRA mutant D482G failed to rescue the sensitivity back to the control level, and the survival rate was similar to the KD cells (Fig. 6.8B, the green curve). The mutant R504A also failed to rescue the KD phenotype, and it appeared to be even more sensitive than the KD cells (Fig. 6.8B, the purple curve), possibly suggesting a dominant negative effect. These data indicate that the SRA domain is critical for UHRF1's function in DNA ICLs repair, consistent with our hypothesis that its direct interaction with the cross-linked DNA supports its function. It would also be important in future to introduce a series of point mutations in the SRA domain to analyze whether the residues recognizing hemi-methylated DNA are the same to recognize DNA ICLs.

Figure 6.7

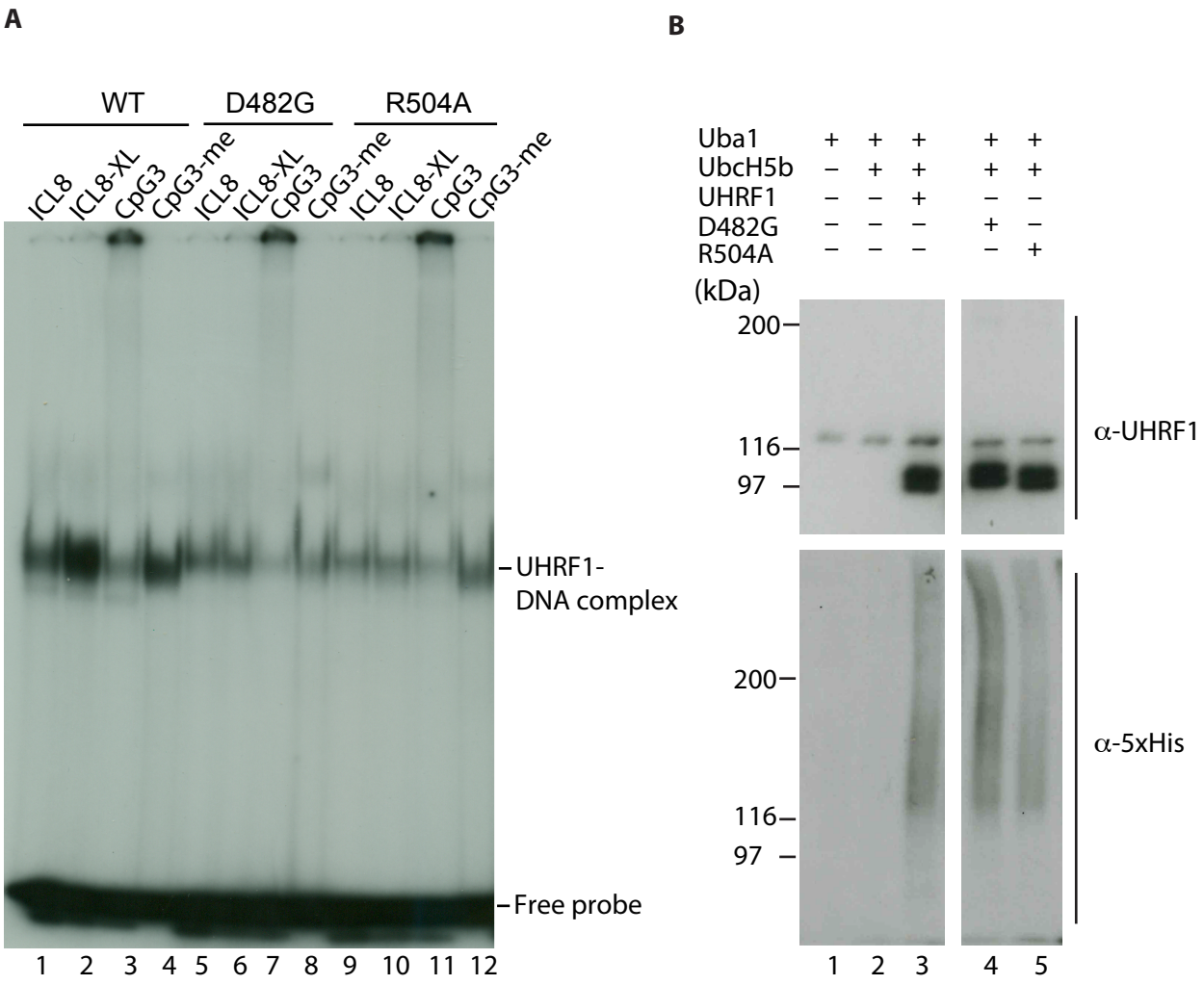

FIG. 6.7 **SRA domain mutations abolish the protein DNA binding specificity, but retain its ubiquitination activity. A.** EMSA shows that two point mutations of the SRA domain, D482G and R504A, abolished the specific binding to ICL8-XL and CpG3-me (lanes 5-8 and lanes 9-12), compared with the WT (lanes 1-4). This experiment was performed by Chih-Chao Liang; **B.** *In vitro* ubiquitination assay shows that the two mutations did not affect UHRF1 auto-ubiquitination activity (lanes 4&5). The WT protein auto-ubiquitination was used as a positive control. The WT and mutant proteins in the reactions are shown in α-UHRF1 (H8) blot, and the ubiquitination product is shown in α-His (34660, for ubiquitin) blot.

Figure 6.8

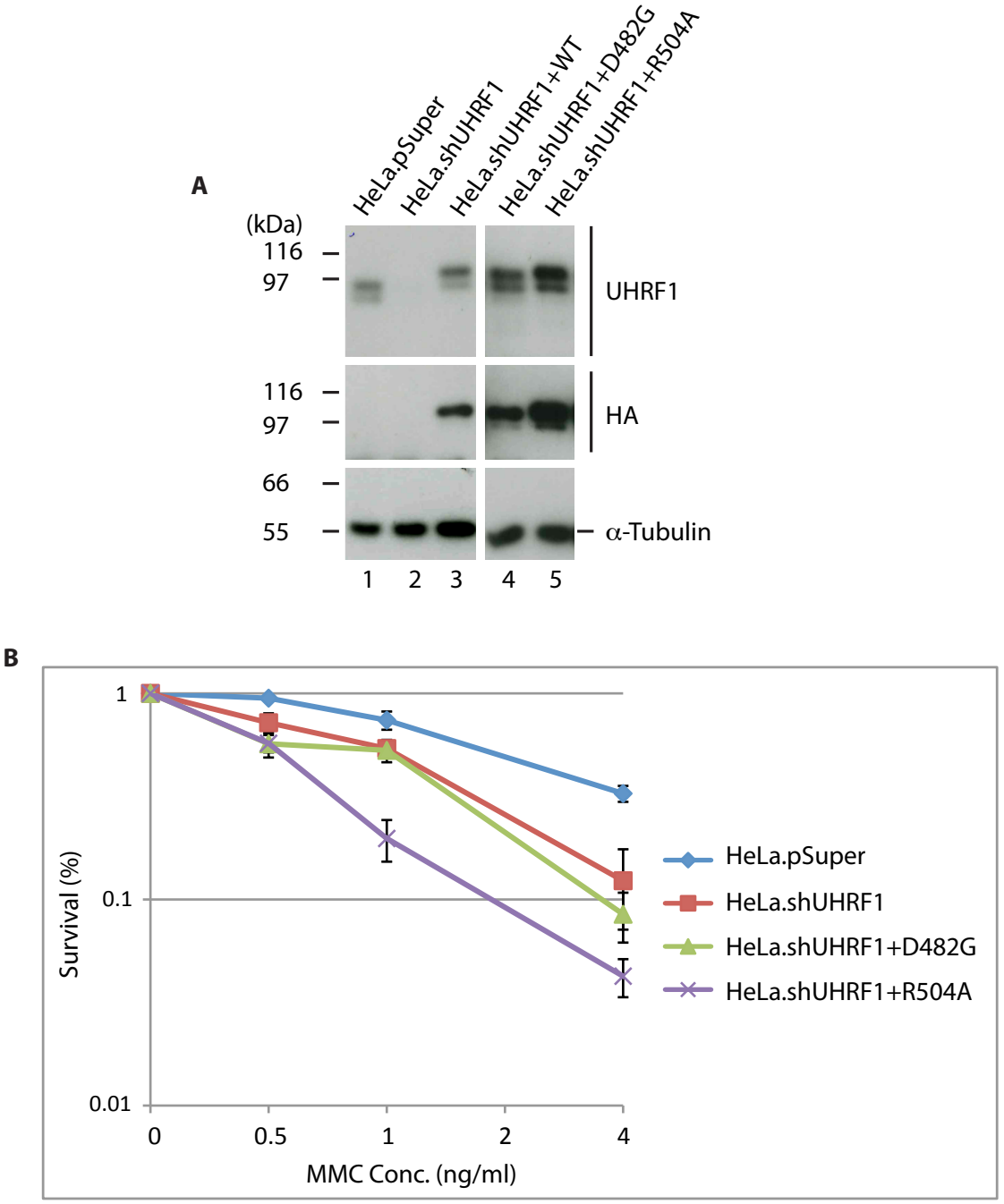

FIG. 6.8 **SRA domain is required for UHRF1's function in the FA pathway. A.** WB shows the expression of exogenous UHRF1 WT and SRA mutant proteins (lanes 3-5) in complementation of the KD (lane 2) in HeLa cells. The UHRF1 (H8) blot includes both the endogenous and exogenous proteins, and the HA (12CA5) blot shows only the exogenous proteins. Tubulin (α-α-Tubulin: DM1A) was used as a loading control. Samples for lanes 1-5 were loaded in the same gel; **B.** MMC survival assay shows that HeLa.shUHRF1 was more sensitive than HeLa.pSuper control cells (the blue and the red curves), and the two SRA mutants could not rescue the hypersensitivity (the green and the purple curves). The R504A mutant caused an even higher sensitivity than UHRF1 KD cells (the purple curve). The experiment was repeated twice with triplicate. Error bars indicate stand error.

RING finger motif was first identified as a zinc binding motif with DNA binding activity, although subsequent studies show that it mediates protein-protein interaction and bears E3 ubiquitin ligase activity (*200*). As the RING domain may also be important for UHRF1's DNA binding activity (Fig. 5.6), and possibly required for the recognition of ICLs, it will be important to measure the effect on cell survival to ICL-inducing agents when the RING domain is disrupted. We have not been able to express the RING domain mutants stably in the HeLa KD cells. One possibility is that although they can be expressed and purified from Sf9 cells, they are not functionally stable in the human cell lines. It may help in future if we introduce the mutants in the inducible KD system instead. Since the SRA mutants are fully defective in rescuing the hypersensitivity of UHRF1 depleted cells, it is likely that some of the RING domain mutants, that reflect the DNA binding defects as we observed in ΔRING mutant, have similar phenotype. Future work is needed to demonstrate the relationship between SRA and RING domains in UHRF1's function in the FA pathway.

From the epistatic analysis, we demonstrated that in the process of DNA ICLs repair, UHRF1 was epistatic with FANCD2, which makes it highly possible that UHRF1 functions within the FA pathway. In the lab, we have established Flag-HA tagged UHRF1, FANCD2 and FANCI expressing HeLa S3 cell lines (in collaboration with Dr. Martin Cohn and Chih-Chao Liang). To date, there has not been detectable direct interaction of UHRF1 with FANCD2 or FANCI by immuno-precipitation followed by WB (Dr. Martin Cohn, Fig. 6.9, panel 1), although we could pull-down FANCD2 by FANCI, and pull-down FANCI by FANCD2, efficiently (panels 2&3). From *in vivo* experiments, it seems that there is some degree of

interaction between UHRF1 and ubiquitinated FANCD2 detected by mass-spectrometry (Chih-Chao Liang, unpublished data). However, the interaction is very mild and possibly indirect. As UHRF1 is a very abundant protein in the cells, and bears other epigenetic functions, the fraction of the protein directly interacting with FA proteins could be relatively small. It may require the presence of DNA, histones or some other protein factors.

6.3 Discussion

UHRF1 has been placed in the DNA repair process by many studies. The degree of the survival reduction in response to MMC is similar to reported treatment such as HU and γ-irridiation (*134, 147*), whereas UHRF1 disruption in mESCs seems to cause a more severe sensitization to UV and MNNG (*134*). Since UHRF1 can recognize both hemi-methylated and inter-strand cross-linked DNA, it may generally have a higher affinity to modified DNA structures, and is required for other DNA repair pathways as well. The increased sensitivity to a variety of DNA damage inducing agents is also observed in some of the characterized FA deficient cells (*57-59, 61*). It has been suggested that the FA pathway can coordinate other types of DNA damage repair processes, for example DNA double-strand break repair, by regulating both recombinational and non-recombinational activity (*61, 201, 202*). It is possible that UHRF1 is essential in regulating different steps of the repair process upon initiation, depending on the cell cycle and its interaction with histones or other DNA repair proteins, and therefore entails its requirement in other types of DNA damage repair as well.

Figure 6.9

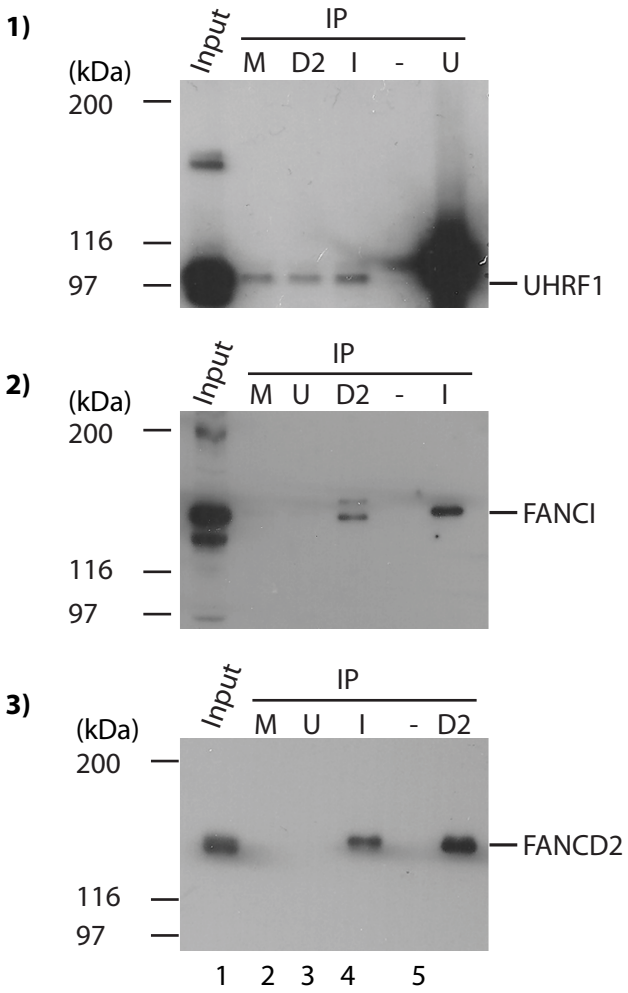

FIG. 6.9 **No direct interaction of UHRF1 with FANCD2 or FANCI observed.** Immuno-precipitation experiment using anti-Flag M2 agarose beads from Flag-HA tagged FANCD2, FANCI and UHRF1 expressing HeLa.S3 cells. HeLa.S3 cells were used as mock purification. 20μg of cell lysate was used as input in lane 1. For lanes 3, 4 and 5: 1) Flag-IP from FANCD2, FANCI and UHRF1 expressing cells, blotting against UHRF1 (H8); 2) IP from UHRF1, FANCD2 and FANCI expressing cells, blotting for FANCI; 3) IP from UHRF1, FANCI and FANCD2 expressing cells, blotting for FANCD2 (FI17). There was 30% of total IP product loaded in lanes 3&4, and 3% in lane 5, in all three panels. This experiment was performed by Dr. Martin Cohn.

Our data suggest that the loss of DNA methylation does not sensitize cells to DNA ICLs damage. However, the knock-out of *Uhrf1* causes an increased sensitivity to MMC, indicating that UHRF1 is required for DNA ICL tolerance independent of DNA methylation. In fact, although UHRF1 has been shown to be critical for DNA methylation maintenance in mESCs (*131*), knock-out of *Dnmt1*, the downstream effector of UHRF1, only causes about 10% of loss of CpG methylation in HCT116 cells (*203*). Therefore it is possible that in the HeLa and HEK293T cell based assays, the effect on DNA methylation caused by UHRF1 KD is very mild, and yet the cells are much more sensitive to MMC than the control cells. However, when DNMT1 and UHRF1 were depleted in human colon carcinoma cells (HCT116), the cells present mitotic catastrophe, suggesting that UHRF1 may be more important for maintaining genomic integrity in these cells than mESCs (*148, 197, 203*), which could also explain the attenuated hypersensitivity we observed in UKO cells compared with UHRF1 KD in HeLa or HEK293T cells.

It is expected that if the SRA domain were critical for DNA ICLs recognition, the mutations of the domain would abolish the protein's function in DNA repair. In general, RING finger motif does not only possess E3 ligase activity, it may bear different functions depending on the protein. In some cases, the integrity of RING domain for maintaining protein-protein interaction is more important than for its ubiquitin ligase activity (*204, 205*). It will be an important next step to determine the regions that are responsible for DNA binding versus E3 ligase activity, and therefore dissect the mechanism of UHRF1's role in the FA pathway.

Chapter 7 *In vivo* characterization of UHRF1 (Part 2): UHRF1 is required for FANCD2 recruitment in response to DNA ICLs

7.1 Introduction

The repair of DNA ICLs requires an intact FA pathway (*107*). The phosphorylation of FANCD2 by ATM and ATR is considered as the first step of the pathway activation (*99, 206*). Phosphorylated FANCD2 is subject to monoubiquitination (*61, 207*), and the ubiquitinated form of FANCD2 has been regarded as a marker of an activated pathway (*107*). Eight proteins (FANCA, B, C, E, F, G, L and M) have been identified to compose the FA core complex, which acquire an E3 ubiquitin ligase activity from FANCL, and mutations of these components can result in failure of FANCD2 activation and recruitment to the sites of DNA damage (*78, 94, 107, 165, 208*).

Although the FA core complex has been proposed to associate with chromatin to some degree in the absence of DNA ICLs (*209*), it is generally believed that FANCD2 is not ubiquitinated or does not form nuclear foci without DNA damage, except a mild activation during replication (*106, 107, 206*). It is unclear how FANCD2 is ubiquitinated in response specifically to DNA ICL damage. Should UHRF1 act as a detector of ICLs, it is possible that UHRF1 regulates FANCD2 ubiquitination. We examined the FANCD2 ubiquitination in UHRF1 KD cells using UVA irridiation in combination with psoralen (PUVA) to introduce ICLs

besides MMC. PUVA creates specific ICLs, and has also long been used for treating skin diseases and for diagnostic differentiation of FA patient cells (*210, 211*).

Many other proteins involved in the FA pathway also form nuclear foci in response to DNA damage, such as FANCA, FAN1, SLX4, etc. (*102, 212, 213*). UHRF1 forms the most distinctive foci during S phase (*117, 118*), although it also has a strong association with heterochromatin independent of cell cycle (*214*). No change in foci formation of UHRF1 is observed using whole cell γ-irridation (*117*), however, when using UV laser in combination with 5-iodo-2-deoxyuridine to introduce localized strand breaks, UHRF1 is recruited to the damage stripes (*148*). It is unknown whether UHRF1's direct interaction with cross-linked DNA *in vitro* can translate into its recognition of ICLs *in vivo*. To answer this question, we conducted immuno-fluorescence microscopy to study whether UHRF1 also formed nuclear foci after ICLs damage.

There has been evidence showing that down-regulation of UHRF1 causes reduction of γH2AX foci formation when double-strand breaks are introduced by γ-irradiation (*147*). γH2AX foci formation is one of the first DNA damage responses, and it is important for the recruitment of several DNA repair factors (*215*). Studies have shown that FANCD2 co-localizes with γH2AX when treated with MMC, and the phosphorylation of H2AX may be required for FANCD2 localization to sites of DNA damage (*216, 217*). However, the mechanism of the recruitment of FANCD2 and downstream repair proteins precisely to the sites of damage remains elusive. Under our hypothesis, if UHRF1 recognizes DNA ICLs

directly and facilitates the FA pathway, it may play a role as a link between the occurrence of DNA ICLs and the repair process by recruiting FANCD2 to the cross-link sites. Hence, we studied the FANCD2 foci formation in UHRF1 KD cells complemented with an SRA domain mutant, to investigate whether UHRF1 recruits FANCD2 to DNA ICLs through its direct recognition of the damage.

7.2 Results

7.2.1 The main role of UHRF1 in the FA pathway does not lie within the regulation of FANCD2 ubiquitination

We treated control HeLa.pSuper and UHRF1 KD HeLa.shUHRF1 cells with 50mJ/cm^2 UVA after 2hr of incubation with 50ng/ml psoralen. Cells were harvested for whole cell lysate after the indicated amount of time for recovery (Fig. 7.1A). From the UHRF1 blot, we could see the level of the protein was reduced by shRNA in HeLa.shUHRF1 cells. For HeLa.pSuper cells, FANCD2 was gradually ubiquitined following the time course (Fig. 7.1A, lanes 1-5). After 6hr of recovery, the ratio of ubiquitinated FANCD2 versus non-ubiquitinated FANCD2 reached about 1:1 in control cells (lane 4), and there was more ubiquitinated than non-ubiquitined form after 8hr of recovery (lane 5). For HeLa.shUHRF1 cells, we also observed the gradual increase of FANCD2 ubiquitination (Fig. 7.1A, lanes 6-10). However, the activation seemed to be slightly delayed, where the ubiquitination level after 8hr recovery was close to 4hr of recovery of the control cells (lane 10 compared with lane 3). The

ubiquitinated FANCD2 never reached the same level as the non-ubiquitinated form. This experiment indicates that although the ubiquitination of FANCD2 is not abolished, there is a degree of reduction when the expression of UHRF1 is reduced.

To investigate whether UHRF1 affects FANCD2 ubiquitination in response to other DNA ICL inducing agents, we used MMC as an alternative treatment. Suspension HeLa.S3 cells were transfected with the pSuperior.TetR.shUHRF1 vector, and in response to doxycycline, UHRF1 expression was reduced (Fig. 7.1B, lanes 6-10 compared with lanes 1-5). Cells were treated with 160ng/ml of MMC, which has been shown to activate DDR effective in mitotic cells (*106*), for indicated period of time. In the control -Dox cells, the ubiquitination of FANCD2 peaked at 4hr when about 50% of the protein was ubiquitinated, and persisted till the 8hr (lanes 3-5). However, the same dynamic was also observed in the +Dox cells, in which the ubiquitination of FANCD2 also peaked at 4hr (lane 8). We noticed that in the MMC treatment, the final ratio of ubiquitinated FANCD2 versus non-ubiquitinated FANCD2 was lower than in the PUVA treatment (Fig. 7.1B, lane 5 compared with Fig. 7.1A, lane 5), even with longer treatment or an increased dosage of MMC up to 240ng/ml (data not shown). It is possible that PUVA causes mainly ICLs, but less other types of DNA damage as seen from cells treated with MMC, and therefore has a more specific activation of the FA pathway. If so, some of the ICL repair phenotype defects in UHRF1 KD cells may be shielded for this reason.

Fig. 7.1

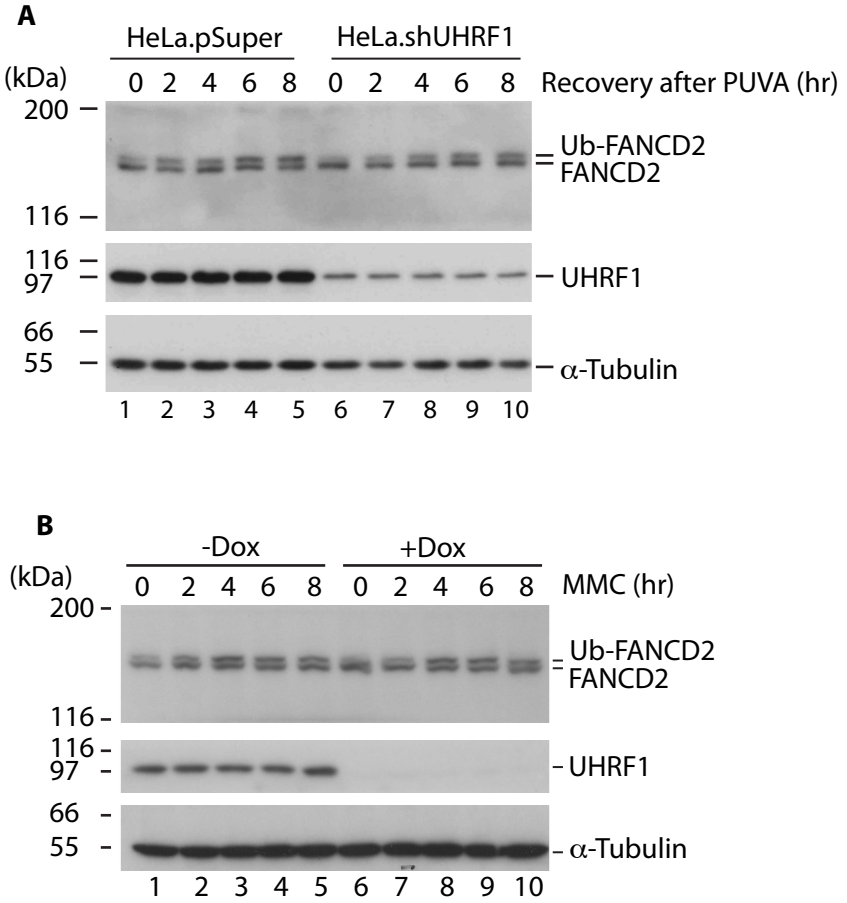

FIG 7.1 **UHRF1 only partially regulate FANCD2 ubiquitination in response to PUVA treatment. A.** HeLa.pSuper and HeLa.shUHRF1 cells were incubated with 50ng/ml of psoralen for 2hr first, and then irridated by 50mJ/cm^2 UVA. Following indicated amount of time for recovery, cells were harvested and processed for whole cell extract. UHRF1 (H8) WB demonstrates the degree of KD in the HeLa.shUHRF1 (lanes 6-10) compared with the control cells (lanes 1-5). FANCD2 (FI17) blot shows the level of ubiquitination in response to the treatment. Tubulin (α-α-Tubulin: DM1A) was used as a loading control; **B.** HeLa.S3.TetR.shUHRF1 cells were treated with (lanes 6-10) or without (lanes 1-5) doxycyline before the addition of MMC. Cells were harvested at the indicated time points for WB.

As we observed a discrepancy of FANCD2 ubiquitination dynamics in UHRF1 KD cells in response to different DNA damage treatments, we hypothesized that the main function of UHRF1 in the FA pathway may not be regulating the ubiquitination of FANCD2. Since it is believed that FANCD2 is ubiquitinated and recruited to the nucleus after DDR activation, we next addressed whether the nuclear recruitment of ubiquitinated FANCD2 was compromised when UHRF1 was down regulated. After MMC treatment, we separated the cells into cytoplasmic and nuclear fractions, to follow the nuclear enrichment of the ubiquitinated protein. Shown in Fig. 7.2A, the nuclear fraction of control cells (-Dox) and UHRF1 KD (+Dox) cells, which were treated with MMC, was analyzed by WB. In both control and KD cells, we noticed an increase of the ubiquitinated form of FANCD2 (lanes 1-5 and lanes 6-10). There might be slightly less of FANCD2 in the KD cells than the control cells at time point 9hr and 24hr, although the difference was very minimal (lanes 4&5 compared with lanes 9&10).

We also used the same way of fractionation to evaluate the FANCD2 ubiquitination and nuclear enrichment in PD20 corrected cell lines, PD20+FANCD2 and PD20+FANCD2.shUHRF1. Possibly due to the high level of FANCD2 expression in these corrected cell lines, FANCD2 ubiquitination has been difficult to observe using whole cell lysate (Dr. Yasunaga Yoshikawa, unpublished data). By using cytoplasmic and nuclear fractionation, we could remove the majority of non-ubiquitinated FANCD2 in the cytoplasm, which was why only ubiquitinated FANCD2 was detected in the nuclear extract in HeLa cells (Fig. 7.2A). However, as FANCD2 was expressed at a much higher level in

PD20+FANCD2 cells, we could not eliminate the non-ubiquitinated FANCD2 entirely, and there was still some left in the nuclear fraction (Fig. 7.2B). Nevertheless, we could observe an increase of exogenous FANCD2 ubiquitination in the corrected PD20 cells. The ratio of ubiquitinated versus non-ubiquitinated FANCD2 is about 1:1 in PD20+FANCD2 cells without the treatment of MMC (Fig. 7.2B, lane 1). The ubiquitinated FANCD2 accumulated in the nuclear fraction following the MMC time course, and reached a higher amount than non-ubiquitinated FANCD2 at 9hr (lane 4). In the UHRF1 KD cells, the ubiquitinated form of FANCD2 was nearly undetectable without the treatment of MMC (lane 5). There was also an increase of ubiquitination, and it reached the same level as the non-ubiquitinated FANCD2 at 9hr (lane 8), which was slightly less than in the control cells. We noticed that in the cells expressing UHRF1 KD shRNA, the degree of KD observed in the nuclear fraction (Fig. 7.2B, lanes 5-8) was less than in the whole cell lysate (Fig. 6.5A, lanes 3, 4 and 6). It is possible that as UHRF1 functions mainly inside the nucleus, when the overall level of the protein is largely reduced, the remaining population becomes more retained in the nucleus to preserve some of the normal activities of the cell.

From the data above, it appears that UHRF1 has very minor regulatory effect on the ubiquitination of FANCD2, or the nuclear enrichment of ubiquitinated FANCD2. However, it remains questionable how ubiquitinated FANCD2 is localized to the damage. Should UHRF1 recognize DNA ICLs, it may be involved in the recruitment of FANCD2 to precise locations, anchoring the ubiquitinated protein to the sites of damage.

Fig. 7.2

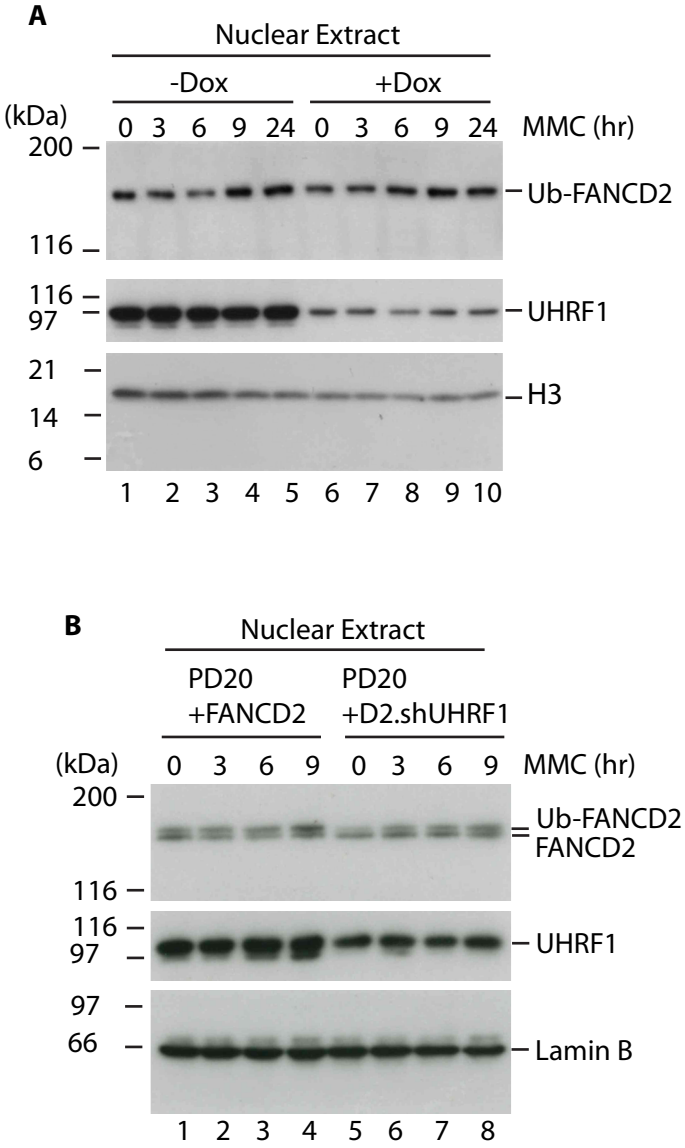

FIG 7.2 **UHRF1 marginally affects the nuclear enrichment of ubiquitinated FANCD2 in response to MMC. A.** The UHRF1 KD in HeLa.S3.TetR.shUHRF1 was introduced by doxycyline, and the cells were treated with MMC. Cells were harvested and subject to cytoplasmic and nuclear fractionation at the indicated time points. The nuclear extract was analyzed, and the WB shows the nuclear enrichment of ubiquitinated FANCD2 (α-UHRF1: H8; α-FANCD2: FI17). Histone H3 (Ab12079-100) was used as a loading control; **B.** PD20+FANCD2 (lanes 1-4) and PD20+FANCD2.shUHRF1 (lanes 5-8) were treated with MMC. Cells were harvested at the indicated time points and fractionated. The exogenous FANCD2 ubiquitination was shown in the nuclear fraction in response to the MMC treatment. Lamin B (sc-6216) was used as a loading control.

7.2.2 UHRF1 is required for FANCD2 foci formation in response to MMC

It has been demonstrated that FANCD2 accumulates at nuclear foci in response to DNA damage, and the increase of the foci formation coincides with FANCD2 ubiquitination, suggesting that the protein is recruited to the sites of damage (*107*). Therefore, we used immuno-fluorescence antibody staining in the cells after treatment of MMC to observe the foci formation of FANCD2 and to study the effect on FANCD2 recruitment when the expression of UHRF1 was reduced. To be able to better visualize the foci formation of nuclear enriched protein, the cytoplasmic fraction of the cells was extracted away before the cells were fixed for staining. Fig. 7.3 shows the endogenous level of UHRF1 in HeLa.pSuper cells (Fig. 7.3, panel b), and the remaining UHRF1 after the KD (panel e). We treated these two cell lines with 160ng/ml MMC for a time course up to 9hr. In the control cells, the number of cells with FANCD2 foci increased after 3hr of MMC treatment, and it continued to increase up to 9hr (Fig. 7.4A, panels b, e, h and k). The quantification of the percentage of cells with FANCD2 foci is shown in Fig. 7.4B. The positive cells increased from 22% at time 0 to 66% after 9hrs. In the UHRF1 KD cells, most of the FANCD2 foci formation was absent, although some cells did respond to the treatment at the end of the time course (Fig. 7.4A, panels n, q, t and w). The quantification of positive cells showed that the population with FANCD2 foci in the KD cells only increased from 12% to 22% during this time course (Fig. 7.4B).

Fig. 7.3

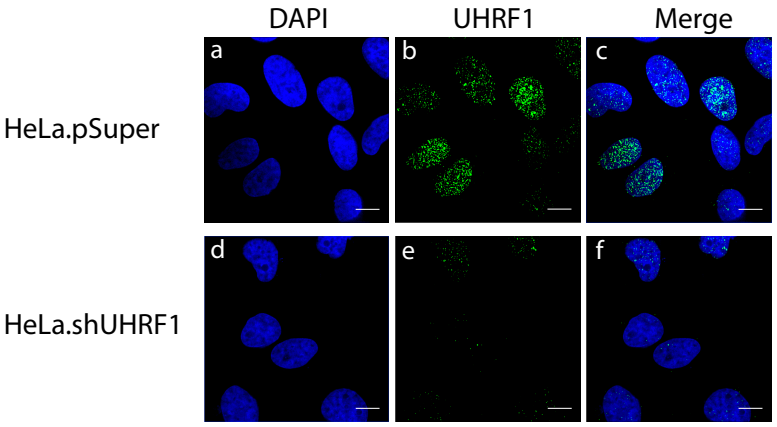

FIG 7.3 **The KD of UHRF1 in HeLa cells confirmed by IF.** HeLa.pSuper and HeLa.shUHRF1 cells were stained with UHRF1 antibody (H8). DAPI was used to stain the nuclear area. The microscopy images demonstrate the level of KD in HeLa.shUHRF1 cells (panel e compared with panel b). Scale bars represent 10μm.

Fig. 7.4

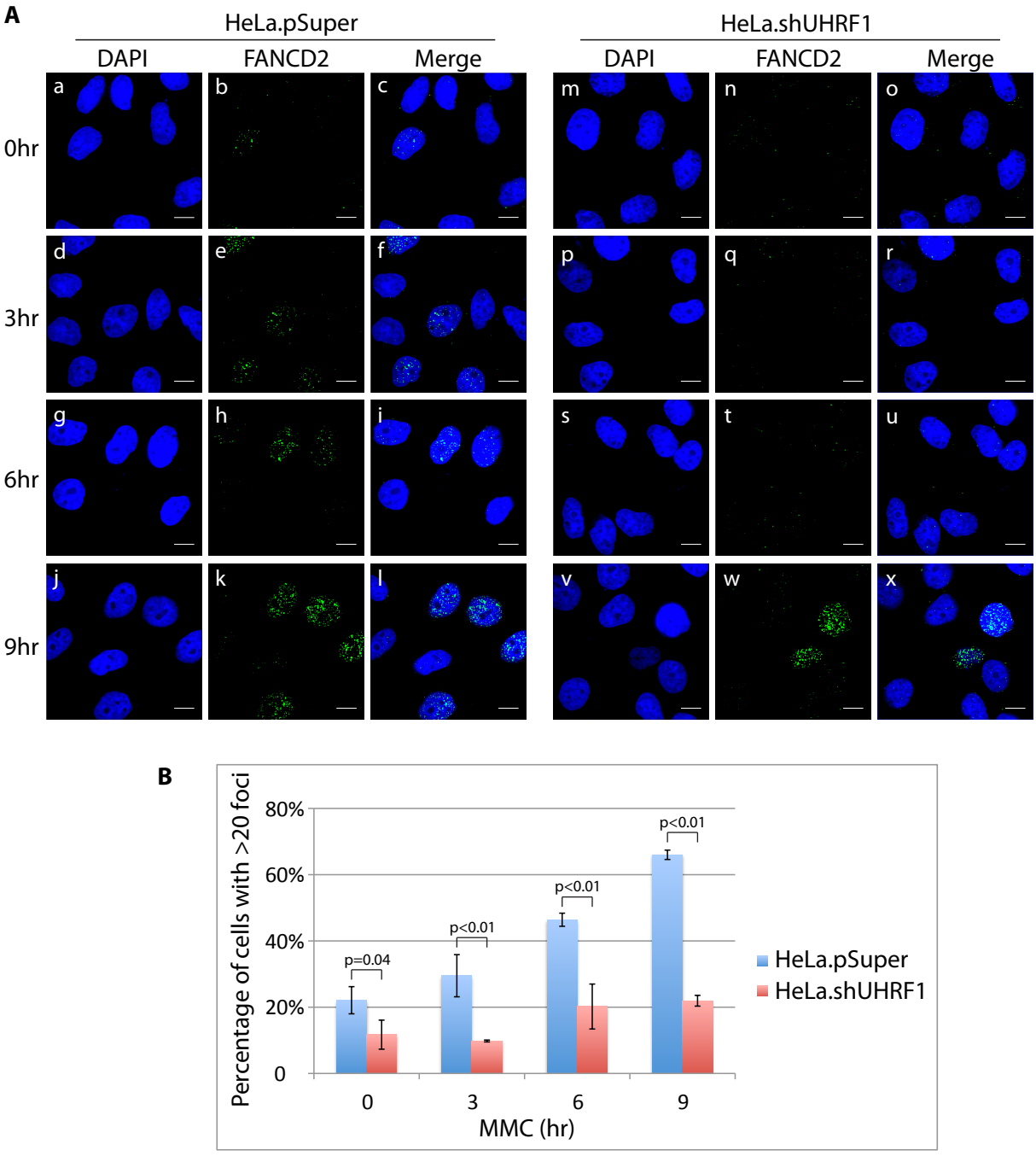

FIG 7.4 **UHRF1 is required for FANCD2 nuclear foci formation. A.** HeLa.pSuper and HeLa.shUHRF1 cells were treated with MMC for the indicated amount of time. After fixation and cytoplasmic pre-extraction, the nuclei were stained with FANCD2 antibody (FI17), showing the nuclear foci formation of the protein; **B.** Quantification of the percentage of cells with greater than 20 foci per cell. The error bars were calculated based on two individual experiments (n=2).

To confirm that UHRF1 is indeed required for FANCD2 recruitment, and to rule out the possibility of artefacts caused by off-target effects of shRNA KD, we used KD cells expressing exogenous WT UHRF1 in a parallel experiment. When treated with MMC for a time course of up to 9hr (images not shown for 3&6hr time points), the exogenous UHRF1 was sufficient to support the FANCD2 foci formation in response to MMC, similar to the endogenous protein (Fig. 7.5A, panels h and q, compared with b and k). The quantification shows that it rescued the phenotype from UHRF1 KD cells back to the control level (Fig. 7.5B).

We conclude that the reduction of UHRF1 disrupts FANCD2 foci formation in response to DNA ICLs. These findings supported our hypothesis, that UHRF1 is required for FANCD2 recruitment to sites of damages, independent of altering its ubiquitination level.

7.2.3 UHRF1 forms nuclear foci independent of DNA damage but may re-locate in response to MMC

So far, whether UHRF1 *in vitro* DNA ICLs binding activity endows its direct interaction *in vivo* remains an open question, as we have not been able to observe this type of interaction directly in the cells. However, by studying the pattern of UHRF1 nuclear staining in response to MMC by IF, we would be able to understand whether UHRF1 could form nuclear foci and be recruited to sites of damage as other FA proteins, e.g. FANCD2.

Fig. 7.5

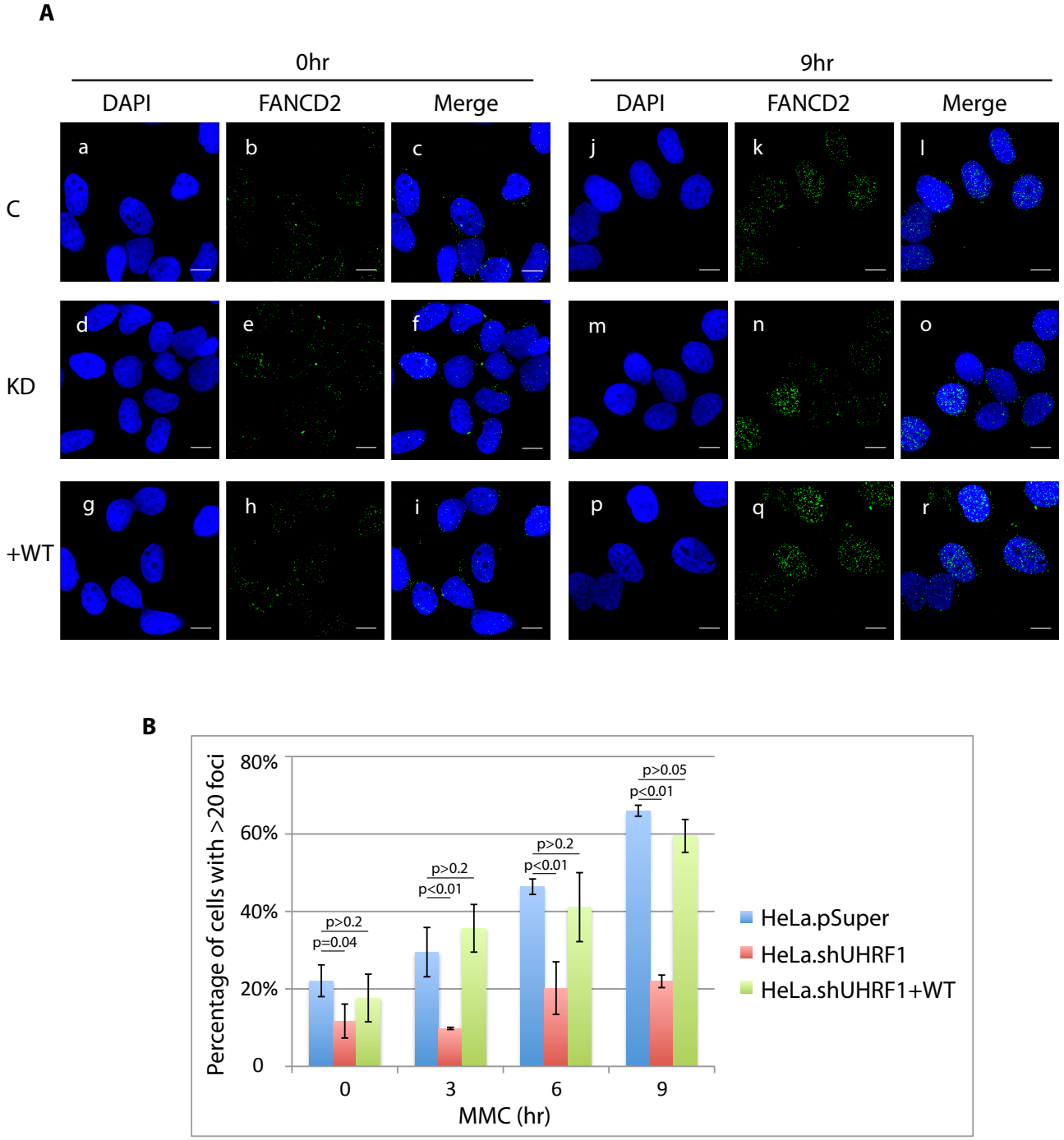

FIG 7.5 **Exogenous UHRF1 can support FANCD2 recruitment in response to MMC. A.** HeLa.pSuper (C), HeLa.shUHRF1 (KD) and HeLa.shUHRF1+WT (+WT) cells were treated with MMC time course for up to 9hr. After fixation and cytoplasm extraction, the nuclei were stained with FANCD2 antibody (FI17), showing the nuclear foci formation of the protein before (0hr) and after (9hr) the treatment. Scale bars represent 10μm; **B.** Quantification of the percentage of cells with greater than 20 foci per cell, in all cell lines. The error bars were calculated based on two individual experiments (n=2). This set of experiments was performed together with the experiment in Fig. 7.4. Therefore, the data points for HeLa.pSuper and HeLa.shUHRF1 are the same as shown in Fig. 7.4.

We treated HeLa.pSuper cells with 160ng/ml of MMC, and used FANCD2 as a positive control for foci formation. After 9hrs, FANCD2 nuclear foci became very pronounced, indicating that the cells were going through the DNA damage response, and the FA pathway was activated (Fig. 7.6A, panels b&h). UHRF1 already formed strong foci before the treatment, and after 9hr of MMC treatment, the percentage of positive cells did not change significantly (Fig. 7.6B, panels b&h).

Interestingly, we noticed that there was an uneven distribution of UHRF1 foci in the untreated cells, where some had very intense foci (Fig. 7.6B, panel b, marked with circles), while others had quite dim or nearly undetectable foci (panel b, marked with arrows). This may reflect UHRF1's localization in association with the cell cycle, which has been shown to form strong nuclear foci during S phase in published studies (*117, 118*). After the treatment of MMC, the majority of cells were positive and the degree of staining in those cells was very similar, with no distinguishable strong or weak patterns (panel h).

These data suggest that there might be a cellular relocation of UHRF1 in response to DNA damage. At this stage, it is not clear whether UHRF1 recognizes DNA ICLs *in vivo* directly. It would be useful to determine the relationship between cell cycle profiles and UHRF1 nuclear staining in the presence and absence of DNA damage by using cell cycle marker such as cyclin proteins and PCNA. This will help us to understand whether UHRF1 can form foci independent of DNA replication and be recruited to sites of DNA damage.

Fig. 7.6

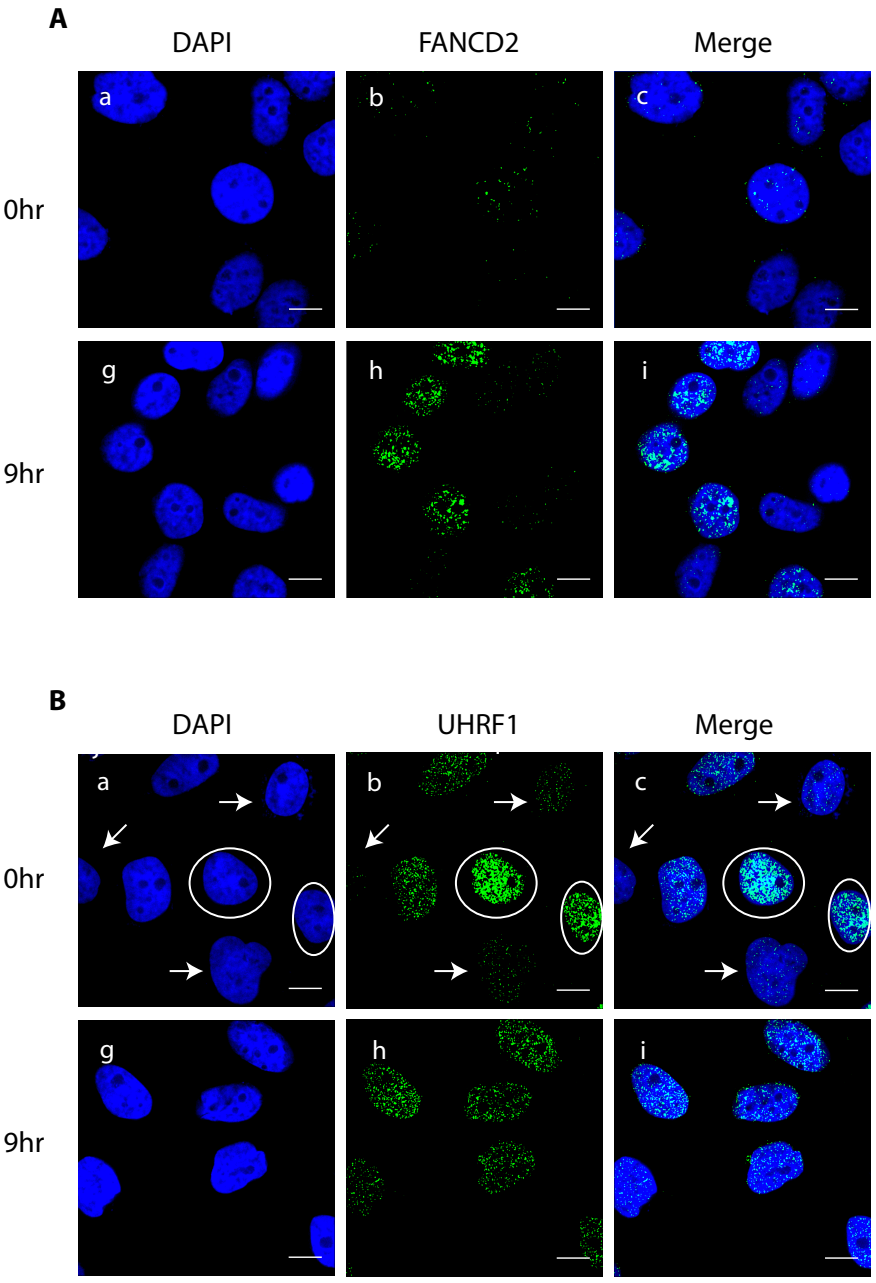

FIG 7.6 **UHRF1 may undergo a re-localization in the presence of DNA damage. A.** HeLa.pSuper cells were treated with MMC for 9hr and the nuclear FANCD2 (FI17) was stained for IF, showing the foci formation (panel b and h). Scale bars represent 10μm; **B.** In the same experiment, the nuclear UHRF1 (H8) in HeLa.pSuper cells was stained for IF. In panel b, the white circles mark the cells with strong and bright foci, whereas the arrows indicate the cells with weak UHRF1 foci.

Another way of studying the recruitment of UHRF1 to sites of DNA damage is to use more localized method to introduce DNA ICLs. For example, UVA laser following psoralen incubation can concentrate the damage to the stripes or spots, which will make the observation of UHRF1 localization more specific.

7.2.4 UHRF1 SRA domain is important for recruiting FANCD2 to form foci

As part of the investigation into the mechanism of UHRF1's function in the FA pathway, we would like to find out whether its DNA binding activity is required for the recruitment FANCD2 to sites of the damages. We introduced a point mutation of UHRF1 in the SRA domain, D482G, into the KD cells, to see if they could complement the KD phenotype and rescue FANCD2 foci formation in response to MMC. The mutation disrupts its DNA binding activity but not the auto-ubiquitination activity (Fig. 6.7A, lanes 5-8, and Fig. 6.7B, lanes 4&5) and its expression could not complement the KD cells (Fig. 6.8B).

Using IF microscopy monitoring FANCD2 recruitment, we saw that the WT protein formed clear foci in HeLa.pSuper cells after 9hr of MMC treatment (Fig. 7.7A, panels b&k), which was greatly reduced in the UHRF1 KD cells (panels e&n). However, the foci formation could not be restored with the SRA mutant D482G (Fig. 7.7A, panels h&q; and Fig. 7.7B). Since SRA domain mainly contributes to the specificity of ICL recognition and the DNA binding activity of UHRF1 *in vitro*, it is likely that the binding to DNA ICLs of UHRF1 facilitates the recruitment of FANCD2. It would also be interesting to investigate whether

mutations in the SRA domain in the cells could affect the re-location of the protein in response to DNA ICL damage as we observed from the WT protein (Fig. 7.6B), to be able to conclude on the relationship between UHRF1 DNA binding activity and its function in the recruitment of FANCD2 *in vivo*.

It is generally believed that ICL repair is DNA replication dependent, and the activation of FANCD2 occurs in S phase (*95, 106*). In this study, we found that using the similar concentration of MMC, 500nM for 24hr, there was about 10% of increase in the population of S and G2/M phase cells (Fig. 7.8A&B). It has been reported that in normal and FA patient derived cells, MMC treatment causes accumulation of cells in G2/M phase (*66*). As we observed more than half of the population of the cells has FANCD2 foci formation after DNA damage, we suspect that some of the FANCD2 foci positive cells were not in S phase. In future, it would be important to use cell cycle marker, such as cyclin proteins, to determine the cell cycle stage of those positive cells. This will help us to understand whether an UHRF1-involved DNA ICL repair is replication-dependent.

Fig. 7.7

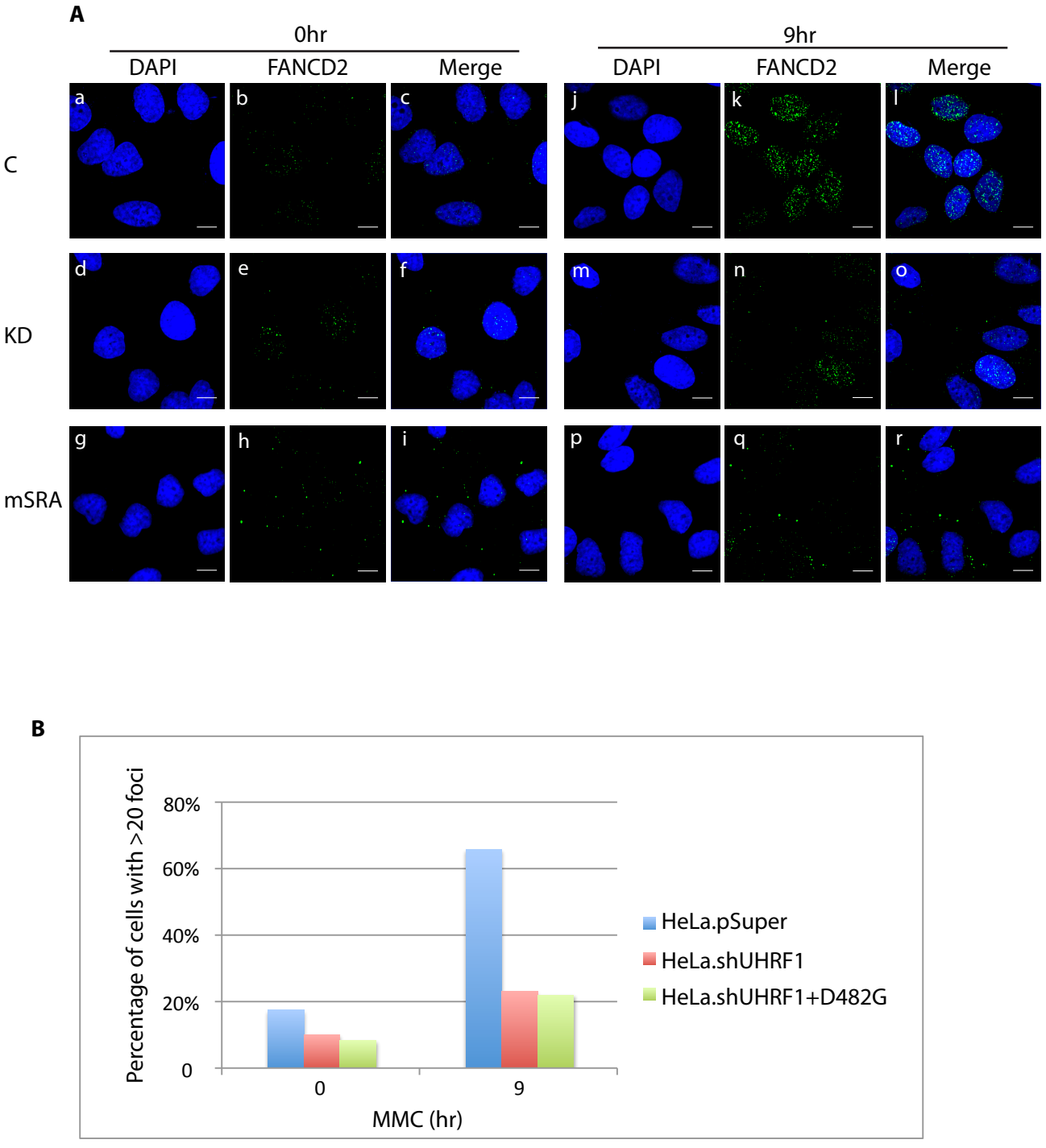

FIG 7.7 **UHRF1 SRA domain is required for FANCD2 nuclear foci formation. A.** HeLa.pSuper (C), HeLa.shUHRF1 (KD), and HeLa.shUHRF1 D482G (mSRA) were treated with MMC for 9hr. The nuclear FANCD2 (FI17) staining before (0hr) and after (9hr) the treatment were shown in the IF images. Scale bars represent 10μm; **B.** Quantification of the percentage of cells with greater than 20 foci per cell (the experiment was performed twice, and the representative data is shown here).

Fig. 7.8

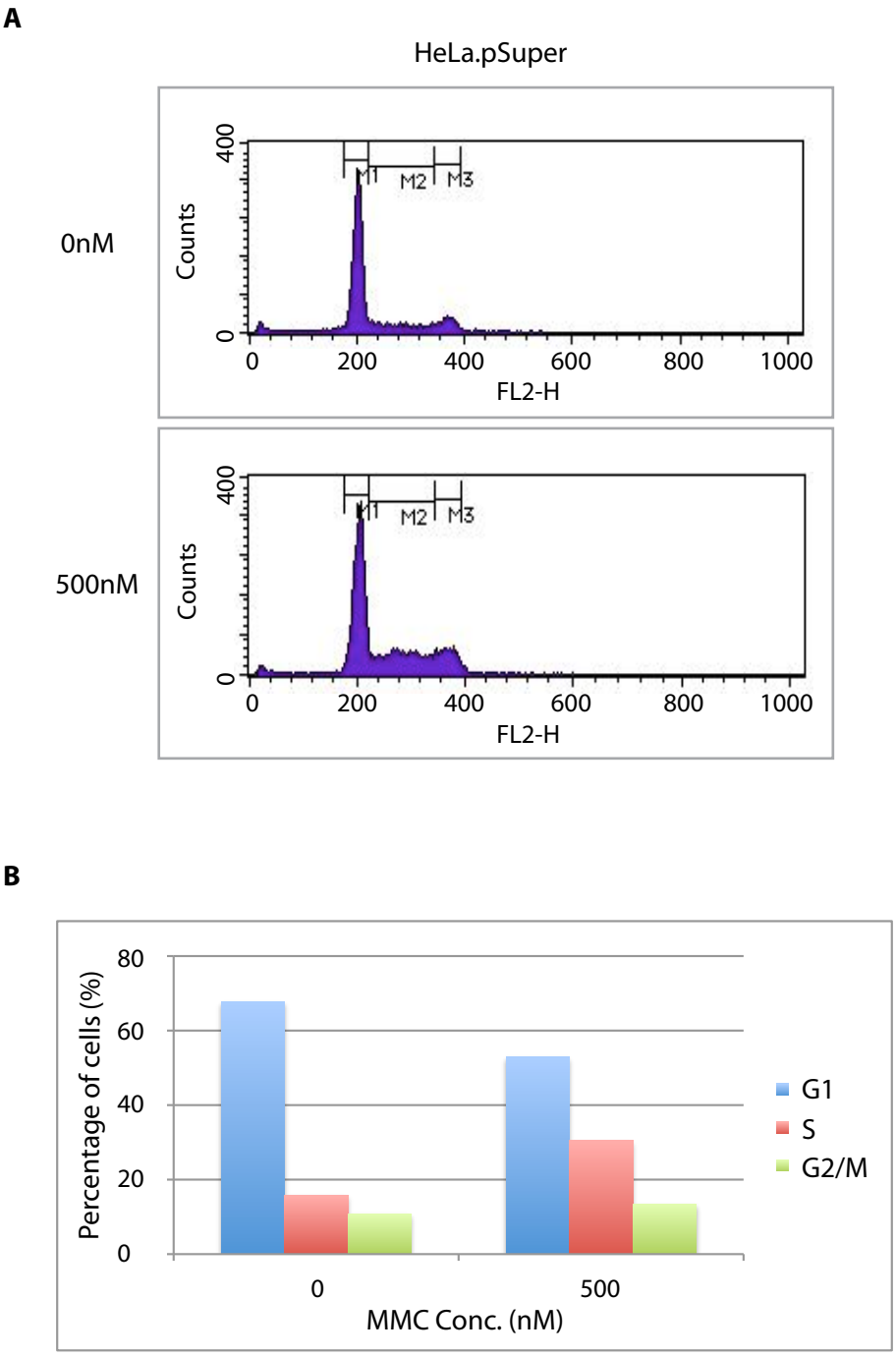

FIG 7.8 **MMC treatment in HeLa cells increases slightly the percentage of S phase cells. A.** HeLa.pSuper cells were treated with (lower panel) or without (upper panel) MMC for 500nM for 24hr. Then the cells were harvested and fixed. The DNA was stained by propidium iodide solution, analyzed by FACS. The PI staining profile was plotted according to the cell count as shown. M1 marks G1 cells, M2 marks most of S phase cells, and M3 marks G2/M cells; **B.** Quantification of percentage of cells in each cell cycle before and after the MMC treatment (experiment was performed for three times, and the representative data is shown here).

7.3 Discussion

The mechanism of FANCD2 ubiquitination by FANCL in association with the FA core complex has been established (*77*). The chromatin affinity by the FA core complex suggests that it is possible that FANCD2 is constantly being ubiquitinated (*209*), but that the USP1/UAF1 deubiquitinase complex regulates its response to DNA damage (*157, 218-220*). Hence, the key to the activation of the FA pathway may lie in the recruitment of FANCL and the FA core complex to the sites of damage, and the balance between ubiquitination and deubiquitination activities during the repair. Therefore, as a potential DNA ICL sensor, UHRF1 may serve a more important role in the recruitment of FANCD2 rather than its ubiquitination.

It has been demonstrated that RAD18-mediated ubiquitination of PCNA may be required for FANCD2 ubiquitination and the Fanconi anemia DNA repair activation (*221*). FANCD2 also co-localizes with PCNA in response to DNA damage (*222*). It has been shown that UHRF1 co-localizes with PCNA during S phase, and possibly through DNMT1 (*118, 223*), but PCNA can be ubiquitinated and form nuclear foci in response to DNA damage independently of DNA replication (*224, 225*). Whether UHRF1 interacts with PCNA outside S phase in response to DNA damage is not clear, however, there is the possibility that UHRF1 recognizes DNA ICLs and anchor PCNA to the sites of damage as an intermediate. Then FANCD2 is subsequently recruited.

If it is indeed by SRA domain that UHRF1 anchors to the sites of cross-links and recruit FANCD2, another important question would be whether mutations in SRA domain disrupt UHRF1 nuclear relocation as well in response to DNA damage. To gain a thorough understanding of the mechanism of FANCD2 recruitment by UHRF1, we also need to study the functions and behaviours of the other domains in response to DNA damage, such as the UBL, TTD and PHD domains. In particular, as the RING domain possesses both DNA binding specificity and possibly E3 ubiquitin ligase activity, it could potentially be a very important regulatory region of the protein function in the FA pathway.

On the other hand, in the absence of DNA damage, UHRF1 is predominantly associated with heterochromatin (*127, 128*). The re-location of UHRF1 in response to MMC may reflect a switch of function between DNA replication/gene expression regulation and DNA damage repair. SRA domain may be important in serving this switch, as it is able to bind to naked DNA (*138, 139*), and possibly recognize histone markers as well (*125*). In animals, SRA domain has only been found in UHRF1 and UHRF2 so far. Its mechanism in potential dual-function, and interaction with other DNA repair proteins are to be further investigated.

Chapter 8. Discussion

8.1 Conclusion

Among the current discovered FA proteins, the structure specific DNA binding factors are functioning towards the downstream of the pathway, such as FANCJ/BRIP1, FANCP/SLX4 and XPF (*85, 92, 212*). Also, the association of upstream FA core complex with chromatin does not seem to be DNA damage dependent (*209*). We confirmed that FANCD2/FANCI complex binds DNA, but does not specifically interact with DNA ICLs. From our ICL DNA interacting protein purification, we identified UHRF1, which can directly recognize cross-linked DNA *in vitro*. Subsequent *in vivo* experiments showed that it is required for cells to tolerate DNA ICL damage, and participates in the FA pathway by recruiting FANCD2 to sites of damage. Therefore, we propose that UHRF1 senses the DNA ICLs in the FA pathway.

8.2 The function of UHRF1 in epigenetics in relations to FA

It seems that UHRF1 has dual functions in DNA methylation and DNA repair, and these two aspects are independent from each other (*203*). We show that the SRA domain is important for binding to ICL DNA besides hemi-methylated DNA, and the amino acids responsible for hemi-methylated DNA binding are also required for ICL binding and repair. However, it remains to be seen whether there are

other amino acids of the SRA domain that can affect DNA ICL recognition but not the hemi-methylation binding.

The significance of UHRF1's function in the two areas may depend on the stage of development. During early development, although stem cells can maintain self-renewal properties and proliferate without DNA methylation, they cannot differentiate (*130, 135*). The embryonic lethality and organ developmental failures have been shown in different organisms when UHRF1 expression is lost (*134, 135, 226*). Also, UHRF1 is suggested to promote the turnover of the promyelocytic leukemia (PML) protein through ubiquitination-mediated degradation, and the knockdown of UHRF1 inhibits the cell migration and *in vitro* capillary tube formation of human umbilical vein endothelial cells (HUVECs) (*183*). When knocked down in hESCs, among the FA genes, FANCD2 and FANCA are shown to cause developmental defects as well, especially in the hematopoietic lineage, but the mechanism is undiscovered (*227*). Given the similarity between UHRF1 and the two FA genes knockdown phenotype during early development, UHRF1 may be the link between developmental abnormalities and defects in DNA repair in the FA patients.

8.3 The association of UHRF1 with heterochromatic DNA ICLs repair

The DNA damage response in heterochromatin is believed to be different from euchromatin (*228*). Although the damage can be sensed in the compact

chromatin structure, as seen in mitotic chromosomes, the damage signaling transduction can be much less efficient than in euchromatin (*229*). The restrained DDR in heterochromatin may be a mechanism that protects cells from undesired consequences such as apoptosis or unregulated recombination (*228*). It has been shown that there is an increased level of heterochromatin instability in the FA cells, and their metaphase chromosomes cannot be separated well (*230*). This is also observed in UHRF1 KD cells, where the heterochromatin shows a more diffused staining pattern than control cells and the S phase progression is prolonged (*126, 127*). Multiple domains of UHRF1 are involved in H3 lysine 9 methylation marker recognition (*128*), which is important for heterochromatic genome stability. Cells defective in H3K9me3 have an increased level of DNA damage in heterochromatin region (*231*). Hence, UHRF1 may also contribute to the maintenance of heterochromatin stability in the presence of DNA damage.

8.4 The role of UHRF1 in the FA pathway

8.4.1 A working model

Our data suggest that UHRF1 can recognize ICL damage through its SRA domain (Fig. 8.1, step A, pathway I), and activates the pathway by recruiting FANCD2 for the downstream repair. It is unclear at this stage whether UHRF1 serves as a structural platform for downstream protein recruitment or it acts as the E3 ubiquitin ligase to contribute to the transduction of signal. In our purification of proteins binding to DNA ICLs, we also identified ATR. Although we could not

detect any direct interaction of ATR and cross-linked DNA from subsequent experiments (data not shown), it is possible that ATR and the FA core complex are localized to the cross-link sites through other protein partners, and UHRF1 may be able to serve this interaction (step B). Then the FANCD2/FANCI complex is phosphorylated and mono-ubiquitinated, followed by its recruitment to the site of damage (step C).

UHRF1 can potentially recruit nucleases to enable the repair as well. SLX4 interacts with different nucleases, and its recruitment depends on FANCD2 mono-ubiquitination and an intact SLX4 ubiquitin binding UBZ domain (*212*). However, it is unclear whether SLX4 binds to the ubiquitination marker of FANCD2 directly. The UBL domain of UHRF1 can also possibly be a binding partner of the UBZ domain of SLX4, and since UHRF1 is required for Eme1 localization in response to DNA damage (*152*), UHRF1 can be very important to coordinate these nucleases to excise the cross-linked nucleotides in the FA pathway, and for the assembly of the downstream repair complex (step D).

Whether UHRF1 E3 ubiquitin ligase activity is required for its function in the FA pathway is unspecified, although evidence indicates that the RING domain is important for UHRF1's DNA binding and is required for DNA damage response (*152, 153*). Histone components are likely to be UHRF1's ubiquitination targets (*124*), and the ubiquitination event may be critical for signaling the FA pathway activation. Upon binding to DNA ICL, UHRF1 may participate in the FA core complex to enhance the overall ubiquitination activity (step E, pathway II). Then UHRF1 and ubiquitinated FANCD2/FANCI recruit the nucleases and other repair

proteins (step F, pathway II). It can also ubiquitinate some other substrates unknown to the current FA proteins (step G, substrates represented by protein X, pathway III). The modified substrate, histones being one possibility, can then propagate the damage signaling, to recruit FANCD2/FANCI (step H, pathway III) (*216*). Finally the nucleases and the downstream repair complex are engaged to complete the repair (step I, pathway III).

8.4.2 Future work

It is notable that there are still several aspects unrevealed in this model. From existing evidence, it seems that UHRF1 can be critical in both DNA DSB and ICL repair. Biochemical data suggest that UHRF1 is the sensor for ICLs, but the immediate downstream events after the damage detection are still unclear. These events may entail UHRF1's connection with other repair pathways. Since there is a high degree of cross talking between DSB and ICL repair, UHRF1 may potentially participate in both pathways. However, it will also be important to determine whether UHRF1 is more specifically demanded in the FA pathway than others, or it is generally involved in all types of DNA damage response. We are currently conducting more *in vitro* DNA binding assays, to test the interaction of UHRF1 with different DNA structures, and to understand if UHRF1 could accommodate and recognize damaged DNA in general.

Moreover, it needs to be clarified whether the enzymatic activity of UHRF1 is required in DNA ICL repair, e.g. by measuring sensitivity to MMC and assessing FANCD2 foci formation when cells express RING domain deletion or mutation.

This would help to position UHRF1 in the pathway in relation to other FA proteins accurately. Should it be required, the substrate of UHRF1 becomes critical in the process. We can examine proteins that are ubiquitinated by UHRF1 both *in vivo* and *in vitro*, and analyze if ubiquitination defects of those proteins causes the same phenotype as UHRF1 RING mutants. Since UHRF1 is unlikely to have a strong interaction with FANCD2/FANCI, it will be necessary to study whether it directly cooperates with other factors, such as ATR, FA core complex, downstream repair proteins and nucleases such as Eme1 and SLX4. Such exploration can enable us to understand the molecular mechanism of how UHRF1 initiates the rest of the FA pathway after recognizing DNA ICLs.

We also identified UHRF2 from our purification. Structurally, UHRF2 is highly identical to UHRF1, and also belongs to the UHRF family. UHRF2 can also interact with hemi-methylated DNA, but seems to be dispensable for DNA methylation maintenance (*214*). So far, UHRF2 has been reported to be involved in apoptosis, but it is unclear whether UHRF2 also have a role in DNA repair (*232*). It would be important to study if UHRF2 can also recognize DNA ICLs and participate in the FA pathway. We can also investigate the cellular phenotype in response to DNA damage when both proteins are knocked-down, to understand if there is any functional redundancy between the proteins.

Given its multi-functions in epigenetic regulation and DNA repair, UHRF1 is a good candidate to answer why we see various facets of defective cell behaviors in FA patients. In future, it may be appropriate to study the functions of UHRF1 in development in relation to the FA phenotype *in vivo*. For example, conditional

Fig. 8.1

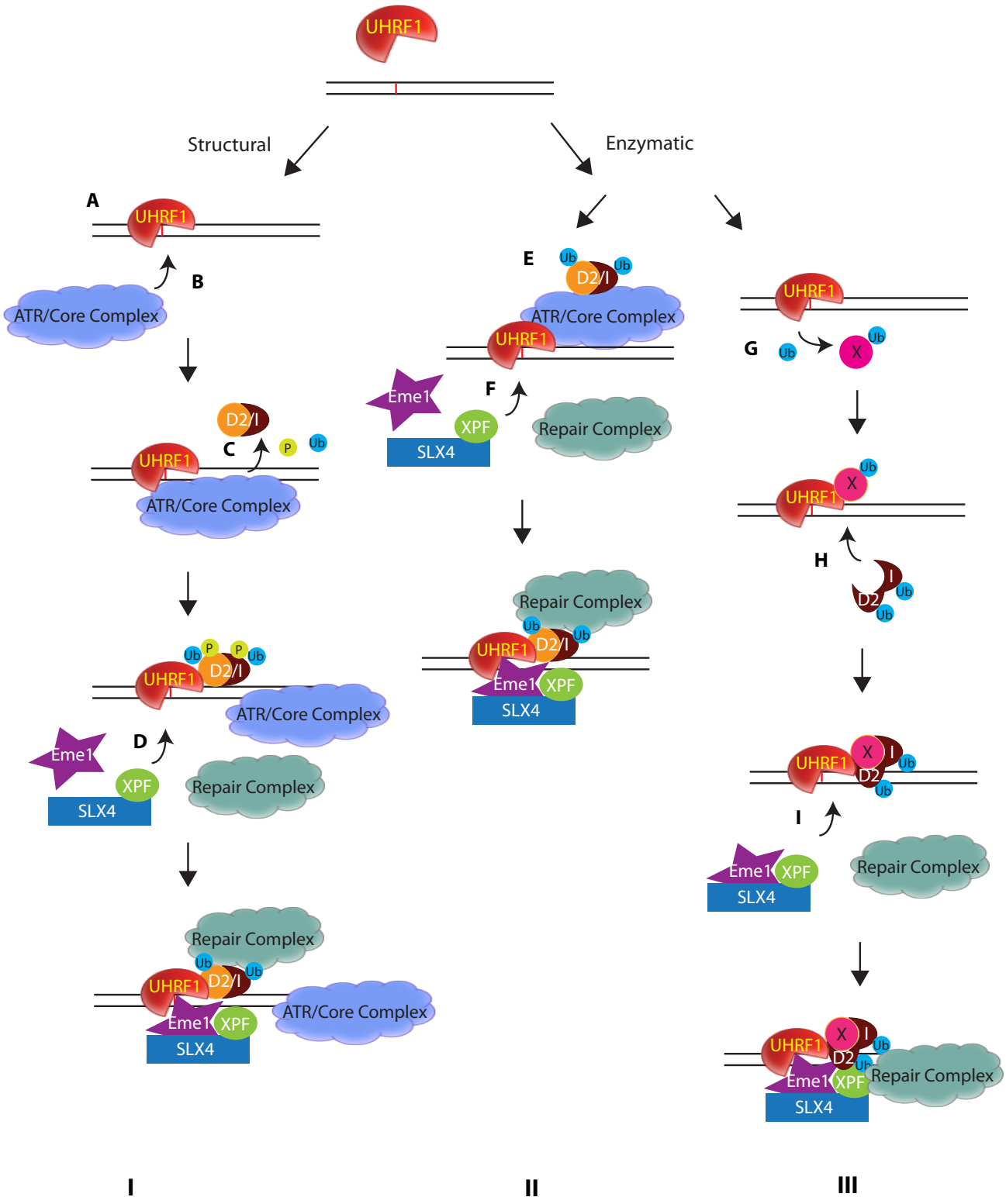

FIG. 8.1 **Schematic diagram illustrating the possible model of UHRF1 in the FA pathway.**

knockdown mice can be generated to study UHRF1's function in different stages of development. This can help us to answer questions such as whether it causes the same type of bone structure and bone marrow malformation, hematologic failures, and other symptoms, which are seen in the FA patients.

Finally, it is still under discussion whether UHRF1 is a specific sensor for DNA ICLs, and also an FA gene, as it is likely that UHRF1 has a general recognition function to damaged DNA. So far, most of the FA patients are categorized into complementation groups corresponding to the 16 FA genes, but several patients are yet to be assigned and there are probably more patients to be identified. It will be very exciting to conduct genetic screen among the FA patient population to study whether any of them can be found with mutations of UHRF1. A better understanding of the molecular mechanisms underlying the FA pathway, including UHRF1, as well as the genetic functional analysis and clinical symptoms, will increase our chances of developing better and more targeted modes of treatment in future.

References

1. Kennedy, R. D., and D'Andrea, A. D. (2005) The Fanconi Anemia/BRCA pathway: new faces in the crowd, *Genes & Development 19*, 2925-2940.
2. Sirbu, B. M., and Cortez, D. (2013) DNA damage response: Three levels of DNA repair regulation, *Cold Spring Harbor Perspectives in Biology*.
3. Cimprich, K. A., and Cortez, D. (2008) ATR: an essential regulator of genome integrity, *Nat Rev Mol Cell Biol 9*, 616-627.
4. Clancy, S. (2008) DNA damage & repair: mechanisms for maintaining DNA integrity, *Nature Education 1*, 103.
5. Kudlow, B. A., Kennedy, B. K., and Monnat, R. J. (2007) Werner and Hutchinson-Gilford progeria syndromes: mechanistic basis of human progeroid diseases, *Nat Rev Mol Cell Biol 8*, 394-404.
6. Goodsell, D. S. (2001) The molecular perspective: Ultraviolet light and pyrimidine dimers, *The Oncologist 6*, 298-299.
7. Kamileri, I., Karakasilioti, I., and Garinis, G. A. (2012) Nucleotide excision repair: new tricks with old bricks, *Trends in genetics : TIG 28*, 566-573.
8. Nishi, R., Okuda, Y., Watanabe, E., Mori, T., Iwai, S., Masutani, C., Sugasawa, K., and Hanaoka, F. (2005) Centrin 2 stimulates nucleotide excision repair by interacting with Xeroderma Pigmentosum group C protein, *Molecular and Cellular Biology 25*, 5664-5674.
9. Oksenych, V., de Jesus, B. B., Zhovmer, A., Egly, J.-M., and Coin, F. (2009) Molecular insights into the recruitment of TFIIH to sites of DNA damage, *EMBO J 28*, 2971-2980.
10. Overmeer, R. M., Moser, J., Volker, M., Kool, H., Tomkinson, A. E., van Zeeland, A. A., Mullenders, L. H. F., and Fousteri, M. (2011) Replication protein A safeguards genome integrity by controlling NER incision events, *The Journal of Cell Biology 192*, 401-415.
11. Ogi, T., Limsirichaikul, S., Overmeer, R. M., Volker, M., Takenaka, K., Cloney, R., Nakazawa, Y., Niimi, A., Miki, Y., Jaspers, N. G., Mullenders, L. H. F., Yamashita, S., Fousteri, M. I., and Lehmann, A. R. (2010) Three DNA polymerases, recruited by different mechanisms, carry out NER repair synthesis in human cells, *Molecular Cell 37*, 714-727.
12. Moser, J., Kool, H., Giakzidis, I., Caldecott, K., Mullenders, L. H. F., and Fousteri, M. I. (2007) Sealing of chromosomal DNA nicks during nucleotide excision repair requires XRCC1 and DNA Ligase III α in a cell-cycle-specific manner, *Molecular Cell 27*, 311-323.
13. Lovell, M. A., Xie, C., and Markesbery, W. R. (2000) Decreased base excision repair and increased helicase activity in Alzheimer's disease brain, *Brain Research 855*, 116-123.
14. Parsons, J. L., and Dianov, G. L. (2013) Co-ordination of base excision repair and genome stability, *DNA Repair 12*, 326-333.
15. Yu, C.-E., Oshima, J., Fu, Y.-H., Wijsman, E. M., Hisama, F., Alisch, R., Matthews, S., Nakura, J., Miki, T., Ouais, S., Martin, G. M., Mulligan, J., and Schellenberg, G. D. (1996) Positional cloning of the Werner's syndrome gene, *Science 272*, 258-262.

16. Lee, J. W., Harrigan, J., Opresko, P. L., and Bohr, V. A. (2005) Pathways and functions of the Werner syndrome protein, *Mechanisms of Ageing and Development 126*, 79-86.
17. Pichierri, P., Franchitto, A., Mosesso, P., and Palitti, F. (2000) Werner's syndrome cell lines are hypersensitive to camptothecin-induced chromosomal damage, *Mutation Research/Fundamental and Molecular Mechanisms of Mutagenesis 456*, 45-57.
18. Antoccia, A., Ricordy, R., Maraschio, P., Prudente, S., and Tanzarella, C. (1997) Chromosomal sensitivity to clastogenic agents and cell cycle perturbations in Nijmegen breakage syndrome lymphoblastoid cell lines, *International journal of radiation biology 71*, 41-49.
19. Canman, C. E., Lim, D. S., Cimprich, K. A., Taya, Y., Tamai, K., Sakaguchi, K., Appella, E., Kastan, M. B., and Siliciano, J. D. (1998) Activation of the ATM Kinase by Ionizing Radiation and Phosphorylation of p53, *Science 281*, 1677-1679.
20. Stewart, G. S., Wang, B., Bignell, C. R., Taylor, A. M. R., and Elledge, S. J. (2003) MDC1 is a mediator of the mammalian DNA damage checkpoint, *Nature 421*, 961-966.
21. Johnson, E. S., Ma, P. C. M., Ota, I. M., and Varshavsky, A. (1995) A proteolytic pathway that recognizes ubiquitin as a degradation signal, *Journal of Biological Chemistry 270*, 17442-17456.
22. Pickart, C. M., and Eddins, M. J. (2004) Ubiquitin: structures, functions, mechanisms, *Biochimica et Biophysica Acta (BBA) - Molecular Cell Research 1695*, 55-72.
23. Huen, M. S. Y., Grant, R., Manke, I., Minn, K., Yu, X., Yaffe, M. B., and Chen, J. (2007) RNF8 transduces the DNA-damage signal via histone ubiquitylation and checkpoint protein assembly, *Cell 131*, 901-914.
24. Mattiroli, F., Vissers, J. H., van Dijk, W. J., Ikpa, P., Citterio, E., Vermeulen, W., Marteijn, J. A., and Sixma, T. K. (2012) RNF168 ubiquitinates K13-15 on H2A/H2AX to drive DNA damage signaling, *Cell 150*, 1182-1195.
25. Mailand, N., Bekker-Jensen, S., Faustrup, H., Melander, F., Bartek, J., Lukas, C., and Lukas, J. (2007) RNF8 ubiquitylates histones at DNA double-strand breaks and promotes assembly of repair proteins, *Cell 131*, 887-900.
26. Wang, B., and Elledge, S. J. (2007) Ubc13/Rnf8 ubiquitin ligases control foci formation of the Rap80/Abraxas/Brca1/Brcc36 complex in response to DNA damage, *Proceedings of the National Academy of Sciences 104*, 20759-20763.
27. You, Z., Shi, L. Z., Zhu, Q., Wu, P., Zhang, Y.-W., Basilio, A., Tonnu, N., Verma, I. M., Berns, M. W., and Hunter, T. (2009) CtIP links DNA double-strand break sensing to resection, *Molecular Cell 36*, 954-969.
28. Jazayeri, A., Falck, J., Lukas, C., Bartek, J., Smith, G. C. M., Lukas, J., and Jackson, S. P. (2006) ATM- and cell cycle-dependent regulation of ATR in response to DNA double-strand breaks, *Nat Cell Biol 8*, 37-45.
29. Dobbs, T. A., Tainer, J. A., and Lees-Miller, S. P. (2010) A structural model for regulation of NHEJ by DNA-PKcs autophosphorylation, *DNA Repair 9*, 1307-1314.
30. Henricksen, L. A., Umbricht, C. B., and Wold, M. S. (1994) Recombinant replication protein A: expression, complex formation, and functional characterization, *Journal of Biological Chemistry 269*, 11121-11132.

31. Zou, L., and Elledge, S. J. (2003) Sensing DNA damage through ATRIP recognition of RPA-ssDNA complexes, *Science 300*, 1542-1548.
32. Choi, J.-H., Lindsey-Boltz, L. A., Kemp, M., Mason, A. C., Wold, M. S., and Sancar, A. (2010) Reconstitution of RPA-covered single-stranded DNA-activated ATR-Chk1 signaling, *Proceedings of the National Academy of Sciences 107*, 13660-13665.
33. Bermudez, V. P., Lindsey-Boltz, L. A., Cesare, A. J., Maniwa, Y., Griffith, J. D., Hurwitz, J., and Sancar, A. (2003) Loading of the human 9-1-1 checkpoint complex onto DNA by the checkpoint clamp loader hRad17-replication factor C complex in vitro, *Proceedings of the National Academy of Sciences 100*, 1633-1638.
34. Delacroix, S., Wagner, J. M., Kobayashi, M., Yamamoto, K.-I., and Karnitz, L. M. (2007) The Rad9-Hus1-Rad1 (9-1-1) clamp activates checkpoint signaling via TopBP1, *Genes & Development 21*, 1472-1477.
35. Smith, J., Mun Tho, L., Xu, N., and Gillespie, D. A. (2010) The ATM-Chk2 and ATR-Chk1 pathways in DNA damage signaling and cancer, *Advances in Cancer Research 108*, 73-112.
36. Sugiyama, T., and Kowalczykowski, S. C. (2002) Rad52 protein associates with replication protein A (RPA)-single-stranded DNA to accelerate Rad51-mediated displacement of RPA and presynaptic complex formation, *Journal of Biological Chemistry 277*, 31663-31672.
37. Sugiyama, T., and Kantake, N. (2009) Dynamic regulatory interactions of Rad51, Rad52, and replication protein-A in recombination intermediates, *Journal of Molecular Biology 390*, 45-55.
38. Liu, J., Doty, T., Gibson, B., and Heyer, W.-D. (2010) Human BRCA2 protein promotes RAD51 filament formation on RPA-covered single-stranded DNA, *Nat Struct Mol Biol 17*, 1260-1262.
39. Paillard, S., and Strauss, F. (1991) Analysis of the mechanism of interaction of simian Ku protein with DNA, *Nucleic Acids Research 19*, 5619-5624.
40. Gottlieb, T. M., and Jackson, S. P. (1993) The DNA-dependent protein kinase: Requirement for DNA ends and association with Ku antigen, *Cell 72*, 131-142.
41. Drouet, J., Frit, P., Delteil, C., de Villartay, J.-P., Salles, B., and Calsou, P. (2006) Interplay between Ku, Artemis, and the DNA-dependent protein kinase catalytic subunit at DNA ends, *Journal of Biological Chemistry 281*, 27784-27793.
42. Xie, A., Kwok, A., and Scully, R. (2009) Role of mammalian Mre11 in classical and alternative nonhomologous end joining, *Nat Struct Mol Biol 16*, 814-818.
43. Chen, L., Trujillo, K., Sung, P., and Tomkinson, A. E. (2000) Interactions of the DNA Ligase IV-XRCC4 complex with DNA ends and the DNA-dependent protein kinase, *Journal of Biological Chemistry 275*, 26196-26205.
44. Lu, H., Pannicke, U., Schwarz, K., and Lieber, M. R. (2007) Length-dependent binding of human XLF to DNA and stimulation of XRCC4-DNA Ligase IV activity, *Journal of Biological Chemistry 282*, 11155-11162.

45. Tomimatsu, N., Mukherjee, B., and Burma, S. (2009) Distinct roles of ATR and DNA-PKcs in triggering DNA damage responses in ATM-deficient cells, *EMBO Rep 10*, 629-635.
46. Fradet-Turcotte, A., Canny, M. D., Escribano-Diaz, C., Orthwein, A., Leung, C. C. Y., Huang, H., Landry, M.-C., Kitevski-LeBlanc, J., Noordermeer, S. M., Sicheri, F., and Durocher, D. (2013) 53BP1 is a reader of the DNA-damage-induced H2A Lys 15 ubiquitin mark, *Nature 499*, 50-54.
47. Iwabuchi, K., Hashimoto, M., Matsui, T., Kurihara, T., Shimizu, H., Adachi, N., Ishiai, M., Yamamoto, K.-i., Tauchi, H., Takata, M., Koyama, H., and Date, T. (2006) 53BP1 contributes to survival of cells irradiated with X-ray during G1 without Ku70 or Artemis, *Genes to Cells 11*, 935-948.
48. Nakamura, K., Sakai, W., Kawamoto, T., Bree, R. T., Lowndes, N. F., Takeda, S., and Taniguchi, Y. (2006) Genetic dissection of vertebrate 53BP1: A major role in non-homologous end joining of DNA double strand breaks, *DNA Repair 5*, 741-749.
49. Yang, K., Weinacht, C. P., and Zhuang, Z. (2013) Regulatory role of ubiquitin in eukaryotic DNA translesion synthesis, *Biochemistry 52*, 3217-3228.
50. Zhuang, Z., and Ai, Y. (2010) Processivity factor of DNA polymerase and its expanding role in normal and translesion DNA synthesis, *Biochimica et Biophysica Acta (BBA) - Proteins and Proteomics 1804*, 1081-1093.
51. Kannouche, P. L., Wing, J., and Lehmann, A. R. (2004) Interaction of human DNA polymerase η with monoubiquitinated PCNA: A possible mechanism for the polymerase switch in response to DNA damage, *Molecular Cell 14*, 491-500.
52. Davies, A. A., Huttner, D., Daigaku, Y., Chen, S., and Ulrich, H. D. (2008) Activation of ubiquitin-dependent DNA damage bypass is mediated by replication protein A, *Molecular Cell 29*, 625-636.
53. Zhang, S., Chea, J., Meng, X., Zhou, Y., Lee, E. Y. C., and Lee, M. Y. W. T. (2008) PCNA is ubiquitinated by RNF8, *Cell Cycle 7*, 3399-3404.
54. Lynch, H. T., and de la Chapelle, A. (1999) Genetic susceptibility to non-polyposis colorectal cancer, *Journal of Medical Genetics 36*, 801-818.
55. Jiricny, J. (2006) The multifaceted mismatch-repair system, *Nat Rev Mol Cell Biol 7*, 335-346.
56. Auerbach, A. D. (2009) Fanconi anemia and its diagnosis, *Mutation Research/Fundamental and Molecular Mechanisms of Mutagenesis 668*, 4-10.
57. Ishida, R., and Buchwald, M. (1982) Susceptibility of Fanconi's anemia lymphoblasts to DNA-cross-linking and alkylating agents, *Cancer Res 42*, 4000 - 4006.
58. Carreau, M., Alon, N., Bosnoyan-Collins, L., Joenje, H., and Buchwald, M. (1999) Drug sensitivity spectra in Fanconi anemia lymphoblastoid cell lines of defined complementation groups, *Mutation Research/DNA Repair 435*, 103-109.
59. Duckworth-Rysiecki, G., and Taylor, A. M. R. (1985) Effects of ionizing radiation on cells from Fanconi's anemia patients, *Cancer Research 45*, 416-420.

60. Heddle, J. A., Lue, C. B., Saunders, E. F., and Benz, R. D. (1978) Sensitivity to five mutagens in Fanconi's anemia as measured by the micronucleus method, *Cancer Research 38*, 2983-2988.
61. Taniguchi, T., Garcia-Higuera, I., Xu, B., Andreassen, P. R., Gregory, R. C., Kim, S.-T., Lane, W. S., Kastan, M. B., and D'Andrea, A. D. (2002) Convergence of the Fanconi anemia and Ataxia telangiectasia signaling pathways, *Cell 109*, 459-472.
62. Zhang, Q.-S., Eaton, L., Snyder, E. R., Houghtaling, S., Mitchell, J. B., Finegold, M., Van Waes, C., and Grompe, M. (2008) Tempol protects against oxidative damage and delays epithelial tumor onset in Fanconi anemia mice, *Cancer Research 68*, 1601-1608.
63. Joenje, H., and Oostra, B. (1983) Effect of oxygen tension on chromosomal aberrations in Fanconi anaemia, *Hum Genet 65*, 99-101.
64. Castillo, P., Bogliolo, M., and Surralles, J. (2011) Coordinated action of the Fanconi anemia and Ataxia telangiectasia pathways in response to oxidative damage, *DNA Repair 10*, 518-525.
65. Langevin, F., Crossan, G. P., Rosado, I. V., Arends, M. J., and Patel, K. J. (2011) Fancd2 counteracts the toxic effects of naturally produced aldehydes in mice, *Nature 475*, 53-58.
66. Heinrich, M., Hoatlin, M., Zigler, A., Silvey, K., Bakke, A., Keeble, W., Zhi, Y., Reifsteck, C., Grompe, M., and Brown, M. (1998) DNA cross-linker-induced G2/M arrest in group C Fanconi anemia lymphoblasts reflects normal checkpoint function, *Blood 91*, 275 - 287.
67. Kottemann, M. C., and Smogorzewska, A. (2013) Fanconi anaemia and the repair of Watson and Crick DNA crosslinks, *Nature 493*, 356-363.
68. Bogliolo, M., Schuster, B., Stoepker, C., Derkunt, B., Su, Y., Raams, A., Trujillo, J. P., Minguillón, J., Ramírez, M. J., Pujol, R., Casado, J. A., Baños, R., Rio, P., Knies, K., Zúñiga, S., Benítez, J., Bueren, J. A., Jaspers, N. G. J., Schärer, O. D., de Winter, J. P., Schindler, D., and Surrallés, J. (2013) Mutations in ERCC4, encoding the DNA-repair endonuclease XPF, cause Fanconi anemia, *American journal of human genetics 92*, 800-806.
69. Kupfer, G., Naf, D., Garcia-Higuera, I., Wasik, J., Cheng, A., Yamashita, T., Tipping, A., Morgan, N., Mathew, C. G., and D'Andrea, A. D. (1999) A patient-derived mutant form of the Fanconi anemia protein, FANCA, is defective in nuclear accumulation, *Experimental Hematology 27*, 587-593.
70. Leung, J. W. C., Wang, Y., Fong, K. W., Huen, M. S. Y., Li, L., and Chen, J. (2012) Fanconi anemia (FA) binding protein FAAP20 stabilizes FA complementation group A (FANCA) and participates in interstrand cross-link repair, *Proceedings of the National Academy of Sciences 109*, 4491-4496.
71. Fei, P., Yin, J., and Wang, W. (2005) New Advances in the DNA Damage Response Network of Fanconi Anemia and BRCA proteins: FAAP95 Replaces BRCA2 as the True FANCB Protein, *Cell Cycle 4*, 80-86.
72. Kupfer, G. M., Naf, D., Suliman, A., Pulsipher, M., and D'Andrea, A. D. (1997) The Fanconi anaemia proteins, FAA and FAC interact to form a nuclear complex, *Nat Genet 17*, 487-490.
73. Pace, P., Johnson, M., Tan, W. M., Mosedale, G., Sng, C., Hoatlin, M., de Winter, J., Joenje, H., Gergely, F., and Patel, K. J. (2002) FANCE: the link

between Fanconi anaemia complex assembly and activity, *EMBO J 21*, 3414-3423.
74. de Winter, J., Rooimans, M., van Der Weel, L., van Berkel, C., Alon, N., Bosnoyan-Collins, L., de Groot, J., Zhi, Y., Waisfisz, Q., and Pronk, J. (2000) The Fanconi anaemia gene FANCF encodes a novel protein with homology to ROM, *Nat Genet 24*, 15 - 16.
75. de Winter, J., Waisfisz, Q., Rooimans, M., van Berkel, C., Bosnoyan-Collins, L., Alon, N., Carreau, M., Bender, O., Demuth, I., and Schindler, D. (1998) The Fanconi anaemia group G gene FANCG is identical with XRCC9, *Nat Genet 20*, 281 - 283.
76. Meetei, A. R., Yan, Z., and Wang, W. (2004) FANCL Replaces BRCA1 as the Likely Ubiquitin Ligase Responsible for FANCD2 Monoubiquitination, *Cell Cycle 3*, 174-176.
77. Alpi, A. F., Pace, P. E., Babu, M. M., and Patel, K. J. (2008) Mechanistic insight into site-restricted monoubiquitination of FANCD2 by Ube2t, FANCL, and FANCI, *Molecular Cell 32*, 767-777.
78. Meetei, A. R., Medhurst, A. L., Ling, C., Xue, Y., Singh, T. R., Bier, P., Steltenpool, J., Stone, S., Dokal, I., Mathew, C. G., Hoatlin, M., Joenje, H., de Winter, J. P., and Wang, W. (2005) A human ortholog of archaeal DNA repair protein Hef is defective in Fanconi anemia complementation group M, *Nat Genet 37*, 958-963.
79. Collis, S. J., Ciccia, A., Deans, A. J., Hořejší, Z., Martin, J. S., Maslen, S. L., Skehel, J. M., Elledge, S. J., West, S. C., and Boulton, S. J. (2008) FANCM and FAAP24 function in ATR-mediated checkpoint signaling independently of the Fanconi anemia core complex, *Molecular Cell 32*, 313-324.
80. Timmers, C., Taniguchi, T., Hejna, J., Reifsteck, C., Lucas, L., Bruun, D., Thayer, M., Cox, B., Olson, S., D'Andrea, A. D., Moses, R., and Grompe, M. (2001) Positional cloning of a novel Fanconi anemia gene, FANCD2, *Molecular Cell 7*, 241-248.
81. Liu, T., Ghosal, G., Yuan, J., Chen, J., and Huang, J. (2010) FAN1 acts with FANCI-FANCD2 to promote DNA interstrand cross-link repair, *Science 329*, 693-696.
82. Smogorzewska, A., Matsuoka, S., Vinciguerra, P., McDonald, E. R., Hurov, K. E., Luo, J., Ballif, B. A., Gygi, S. P., Hofmann, K., D'Andrea, A. D., and Elledge, S. J. (2007) Identification of the FANCI protein, a monoubiquitinated FANCD2 paralog required for DNA repair, *Cell 129*, 289-301.
83. Howlett, N., Taniguchi, T., Olson, S., Cox, B., Waisfisz, Q., De Die-Smulders, C., Persky, N., Grompe, M., Joenje, H., and Pals, G. (2002) Biallelic inactivation of BRCA2 in Fanconi anemia, *Science 297*, 606 - 609.
84. Levitus, M., Waisfisz, Q., Godthelp, B. C., Vries, Y. d., Hussain, S., Wiegant, W. W., Elghalbzouri-Maghrani, E., Steltenpool, J., Rooimans, M. A., Pals, G., Arwert, F., Mathew, C. G., Zdzienicka, M. Z., Hiom, K., De Winter, J. P., and Joenje, H. (2005) The DNA helicase BRIP1 is defective in Fanconi anemia complementation group J, *Nat Genet 37*, 934-935.
85. Suhasini, A. N., Rawtani, N. A., Wu, Y., Sommers, J. A., Sharma, S., Mosedale, G., North, P. S., Cantor, S. B., Hickson, I. D., and Brosh, R. M. (2011) Interaction between the helicases genetically linked to Fanconi anemia group J and Bloom's syndrome, *EMBO J 30*, 692-705.

86. Reid, S., Schindler, D., Hanenberg, H., Barker, K., Hanks, S., Kalb, R., Neveling, K., Kelly, P., Seal, S., Freund, M., Wurm, M., Batish, S. D., Lach, F. P., Yetgin, S., Neitzel, H., Ariffin, H., Tischkowitz, M., Mathew, C. G., Auerbach, A. D., and Rahman, N. (2007) Biallelic mutations in PALB2 cause Fanconi anemia subtype FA-N and predispose to childhood cancer, *Nat Genet 39*, 162-164.
87. Vaz, F., Hanenberg, H., Schuster, B., Barker, K., Wiek, C., Erven, V., Neveling, K., Endt, D., Kesterton, I., Autore, F., Fraternali, F., Freund, M., Hartmann, L., Grimwade, D., Roberts, R. G., Schaal, H., Mohammed, S., Rahman, N., Schindler, D., and Mathew, C. G. (2010) Mutation of the RAD51C gene in a Fanconi anemia-like disorder, *Nat Genet 42*, 406-409.
88. Kim, Y., Lach, F. P., Desetty, R., Hanenberg, H., Auerbach, A. D., and Smogorzewska, A. (2011) Mutations of the SLX4 gene in Fanconi anemia, *Nat Genet 43*, 142-146.
89. Crossan, G. P., van der Weyden, L., Rosado, I. V., Langevin, F., Gaillard, P.-H. L., McIntyre, R. E., Gallagher, F., Kettunen, M. I., Lewis, D. Y., Brindle, K., Arends, M. J., Adams, D. J., and Patel, K. J. (2011) Disruption of mouse Slx4, a regulator of structure-specific nucleases, phenocopies Fanconi anemia, *Nat Genet 43*, 147-152.
90. Hanada, K., Budzowska, M., Modesti, M., Maas, A., Wyman, C., Essers, J., and Kanaar, R. (2006) The structure-specific endonuclease Mus81-Eme1 promotes conversion of interstrand DNA crosslinks into double-strands breaks, *EMBO J 25*, 4921-4932.
91. Muñoz, I. M., Hain, K., Déclais, A.-C., Gardiner, M., Toh, G. W., Sanchez-Pulido, L., Heuckmann, J. M., Toth, R., Macartney, T., Eppink, B., Kanaar, R., Ponting, C. P., Lilley, D. M. J., and Rouse, J. (2009) Coordination of structure-specific nucleases by human SLX4/BTBD12 is required for DNA repair, *Molecular Cell 35*, 116-127.
92. Bhagwat, N., Olsen, A. L., Wang, A. T., Hanada, K., Stuckert, P., Kanaar, R., D'Andrea, A., Niedernhofer, L. J., and McHugh, P. J. (2009) XPF-ERCC1 participates in the Fanconi anemia pathway of cross-link repair, *Molecular and Cellular Biology 29*, 6427-6437.
93. Smogorzewska, A., Matsuoka, S., Vinciguerra, P., McDonald, E.R., Illf, Hurov, K.E., Luo, J., Ballif, B.A., Gygi, S.P., Hofmann, K., D'Andrea, A.D., Elledge, S.J. (2007) Identification of the FANCI protein, a monomonoubiquitinated FANCD2 paralog required for DNA repair., *Cell 129*, 289-310.
94. Meetei, A. R., de Winter, J. P., Medhurst, A. L., Wallisch, M., Waisfisz, Q., van de Vrugt, H. J., Oostra, A. B., Yan, Z., Ling, C., Bishop, C. E., Hoatlin, M. E., Joenje, H., and Wang, W. (2003) A novel ubiquitin ligase is deficient in Fanconi anemia, *Nat Genet 35*, 165-170.
95. Knipscheer, P., Raschle, M., Smogorzewska, A., Enoiu, M., Ho, T. V., Scharer, O. D., Elledge, S. J., and Walter, J. C. (2009) The Fanconi anemia pathway promotes replication-cependent DNA interstrand cross-link repair, *Science 326*, 1698-1701.
96. Joo, W., Xu, G., Persky, N. S., Smogorzewska, A., Rudge, D. G., Buzovetsky, O., Elledge, S. J., and Pavletich, N. P. (2011) Structure of the FANCI-FANCD2 complex: Insights into the Fanconi anemia DNA repair pathway, *Science 333*, 312-316.

97. Park, W. H., Margossian, S., Horwitz, A.A., Simons, A.M., D'Andrea, A.D., Parvin, J.D. . (2005) Direct DNA binding activity of the Fanconi anemia D2 protein. , *J.Biol.Chem. 280*, 6.
98. Longerich, S., San Filippo, J., Liu, D., and Sung, P. (2009) FANCI binds branched DNA and is monoubiquitinated by UBE2T-FANCL, *Journal of Biological Chemistry 284*, 23182-23186.
99. Pichierri, P., and Rosselli, F. (2004) The DNA crosslink-induced S-phase checkpoint depends on ATR-CHK1 and ATR-NBS1-FANCD2 pathways, *EMBO J 23*, 1178-1187.
100. Ishiai, M., Kitao, H., Smogorzewska, A., Tomida, J., Kinomura, A., Uchida, E., Saberi, A., Kinoshita, E., Kinoshita-Kikuta, E., Koike, T., Tashiro, S., Elledge, S. J., and Takata, M. (2008) FANCI phosphorylation functions as a molecular switch to turn on the Fanconi anemia pathway, *Nat Struct Mol Biol 15*, 1138-1146.
101. Shigechi, T., Tomida, J., Sato, K., Kobayashi, M., Eykelenboom, J. K., Pessina, F., Zhang, Y., Uchida, E., Ishiai, M., Lowndes, N. F., Yamamoto, K., Kurumizaka, H., Maehara, Y., and Takata, M. (2012) ATR-ATRIP kinase complex triggers activation of the Fanconi anemia DNA repair pathway, *Cancer Research 72*, 1149-1156.
102. MacKay, C., Déclais, A.-C., Lundin, C., Agostinho, A., Deans, A. J., MacArtney, T. J., Hofmann, K., Gartner, A., West, S. C., Helleday, T., Lilley, D. M. J., and Rouse, J. (2010) Identification of KIAA1018/FAN1, a DNA repair nuclease recruited to DNA damage by monoubiquitinated FANCD2, *Cell 142*, 65-76.
103. Pichierri, P., Averbeck, D., and Rosselli, F. (2002) DNA cross-link-dependent RAD50/MRE11/NBS1 subnuclear assembly requires the Fanconi anemia C protein, *Human Molecular Genetics 11*, 2531-2546.
104. Taniguchi, T., Tischkowitz, M., Ameziane, N., Hodgson, S. V., Mathew, C. G., Joenje, H., Mok, S. C., and D'Andrea, A. D. (2003) Disruption of the Fanconi anemia-BRCA pathway in cisplatin-sensitive ovarian tumors, *Nat Med 9*, 568-574.
105. Wang, X., Andreassen, P. R., and D'Andrea, A. D. (2004) Functional Interaction of Monoubiquitinated FANCD2 and BRCA2/FANCD1 in Chromatin, *Mol. Cell. Biol. 24*, 5850-5862.
106. Taniguchi, T., Garcia-Higuera, I., Andreassen, P. R., Gregory, R. C., Grompe, M., and D'Andrea, A. D. (2002) S-phase specific interaction of the Fanconi anemia protein, FANCD2, with BRCA1 and RAD51, *Blood 100*, 2414-2420.
107. Garcia-Higuera, I., Taniguchi, T., Ganesan, S., Meyn, M. S., Timmers, C., Hejna, J., Grompe, M., and D'Andrea, A. D. (2001) Interaction of the Fanconi anemia proteins and BRCA1 in a common pathway, *Molecular Cell 7*, 249-262.
108. Bunting, S. F., Callén, E., Kozak, M. L., Kim, J. M., Wong, N., López-Contreras, A. J., Ludwig, T., Baer, R., Faryabi, R. B., Malhowski, A., Chen, H.-T., Fernandez-Capetillo, O., D'Andrea, A., and Nussenzweig, A. (2012) BRCA1 functions independently of homologous recombination in DNA interstrand crosslink repair, *Molecular Cell 46*, 125-135.
109. Feng, L., Fong, K.-W., Wang, J., Wang, W., and Chen, J. (2013) RIF1 counteracts BRCA1-mediated end resection during DNA repair, *Journal of Biological Chemistry*.

110. Adamo, A., Collis, S. J., Adelman, C. A., Silva, N., Horejsi, Z., Ward, J. D., Martinez-Perez, E., Boulton, S. J., and La Volpe, A. (2010) Preventing nonhomologous end joining suppresses DNA repair defects of Fanconi anemia, *Molecular Cell 39*, 25-35.
111. Pace, P., Mosedale, G., Hodskinson, M. R., Rosado, I. V., Sivasubramaniam, M., and Patel, K. J. (2010) Ku70 corrupts DNA repair in the absence of the Fanconi anemia pathway, *Science 329*, 219-223.
112. Shen, X., Do, H., Li, Y., Chung, W.-H., Tomasz, M., de Winter, J. P., Xia, B., Elledge, S. J., Wang, W., and Li, L. (2009) Recruitment of Fanconi anemia and breast cancer proteins to DNA damage sites is differentially governed by replication, *Molecular Cell 35*, 716-723.
113. Williams, S. A., Wilson, J. B., Clark, A. P., Mitson-Salazar, A., Tomashevski, A., Ananth, S., Glazer, P. M., Semmes, O. J., Bale, A. E., Jones, N. J., and Kupfer, G. M. (2011) Functional and physical interaction between the mismatch repair and FA-BRCA pathways, *Human Molecular Genetics 20*, 4395-4410.
114. Wu, L., and Hickson, I. D. (2003) The Bloom's syndrome helicase suppresses crossing over during homologous recombination, *Nature 426*, 870-874.
115. Chaudhury, I., Sareen, A., Raghunandan, M., and Sobeck, A. (2013) FANCD2 regulates BLM complex functions independently of FANCI to promote replication fork recovery, *Nucleic Acids Research 41*, 6444-6459.
116. Fujimori, A., Matsuda, Y., Takemoto, Y., Hashimoto, Y., Kubo, E., Araki, R., Fukumura, R., Mita, K., Tatsumi, K., and Muto, M. (1998) Cloning and mapping of Np95 gene which encodes a novel nuclear protein associated with cell proliferation, *Mammalian Genome 9*, 1032-1035.
117. Miura, M., Watanabe, H., Sasaki, T., Tatsumi, K., and Muto, M. (2001) Dynamic changes in subnuclear Np95 location during the cell cycle and its spatial relationship with DNA replication foci, *Experimental Cell Research 263*, 202-208.
118. Uemura, T., Kubo, E., Kanari, Y., Ikemura, T., Tatsumi, K., and Muto, M. (2000) Temporal and spatial localization of novel nuclear protein Np95 in mitotic and meiotic cells, *Cell Structure and Function 25*, 149-159.
119. Raphaël Hopfner, M. M., Jean-Marc Jeltsch, Angélique Voulgaris, Yves Lutz, Cristi Marin, Jean-Pierre Bellocq, Pierre Oudet, and Christian Bronner. (2000) ICBP90, a novel human CCAAT binding protein, involved in the regulation of Topoisomerase II α expression, *Cancer Research 60*, 121-128.
120. Mousli, M., Hopfner, R., Abbady, A. Q., Monte, D., Jeanblanc, M., Oudet, P., Louis, B., and Bronner, C. (2003) ICBP90 belongs to a new family of proteins with an expression that is deregulated in cancer cells, *Br J Cancer 89*, 120-127.
121. Unoki, M., Nishidate, T., and Nakamura, Y. (2004) ICBP90, an E2F-1 target, recruits HDAC1 and binds to methyl-CpG through its SRA domain, *Oncogene 23*, 7601-7610.
122. Taylor, E. M., Bonsu, N. M., Price, R. J., and Lindsay, H. D. (2013) Depletion of Uhrf1 inhibits chromosomal DNA replication in Xenopus egg extracts, *Nucleic Acids Research*.

123. Nishiyama, A., Yamaguchi, L., Sharif, J., Johmura, Y., Kawamura, T., Nakanishi, K., Shimamura, S., Arita, K., Kodama, T., Ishikawa, F., Koseki, H., and Nakanishi, M. (2013) Uhrf1-dependent H3K23 ubiquitylation couples maintenance DNA methylation and replication, *Nature advance online publication*.
124. Citterio, E., Papait, R., Nicassio, F., Vecchi, M., Gomiero, P., Mantovani, R., Di Fiore, P. P., and Bonapace, I. M. (2004) Np95 is a histone-binding protein endowed with ubiquitin ligase activity, *Molecular and Cellular Biology 24*, 2526-2535.
125. Karagianni, P., Amazit, L., Qin, J., and Wong, J. (2008) ICBP90, a novel methyl K9 H3 binding protein linking protein ubiquitination with heterochromatin formation, *Mol. Cell. Biol. 28*, 705-717.
126. Papait, R., Pistore, C., Negri, D., Pecoraro, D., Cantarini, L., and Bonapace, I. M. (2007) Np95 is implicated in pericentromeric heterochromatin replication and in major satellite silencing, *Molecular Biology of the Cell 18*, 1098-1106.
127. Papait, R., Pistore, C., Grazini, U., Babbio, F., Cogliati, S., Pecoraro, D., Brino, L., Morand, A.-L., Dechampesme, A.-M., Spada, F., Leonhardt, H., McBlane, F., Oudet, P., and Bonapace, I. M. (2008) The PHD domain of Np95 (mUHRF1) is involved in large-scale reorganization of pericentromeric heterochromatin, *Molecular Biology of the Cell 19*, 3554-3563.
128. Nady, N., Lemak, A., Walker, J. R., Avvakumov, G. V., Kareta, M. S., Achour, M., Xue, S., Duan, S., Allali-Hassani, A., Zuo, X., Wang, Y.-X., Bronner, C., Chédin, F., Arrowsmith, C. H., and Dhe-Paganon, S. (2011) Recognition of multivalent histone states associated with heterochromatin by UHRF1 protein, *Journal of Biological Chemistry 286*, 24300-24311.
129. Cheng, J., Yang, Y., Fang, J., Xiao, J., Zhu, T., Chen, F., Wang, P., Li, Z., Yang, H., and Xu, Y. (2013) Structural insight into coordinated recognition of trimethylated histone H3 lysine 9 (H3K9me3) by the Plant Homeodomain (PHD) and Tandem Tudor Domain (TTD) of UHRF1 (Ubiquitin-like, Containing PHD and RING Finger Domains, 1) protein, *Journal of Biological Chemistry 288*, 1329-1339.
130. Tsumura, A., Hayakawa, T., Kumaki, Y., Takebayashi, S.-i., Sakaue, M., Matsuoka, C., Shimotohno, K., Ishikawa, F., Li, E., Ueda, H. R., Nakayama, J.-i., and Okano, M. (2006) Maintenance of self-renewal ability of mouse embryonic stem cells in the absence of DNA methyltransferases Dnmt1, Dnmt3a and Dnmt3b, *Genes to Cells 11*, 805-814.
131. Bostick, M., Kim, J. K., Esteve, P.-O., Clark, A., Pradhan, S., and Jacobsen, S. E. (2007) UHRF1 plays a role in maintaining DNA methylation in mammalian cells, *Science 317*, 1760-1764.
132. Okano, M., Bell, D. W., Haber, D. A., and Li, E. (1999) DNA methyltransferases Dnmt3a and Dnmt3b are essential for de novo methylation and mammalian development, *Cell 99*, 247-257.
133. Howell, C. Y., Bestor, T. H., Ding, F., Latham, K. E., Mertineit, C., Trasler, J. M., and Chaillet, J. R. (2001) Genomic imprinting disrupted by a maternal effect mutation in the Dnmt1 gene, *Cell 104*, 829-838.
134. Muto, M., Kanari, Y., Kubo, E., Takabe, T., Kurihara, T., Fujimori, A., and Tatsumi, K. (2002) Targeted disruption of Np95 gene renders murine

embryonic stem cells hypersensitive to DNA damaging agents and DNA replication blocks, *Journal of Biological Chemistry 277*, 34549-34555.
135. Sadler, K. C., Krahn, K. N., Gaur, N. A., and Ukomadu, C. (2007) Liver growth in the embryo and during liver regeneration in zebrafish requires the cell cycle regulator, Uhrf1, *Proceedings of the National Academy of Sciences 104*, 1570-1575.
136. Achour, M., Jacq, X., Rondé, P., Alhosin, M., Charlot, C., Chataigneau, T., Jeanblanc, M., Macaluso, M., Giordano, A., Hughes, A. D., Schini-Kerth, V. B., and Bronner, C. (2007) The interaction of the SRA domain of ICBP90 with a novel domain of DNMT1 is involved in the regulation of VEGF gene expression, *Oncogene 27*, 2187-2197.
137. Rajakumara, E., Law, J. A., Simanshu, D. K., Voigt, P., Johnson, L. M., Reinberg, D., Patel, D. J., and Jacobsen, S. E. (2011) A dual flip-out mechanism for 5mC recognition by the Arabidopsis SUVH5 SRA domain and its impact on DNA methylation and H3K9 dimethylation in vivo, *Genes & Development 25*, 137-152.
138. Johnson, L. M., Bostick, M., Zhang, X., Kraft, E., Henderson, I., Callis, J., and Jacobsen, S. E. (2007) The SRA methyl-cytosine-binding domain links DNA and histone methylation, *Current Biology 17*, 379-384.
139. Hashimoto, H., Horton, J. R., Zhang, X., Bostick, M., Jacobsen, S. E., and Cheng, X. (2008) The SRA domain of UHRF1 flips 5-methylcytosine out of the DNA helix, *Nature 455*, 826-829.
140. Arita, K., Ariyoshi, M., Tochio, H., Nakamura, Y., and Shirakawa, M. (2008) Recognition of hemi-methylated DNA by the SRA protein UHRF1 by a base-flipping mechanism, *Nature 455*, 818-821.
141. Sharif, J., Muto, M., Takebayashi, S.-I., Suetake, I., Iwamatsu, A., Endo, T. A., Shinga, J., Mizutani-Koseki, Y., Toyoda, T., Okamura, K., Tajima, S., Mitsuya, K., Okano, M., and Koseki, H. (2007) The SRA protein Np95 mediates epigenetic inheritance by recruiting Dnmt1 to methylated DNA, *Nature 450*, 908-912.
142. Marhold, J., Rothe, N., Pauli, A., Mund, C., Kuehle, K., Brueckner, B., and Lyko, F. (2004) Conservation of DNA methylation in dipteran insects, *Insect Molecular Biology 13*, 117-123.
143. Lyko, F., Ramsahoye, B. H., and Jaenisch, R. (2000) Development: DNA methylation in Drosophila melanogaster, *Nature 408*, 538-540.
144. Edelheit, S., Schwartz, S., Mumbach, M. R., Wurtzel, O., and Sorek, R. (2013) Transcriptome-wide mapping of 5-methylcytidine RNA modifications in bacteria, archaea, and yeast reveals m5C within archaeal mRNAs, *PLoS Genet 9*, e1003602.
145. Feng, S., Cokus, S. J., Zhang, X., Chen, P.-Y., Bostick, M., Goll, M. G., Hetzel, J., Jain, J., Strauss, S. H., Halpern, M. E., Ukomadu, C., Sadler, K. C., Pradhan, S., Pellegrini, M., and Jacobsen, S. E. (2010) Conservation and divergence of methylation patterning in plants and animals, *Proceedings of the National Academy of Sciences*.
146. Muto, M., Fujimori, A., Nenoi, M., Daino, K., Matsuda, Y., Kuroiwa, A., Kubo, E., Kanari, Y., Utsuno, M., Tsuji, H., Ukai, H., Mita, K., Takahagi, M., and Tatsumi, K. (2006) Isolation and characterization of a novel human radiosusceptibility gene, Np95, *Radiation Research 166*, 723-733.

147. Mistry, H., Tamblyn, L., Butt, H., Sisgoreo, D., Gracias, A., Larin, M., Gopalakrishnan, K., Hande, M., and McPherson, J. (2010) UHRF1 is a genome caretaker that facilitates the DNA damage response to gamma-irradiation, *Genome Integrity 1*, 7.
148. Tien AL, S. S., Kulkarni A, Mudbhary R, Goudreau B, Ganesan S, Sadler KC, Ukomadu C. (2011) UHRF1 depletion causes a G2/M arrest, activation of DNA damage response and apoptosis., *Biochem J. 435*, 175-185.
149. Unoki, M., Kelly, J. D., Neal, D. E., Ponder, B. A. J., Nakamura, Y., and Hamamoto, R. (2009) UHRF1 is a novel molecular marker for diagnosis and the prognosis of bladder cancer, *Br J Cancer 101*, 98-105.
150. Jin, W., Chen, L., Chen, Y., Xu, S.-G., Di, G.-H., Yin, W.-J., Wu, J., and Shao, Z.-M. (2010) UHRF1 is associated with epigenetic silencing of BRCA1 in sporadic breast cancer, *Breast Cancer Research and Treatment 123*, 359-373.
151. Lallous, N., Legrand, P., McEwen, A. G., Ramón-Maiques, S., Samama, J.-P., and Birck, C. (2011) The PHD Finger of Human UHRF1 Reveals a New Subgroup of Unmethylated Histone H3 Tail Readers, *PLoS ONE 6*, e27599.
152. Mistry, H., Gibson, L., Yun, J. W., Sarras, H., Tamblyn, L., and McPherson, J. P. (2008) Interplay between Np95 and Eme1 in the DNA damage response, *Biochemical and Biophysical Research Communications 375*, 321-325.
153. Jenkins, Y., Markovtsov, V., Lang, W., Sharma, P., Pearsall, D., Warner, J., Franci, C., Huang, B., Huang, J., Yam, G. C., Vistan, J. P., Pali, E., Vialard, J., Janicot, M., Lorens, J. B., Payan, D. G., and Hitoshi, Y. (2005) Critical role of the ubiquitin ligase activity of UHRF1, a nuclear RING finger protein, in tumor cell growth, *Mol. Biol. Cell 16*, 5621-5629.
154. Esposito, F., Brankamp, R. G., and Sinden, R. R. (1988) DNA sequence specificity of 4,5',8-trimethylpsoralen cross-linking. Effect of neighboring bases on cross-linking the 5'-TA dinucleotide, *Journal of Biological Chemistry 263*, 11466-11472.
155. Sambrook, J., Fritsch, E. F., and Maniatis, T. (1989) *Molecular Cloning: A Laboratory Manual*, Cold Spring Harbor Laboratory Press.
156. Dignam, J. D., Martin, P. L., Shastry, B. S., and Roeder, R. G. (1983) Eukaryotic gene transcription with purified components, In *Methods in Enzymology* (Ray Wu, L. G. K. M., Ed.), pp 582-598, Academic Press.
157. Cohn, M. A., Kowal, P., Yang, K., Haas, W., Huang, T. T., Gygi, S. P., and D'Andrea, A. D. (2007) A UAF1-containing multisubunit protein complex regulates the Fanconi anemia pathway, *Molecular cell 28*, 786-797.
158. Nakatani, Y., and Ogryzko, V. (2003) Immunoaffinity purification of mammalian protein complexes., *Methods Enzymol. 379*, 430-444.
159. Markowitz, D., Goff, S., and Bank, A. (1989) Construction of a safe and efficient retrovirus packaging cell line, In *Molecular Biology of Hemopoiesis* (Tavassoli, M., Zanjani, E. D., Ascensao, J. L., Abraham, N. G., and Levine, A. S., Eds.), pp 35-40, Springer US.
160. Cimino, G. D., Gamper, H. B., Isaacs, S. T., and Hearst, J. E. (1985) Psoralens as photoactive probes of nucleic acid structure and function: Organic chemistry, photochemistry, and biochemistry, *Annual Review of Biochemistry 54*, 1151-1193.

161. Smogorzewaska, A., Matsuoka, S., Vinciguerra, P., McDonald, E.R., Illf, Hurov, K.E., Luo, J., Ballif, B.A., Gygi, S.P., Hofmann, K., D'Andrea, A.D., Elledge, S.J. (2007) Identification of the FANCI protein, a monoubiquitinated FANCD2 paralog required for DNA repair, *Cell*, 12.
162. Chatterjee, P. K., and Cantor, C. R. (1978) Photochemical production of psoralen - DNA monoadducts capable of subsequent photocrosslinking, *Nucleic Acids Research 5*, 3619-3634.
163. Roques, C., Coulombe, Y., Delannoy, M., Vignard, J., Grossi, S., Brodeur, I., Rodrigue, A., Gautier, J., Stasiak, A. Z., Stasiak, A., Constantinou, A., and Masson, J.-Y. (2009) MRE11-RAD50-NBS1 is a critical regulator of FANCD2 stability and function during DNA double-strand break repair, *EMBO J 28*, 2400-2413.
164. Park, W.-H., Margossian, S., Horwitz, A. A., Simons, A. M., D'Andrea, A. D., and Parvin, J. D. (2005) Direct DNA binding activity of the Fanconi anemia D2 protein, *Journal of Biological Chemistry 280*, 23593-23598.
165. Medhurst, A. L., Laghmani, E. H., Steltenpool, J., Ferrer, M., Fontaine, C., de Groot, J., Rooimans, M. A., Scheper, R. J., Meetei, A. R., Wang, W., Joenje, H., and de Winter, J. P. (2006) Evidence for subcomplexes in the Fanconi anemia pathway, *Blood 108*, 2072-2080.
166. Yuan, F., Qian, L., Zhao, X., Liu, J. Y., Song, L., D'Urso, G., Jain, C., and Zhang, Y. (2012) Fanconi anemia complementation group A (FANCA) protein has intrinsic affinity for nucleic acids with preference for single-stranded forms, *Journal of Biological Chemistry 287*, 4800-4807.
167. Gari, K., Décaillet, C., Stasiak, A. Z., Stasiak, A., and Constantinou, A. (2008) The Fanconi anemia protein FANCM can promote branch migration of Holliday junctions and replication forks, *Molecular Cell 29*, 141-148.
168. Holmberg, A., Blomstergren, A., Nord, O., Lukacs, M., Lundeberg, J., and Uhlén, M. (2005) The biotin-streptavidin interaction can be reversibly broken using water at elevated temperatures, *Electrophoresis 26*, 501-510.
169. Hofmann, K., Wood, S. W., Brinton, C. C., Montibeller, J. A., and Finn, F. M. (1980) Iminobiotin affinity columns and their application to retrieval of streptavidin, *Proceedings of the National Academy of Sciences 77*, 4666-4668.
170. Updyke, T. V., and Nicolson, G. L. (1984) Immunoaffinity isolation of membrane antigens with biotinylated monoclonal antibodies and immobilized streptavidin matrices, *Journal of Immunological Methods 73*, 83-95.
171. Waisfisz, Q., Miyazato, A., de Winter, J., Liu, J., and Joenje, H. (2002) Analysis of baseline and cisplatin-inducible gene expression in Fanconi anemia cells using oligonucleotide-based microarrays, *BMC Blood Disorders 2*, 5.
172. Hale, J. E., Butler, J. P., Gelfanova, V., You, J.-S., and Knierman, M. D. (2004) A simplified procedure for the reduction and alkylation of cysteine residues in proteins prior to proteolytic digestion and mass spectral analysis, *Analytical Biochemistry 333*, 174-181.
173. Sechi, S., and Chait, B. T. (1998) Modification of cysteine residues by alkylation: A tool in peptide mapping and protein identification, *Analytical Chemistry 70*, 5150-5158.

174. Bronner, C., Achour, M., Arima, Y., Chataigneau, T., Saya, H., and Schini-Kerth, V. B. (2007) The UHRF family: Oncogenes that are drugable targets for cancer therapy in the near future?, *Pharmacology & Therapeutics 115*, 419-434.
175. Zhu, G., and Lippard, S. J. (2009) Photoaffinity labeling reveals nuclear proteins that uniquely recognize cisplatin-DNA interstrand cross-links, *Biochemistry 48*, 4916-4925.
176. Guggenheim, E. R., Xu, D., Zhang, C. X., Chang, P. V., and Lippard, S. J. (2009) Photoaffinity isolation and identification of proteins in cancer cell extracts that bind to platinum-modified DNA, *ChemBioChem 10*, 141-157.
177. Kim, J. K., Esteve, P.-O., Jacobsen, S. E., and Pradhan, S. (2009) UHRF1 binds G9a and participates in p21 transcriptional regulation in mammalian cells, *Nucleic Acids Research 37*, 493-505.
178. Alhosin, M., Sharif, T., Mousli, M., Etienne-Selloum, N., Fuhrmann, G., Schini-Kerth, V., and Bronner, C. (2011) Down-regulation of UHRF1, associated with re-expression of tumor suppressor genes, is a common feature of natural compounds exhibiting anti-cancer properties, *Journal of Experimental & Clinical Cancer Research 30*, 41.
179. Joazeiro, C. A. P., and Weissman, A. M. (2000) RING finger proteins: Mediators of ubiquitin ligase activity, *Cell 102*, 549-552.
180. Jackson, P. K., Eldridge, A. G., Freed, E., Furstenthal, L., Hsu, J. Y., Kaiser, B. K., and Reimann, J. D. R. (2000) The lore of the RINGs: substrate recognition and catalysis by ubiquitin ligases, *Trends in Cell Biology 10*, 429-439.
181. Qin, W., Leonhardt, H., and Spada, F. (2011) Usp7 and Uhrf1 control ubiquitination and stability of the maintenance DNA methyltransferase Dnmt1, *Journal of Cellular Biochemistry 112*, 439-444.
182. Du, Z., Song, J., Wang, Y., Zhao, Y., Guda, K., Yang, S., Kao, H.-Y., Xu, Y., Willis, J., Markowitz, S. D., Sedwick, D., Ewing, R. M., and Wang, Z. (2010) DNMT1 stability is regulated by proteins coordinating deubiquitination and acetylation-driven ubiquitination, *Sci. Signal. 3*, ra80.
183. Guan, D., Factor, D., Liu, Y., Wang, Z., and Kao, H. Y. (2012) The epigenetic regulator UHRF1 promotes ubiquitination-mediated degradation of the tumor-suppressor protein promyelocytic leukemia protein, *Oncogene*, 3819-3828.
184. Hoeller, D., Hecker, C.-M., Wagner, S., Rogov, V., Dötsch, V., and Dikic, I. (2007) E3-Independent monoubiquitination of ubiquitin-binding proteins, *Molecular Cell 26*, 891-898.
185. Sakata, E., Satoh, T., Yamamoto, S., Yamaguchi, Y., Yagi-Utsumi, M., Kurimoto, E., Tanaka, K., Wakatsuki, S., and Kato, K. (2010) Crystal structure of UbcH5b~ubiquitin intermediate: Insight into the formation of the self-assembled E2~Ub conjugates, *Structure 18*, 138-147.
186. Rothbart, S. B., Dickson, B. M., Ong, M. S., Krajewski, K., Houliston, S., Kireev, D. B., Arrowsmith, C. H., and Strahl, B. D. (2013) Multivalent histone engagement by the linked tandem Tudor and PHD domains of UHRF1 is required for the epigenetic inheritance of DNA methylation, *Genes & Development 27*, 1288-1298.
187. Rajakumara, E., Wang, Z., Ma, H., Hu, L., Chen, H., Lin, Y., Guo, R., Wu, F., Li, H., Lan, F., Shi, Y. G., Xu, Y., Patel, D. J., and Shi, Y. (2011) PHD finger

recognition of unmodified histone H3R2 Links UHRF1 to regulation of euchromatic Gene expression, *Molecular Cell 43*, 275-284.
188. Yun, J.-H., Ko, S., Lee, C.-K., Cheong, H.-K., Cheong, C., Yoon, J.-B., and Lee, W. (2013) Solution structure and Rpn1 interaction of the UBL domain of human RNA polymerase II C-terminal domain phosphatase, *PLoS ONE 8*, e62981.
189. Xu, Y., Liu, Y., Lee, J.-g., and Ye, Y. (2013) A Ubiquitin-like Domain Recruits an Oligomeric Chaperone to a Retrotranslocation Complex in Endoplasmic Reticulum-associated Degradation, *Journal of Biological Chemistry 288*, 18068-18076.
190. Smith, G. E., Summers, M. D., and Fraser, M. J. (1983) Production of human beta interferon in insect cells infected with a baculovirus expression vector, *Molecular and Cellular Biology 3*, 2156-2165.
191. Pan, M.-R., Peng, G., Hung, W.-C., and Lin, S.-Y. (2011) Monoubiquitination of H2AX protein regulates DNA damage response signaling, *Journal of Biological Chemistry 286*, 28599-28607.
192. Ginjala, V., Nacerddine, K., Kulkarni, A., Oza, J., Hill, S. J., Yao, M., Citterio, E., van Lohuizen, M., and Ganesan, S. (2011) BMI1 is recruited to DNA breaks and contributes to DNA damage-induced H2A ubiquitination and repair, *Molecular and Cellular Biology 31*, 1972-1982.
193. Ismail, I. H., Andrin, C., McDonald, D., and Hendzel, M. J. (2010) BMI1-mediated histone ubiquitylation promotes DNA double-strand break repair, *The Journal of Cell Biology 191*, 45-60.
194. Spielmann, H. P., Dwyer, T. J., Hearst, J. E., and Wemmer, D. E. (1995) Solution structures of psoralen monoadducted and cross-linked DNA oligomers by NMR spectroscopy and restrained molecular dynamics, *Biochemistry 34*, 12937-12953.
195. Klug, A. (1999) Zinc finger peptides for the regulation of gene expression, *Journal of Molecular Biology 293*, 215-218.
196. Hall, T. M. T. (2005) Multiple modes of RNA recognition by zinc finger proteins, *Current Opinion in Structural Biology 15*, 367-373.
197. Arima, Y., Hirota, T., Bronner, C., Mousli, M., Fujiwara, T., Niwa, S.-I., Ishikawa, H., and Saya, H. (2004) Down-regulation of nuclear protein ICBP90 by p53/p21Cip1/WAF1-dependent DNA-damage checkpoint signals contributes to cell cycle arrest at G1/S transition, *Genes to Cells 9*, 131-142.
198. Cervenka, J., Arthur, D., and Yasis, C. (1981) Mitomycin C test for diagnostic differentiation of idiopathic aplastic anemia and Fanconi anemia, *Pediatrics 67*, 119-127.
199. Plooy, A. C. M., van Dijk, M., Berends, F., and Lohman, P. H. M. (1985) Formation and repair of DNA interstrand cross-links in relation to cytotoxicity and unscheduled DNA synthesis induced in control and mutant human cells treated with cis-diamminedichloroplatinum(II), *Cancer Research 45*, 4178-4184.
200. Lovering, R., Hanson, I. M., Borden, K. L., Martin, S., O'Reilly, N. J., Evan, G. I., Rahman, D., Pappin, D. J., Trowsdale, J., and Freemont, P. S. (1993) Identification and preliminary characterization of a protein motif related to the zinc finger, *Proceedings of the National Academy of Sciences 90*, 2112-2116.

201. Seki, S., Ohzeki, M., Uchida, A., Hirano, S., Matsushita, N., Kitao, H., Oda, T., Yamashita, T., Kashihara, N., Tsubahara, A., Takata, M., and Ishiai, M. (2007) A requirement of FancL and FancD2 monoubiquitination in DNA repair, *Genes to Cells 12*, 299-310.
202. Donahue, S. L., Lundberg, R., Saplis, R., and Campbell, C. (2003) Deficient regulation of DNA double-strand break repair in Fanconi anemia fibroblasts, *Journal of Biological Chemistry 278*, 29487-29495.
203. Chen, T., Hevi, S., Gay, F., Tsujimoto, N., He, T., Zhang, B., Ueda, Y., and Li, E. (2007) Complete inactivation of DNMT1 leads to mitotic catastrophe in human cancer cells, *Nat Genet 39*, 391-396.
204. Shakya, R., Reid, L. J., Reczek, C. R., Cole, F., Egli, D., Lin, C.-S., deRooij, D. G., Hirsch, S., Ravi, K., Hicks, J. B., Szabolcs, M., Jasin, M., Baer, R., and Ludwig, T. (2011) BRCA1 tumor suppression depends on BRCT phosphoprotein binding, but not its E3 ligase activity, *Science 334*, 525-528.
205. Drost, R., Bouwman, P., Rottenberg, S., Boon, U., Schut, E., Klarenbeek, S., Klijn, C., van der Heijden, I., van der Gulden, H., Wientjens, E., Pieterse, M., Catteau, A., Green, P., Solomon, E., Morris, J. R., and Jonkers, J. (2011) BRCA1 RING function is essential for tumor suppression but dispensable for therapy resistance, *Cancer cell 20*, 797-809.
206. Ho, G. P. H., Margossian, S., Taniguchi, T., and D'Andrea, A. D. (2006) Phosphorylation of FANCD2 on two novel sites is required for mitomycin C resistance, *Molecular and Cellular Biology 26*, 7005-7015.
207. Andreassen, P. R., D'Andrea, A. D., and Taniguchi, T. (2004) ATR couples FANCD2 monoubiquitination to the DNA-damage response, *Genes & Development 18*, 1958-1963.
208. Medhurst, A. L., Huber, P. A. J., Waisfisz, Q., de Winter, J. P., and Mathew, C. G. (2001) Direct interactions of the five known Fanconi anaemia proteins suggest a common functional pathway, *Human Molecular Genetics 10*, 423-429.
209. Alpi, A., Langevin, F., Mosedale, G., Machida, Y. J., Dutta, A., and Patel, K. J. (2007) UBE2T, the Fanconi anemia core complex, and FANCD2 are recruited independently to chromatin: A basis for the regulation of FANCD2 monoubiquitination, *Molecular and Cellular Biology 27*, 8421-8430.
210. Parrish, J. A. (1977) Treatment of psoriasis with long-wave ultraviolet light, *Archives of Dermatology 113*, 1525-1528.
211. Bredberg, A., Sandor, Z., and Brant, M. (1995) Mutational response of Fanconi anaemia cells to shuttle vector site-specific psoralen cross-links, *Carcinogenesis 16*, 555-561.
212. Yamamoto, K. N., Kobayashi, S., Tsuda, M., Kurumizaka, H., Takata, M., Kono, K., Jiricny, J., Takeda, S., and Hirota, K. (2011) Involvement of SLX4 in interstrand cross-link repair is regulated by the Fanconi anemia pathway, *Proceedings of the National Academy of Sciences 108*, 6492-6496.
213. Sridharan, D., Brown, M., Lambert, W. C., McMahon, L. W., and Lambert, M. W. (2003) Nonerythroid α II spectrin is required for recruitment of FANCA and XPF to nuclear foci induced by DNA interstrand cross-links, *Journal of Cell Science 116*, 823-835.
214. Zhang, J., Gao, Q., Li, P., Liu, X., Jia, Y., Wu, W., Li, J., Dong, S., Koseki, H., and Wong, J. (2011) S phase-dependent interaction with DNMT1 dictates the

role of UHRF1 but not UHRF2 in DNA methylation maintenance, *Cell Res 21*, 1723-1739.
215. Paull, T. T., Rogakou, E. P., Yamazaki, V., Kirchgessner, C. U., Gellert, M., and Bonner, W. M. (2000) A critical role for histone H2AX in recruitment of repair factors to nuclear foci after DNA damage, *Current biology : CB 10*, 886-895.
216. Bogliolo, M., Lyakhovich, A., Callen, E., Castella, M., Cappelli, E., Ramirez, M. J., Creus, A., Marcos, R., Kalb, R., Neveling, K., Schindler, D., and Surralles, J. (2007) Histone H2AX and Fanconi anemia FANCD2 function in the same pathway to maintain chromosome stability, *EMBO J 26*, 1340-1351.
217. Valeri, A., Rio, P., Agirre, X., Prosper, F., and Bueren, J. A. (2012) Unraveling the role of FANCD2 in chronic myeloid leukemia, *Leukemia 26*, 1447-1448.
218. Nijman, S. M. B., Huang, T. T., Dirac, A. M. G., Brummelkamp, T. R., Kerkhoven, R. M., D'Andrea, A. D., and Bernards, R. (2005) The deubiquitinating enzyme USP1 regulates the Fanconi anemia pathway, *Molecular Cell 17*, 331-339.
219. Oestergaard, V. H., Langevin, F., Kuiken, H. J., Pace, P., Niedzwiedz, W., Simpson, L. J., Ohzeki, M., Takata, M., Sale, J. E., and Patel, K. J. (2007) Deubiquitination of FANCD2 is required for DNA crosslink repair, *Molecular Cell 28*, 798-809.
220. Kim, J. M., Parmar, K., Huang, M., Weinstock, D. M., Ruit, C. A., Kutok, J. L., and D'Andrea, A. D. (2009) Inactivation of murine Usp1 results in genomic instability and a Fanconi anemia phenotype, *Developmental cell 16*, 314-320.
221. Geng, L., Huntoon, C. J., and Karnitz, L. M. (2010) RAD18-mediated ubiquitination of PCNA activates the Fanconi anemia DNA repair network, *The Journal of Cell Biology 191*, 249-257.
222. Howlett, N. G., Taniguchi, T., Durkin, S. G., D'Andrea, A. D., and Glover, T. W. (2005) The Fanconi anemia pathway is required for the DNA replication stress response and for the regulation of common fragile site stability, *Human Molecular Genetics 14*, 693-701.
223. Hervouet, E., Lalier, L., Debien, E., Cheray, M., Geairon, A., Rogniaux, H., Loussouarn, D., Martin, S. A., Vallette, F. M., and Cartron, P.-F. (2010) Disruption of Dnmt1/PCNA/UHRF1 interactions promotes tumorigenesis from human and mice glial cells, *PLoS ONE 5*, e11333.
224. Oda, H., Hübner, M. R., Beck, D. B., Vermeulen, M., Hurwitz, J., Spector, D. L., and Reinberg, D. (2010) Regulation of the histone H4 monomethylase PR-Set7 by CRL4(Cdt2)-mediated PCNA-dependent degradation during DNA damage, *Molecular Cell 40*, 364-376.
225. Yang, Y., Durando, M., Smith-Roe, S. L., Sproul, C., Greenwalt, A. M., Kaufmann, W., Oh, S., Hendrickson, E. A., and Vaziri, C. (2013) Cell cycle stage-specific roles of Rad18 in tolerance and repair of oxidative DNA damage, *Nucleic Acids Research 41*, 2296-2312.
226. Tittle, R. K., Sze, R., Ng, A., Nuckels, R. J., Swartz, M. E., Anderson, R. M., Bosch, J., Stainier, D. Y. R., Eberhart, J. K., and Gross, J. M. (2011) Uhrf1 and Dnmt1 are required for development and maintenance of the zebrafish lens, *Developmental Biology 350*, 50-63.

227. Tulpule, A., Lensch, M. W., Miller, J. D., Austin, K., D'Andrea, A., Schlaeger, T. M., Shimamura, A., and Daley, G. Q. (2010) Knockdown of Fanconi anemia genes in human embryonic stem cells reveals early developmental defects in the hematopoietic lineage, *Blood 115*, 3453-3462.
228. Burgess, R. C., Misteli, T., and Oberdoerffer, P. (2012) DNA damage, chromatin, and transcription: The trinity of aging, *Current Opinion in Cell Biology 24*, 724-730.
229. Giunta, S., Belotserkovskaya, R., and Jackson, S. P. (2010) DNA damage signaling in response to double-strand breaks during mitosis, *The Journal of Cell Biology 190*, 197-207.
230. Lin, Y. J., and Edelman, J. R. (2001) Unstable heterochromatin in Fanconi's anemia cells, *Cytologia 66*, 403-407.
231. Peng, J. C., and Karpen, G. H. (2009) Heterochromatic genome stability requires regulators of histone H3 K9 methylation, *PLoS Genet 5*, e1000435.
232. Lu, H., and Hallstrom, T. C. (2013) The Nuclear Protein UHRF2 Is a Direct Target of the Transcription Factor E2F1 in the Induction of Apoptosis, *Journal of Biological Chemistry 288*, 23833-23843.